DEVELOPMENT OF A LACTOFERRIN AND LYSOZYME-CONTAINING PLURONIC-BASED HYDROGEL FOR WOUND HEALING

by
Perihan Ünver Uçkaç

Submitted to Graduate School of Natural and Applied Sciences
in Partial Fulfillment of the Requirements
for the Degree of Doctor of Philosophy in
Biotechnology

Yeditepe University
2022

DEVELOPMENT OF A LACTOFERRIN AND LYSOZYME-CONTAINING PLURONIC-BASED HYDROGEL FOR WOUND HEALING

APPROVED BY:

Assist. Prof. Dr. Gülengül Duman ……
(Thesis Supervisor)
(Yeditepe University)

Prof. Dr. Fikrettin Şahin
(Thesis Co-Supervisor)
(Yeditepe University)

Prof. Dr. Ece Genç ……
(Yeditepe University)

Prof. Dr. Gamze Torun Köse ……
(Yeditepe University)

Assist. Prof. Dr. Çiğdem Sezer Zhmurov ……
(Üsküdar University)

Assist. Prof. Dr. Yuk Yin Ng ……
(İstanbul Bilgi University)

DATE OF APPROVAL: …./…./20…

I hereby declare that this thesis is my own work and that all information in this thesis has been obtained and presented in accordance with academic rules and ethical conduct. I have fully cited and referenced all material and results as required by these rules and conduct, and this thesis study does not contain any plagiarism. If any material used in the thesis requires copyright, the necessary permissions have been obtained. No material from this thesis has been used for the award of another degree.

I accept all kinds of legal liability that may arise in case contrary to these situations.

Name, Last name Perihan Ünver Uçkaç

Signature …..…….……..

ACKNOWLEDGEMENTS

I would like to express my sincere appreciation to my dear supervisor Assist. Prof. Dr. Gülengül Duman for trusting and supporting me in all my decisions during this study. She taught me that the key to success is to work with the right people and I am glad I had a chance to pursue my thesis under the supervision of such a nice person. I also thank my co-supervisor Prof. Dr. Fikrettin Şahin for his generous support during this study.

I extend my gratitudes to Prof. Dr. Ece Genç, Prof. Dr. Gamze Torun Köse, Assist. Prof. Dr. Yuk Yin Ng and Assist. Prof. Dr. Çiğdem Sezer Zhmurov, who honored me by participating in my jury and sharing their invaluable critiques to improve this thesis. I especially thank Assist. Prof. Dr. Yuk Yin Ng for sharing his lab and resources with me generously. I also would like to thank Assist. Prof. Dr. Alev Cumbul for her contribution to the histopathological analysis, and laboratory technician Bilal Şenkal for his effort in hydrogel preparations.

I am grateful to all my professors and my colleagues Dr. Tuğba Köse, Melike Belenli Gümüş and Semra Özdemir Salihoğlu at Istanbul Bilgi University, Department of Genetics and Bioengineering, for the support and peaceful working environment they provided. I also thank laboratory technicians Dr. Fulya Günay and Murat Akkuş not only for helping me with the experimental setups, but also for the fun conversations we had in the lab, which I will miss. I wish I could have shared this thesis also with Assist. Prof. Dr. Özgür Gül, who influenced me a lot at several stages of my academic development not only as a PhD student but also as an educator. I hope he got the news from heaven and got proud of me.

Last but not least, I would like to express how lucky I am to have my family; I wouldn't be able to do it without the endless faith of my beloved husband Özgür Doğan Uçkaç, who was the closest witness and consolation to my struggle. Also, my sisters Meral Ünver and Gamze Tanyeri, my niece Defne Tanyeri, and of course, my parents Füsun Ünver and Murat Ünver… I cannot thank them enough for being with me with all their love and trust no matter what happens and what others say. I am grateful to them for telling me not to give up whenever I am exhausted. I appreciate the effort and time they spent supporting me. I thank them all, from the bottom of my heart, for being so patient and self-sacrificing.

Above all, this thesis is dedicated to my daughter Gökçe, who is "my sky full of stars".

ABSTRACT

DEVELOPMENT OF A LACTOFERRIN AND LYSOZYME-CONTAINING PLURONIC-BASED HYDROGEL FOR WOUND HEALING

The wound healing process consists of three overlapping phases: Inflammation, proliferation and remodeling. Although these stages generally occur spontaneously following an injury, some malfunctioning mechanisms in this process may sometimes cause problems like non-healing wounds or extensive scar formation and the process needs to be supported by a drug formulation in order to accelerate healing. Therefore, hydrogel formulations are of great interest as they may help regulate the mechanisms laying behind the wound healing phases and make great carriers for bioactive molecules, as well as promoting or mimicking extracellular matrix, while providing an antimicrobial environment to prevent infections. It was aimed in this study to develop such a hydrogel formulation made up of Pluronic® F127 and hyaluronic acid as the carrier, containing lactoferrin from human milk and lysozyme from chicken egg white as the bioactive molecules. In order to reveal the combinatorial effects of these two proteins on fibroblast proliferation and migration *in vitro*, MTT, migration and scratch wound healing assays were performed on NIH/3T3 mouse fibroblast cells treated with lactoferrin and/or lysozyme. Moreover, *in vivo* wound healing activity of the generated hydrogels containing lactoferrin and/or lysozyme were also tested on cutaneous skin wounds in rats. According to the results obtained from the MTT assay, the best concentrations of lactoferrin and lysozyme were determined and they were used in migration assays. As a result, it was shown that lactoferrin and lysozyme can be used and combined for inducing fibroblast migration. On the other hand, *in vivo* wound healing results revealed that even though lactoferrin and lysozyme can be formulated in a poloxamer-based hydrogel for wound healing, lactoferrin and/or lysozyme-containing hydrogels showed no significant difference in terms of wound contraction when compared to the blank hydrogel. However, histopathological examination unveiled that the hydrogels containing lactoferrin and lysozyme lead to better wound healing than the hydrogel itself. So, it was concluded that although the concentrations of lactoferrin and lysozyme in question can be used in wound healing hydrogels, more characterization and further testing in the concentrations may end up with a hydrogel with a better healing effect.

ÖZET

YARA İYİLEŞMESİ İÇİN LAKTOFERİN VE LİZOZİM İÇEREN PLURONİK BAZLI BİR HİDROJEL GELİŞTİRİLMESİ

Yara iyileşme süreci birbiriyle örtüşen üç aşamadan oluşur: Enflamasyon, çoğalma ve yeniden şekillenme. Bu aşamalar genellikle bir yaralanma sonrasında kendiliğinden oluşsa da, bu süreçteki bazı arıza mekanizmaları bazen iyileşmeyen yaralar veya yaygın skar oluşumu gibi sorunlara neden olabilir ve iyileşmeyi hızlandırmak için sürecin bir ilaç formülasyonu ile desteklenmesi gerekir. Bu nedenle, hidrojel formülasyonları, yara iyileşme evrelerinin arkasında yatan mekanizmaları düzenlemeye yardımcı olabileceğinden ve biyoaktif moleküller için mükemmel taşıyıcılar oluşturmanın yanı sıra, enfeksiyonları önlemek için antimikrobiyal bir ortam sağlarken hücre dışı matrisi teşvik veya taklit etmede yardımcı olabileceğinden büyük ilgi görmektedir. Bu çalışmada biyoaktif moleküller olarak insan sütünden laktoferrin ve tavuk yumurta beyazından lizozim içeren, taşıyıcı olarak Pluronic® F127 ve hyaluronik asitten oluşan böyle bir hidrojel formülasyonunun geliştirilmesi amaçlanmıştır. Bu iki proteinin *in vitro* fibroblast proliferasyonu ve göçü üzerindeki kombinasyonel etkilerini ortaya çıkarmak için, laktoferrin ve/veya lizozim ile tedavi edilen NIH/3T3 fare fibroblast hücreleri üzerinde MTT, hücre göçü ve çizik yara iyileştirme deneyleri yapıldı. Ayrıca, üretilmiş olan laktoferrin ve/veya lizozim içeren hidrojellerin *in vivo* yara iyileştirme aktivitesi, sıçanlarda kutanöz cilt yaraları üzerinde de test edildi. MTT tahlilinden elde edilen sonuçlara göre, en iyi laktoferrin ve lizozim konsantrasyonları belirlendi ve migrasyon tahlillerinde kullanıldı. Sonuç olarak, laktoferrin ve lizozimin fibroblast göçünü indüklemek için kullanılabileceği ve birleştirilebileceği gösterildi. Öte yandan, *in vivo* yara iyileşmesi sonuçları, laktoferrin ve lizozimin yara iyileşmesi için poloksamer bazlı bir hidrojelde formüle edilebilmesine rağmen, laktoferrin ve/veya lizozim içeren hidrojellerin, yara büzülmesi açısından boş hidrojele kıyasla önemli bir fark göstermediğini ortaya koydu. Ancak histopatolojik inceleme, laktoferrin ve lizozim içeren hidrojellerin hidrojelin kendisinden daha iyi yara iyileşmesine yol açtığını ortaya çıkardı. Bu nedenle, söz konusu laktoferrin ve lizozim konsantrasyonlarının yara iyileştirici hidrojellerde kullanılabilmesine rağmen, daha fazla karakterizasyon ve konsantrasyonlarda daha fazla test yapılmasının daha iyi bir iyileştirici etkiye sahip bir hidrojel ile sonuçlanabileceği sonucuna varılmıştır.

TABLE OF CONTENTS

LIST OF FIGURES

LIST OF TABLES

LIST OF SYMBOLS/ABBREVIATIONS

®	Registered trademark
Abl	Abelson tyrosine-protein kinase
Akt	Protein kinase B
ANOVA	Analysis of variance
bFGF	Basic fibroblast growth factor
CD44	Cluster of differentiation 44
cDNA	Complementary deoxyribonucleic acid
CMC	Critical micelle concentration
Col1a1	Collagen type 1 alpha 1
Col3a1	Collagen type 3 alpha 1
DMEM	Dulbecco's modified eagle medium
DPBS	Dulbecco's phosphate buffered saline
E. coli	*Escherichia coli*
ECM	Extracellular matrix
EDTA	Ethylenediamine tetra-acetic acid
EGF	Epidermal growth factor
ERK	Extracellular signal-regulated kinase
FBS	Fetal bovine serum
FGF	Fibroblast growth factor
HA	Hyaluronic acid
HaCaT	Cultured human keratinocyte cell line
Has1	Hyaluronan synthase 1
HAS2	Hyaluronan synthase 2
hASC	Human adipose-derived stem cell
HIF	Hypoxia-inducible factor
HUVEC	Human umbilical vein endothelial cells
IGF-1	Insulin-like growth factor 1
IL-18	Interleukin 18
IL-1β	Interleukin 1 beta
IL-6	Interleukin 6

IL-8	Interleukin 8
IPN	Interpenetrating polymer networks
KGF	Keratinocyte growth factor
LF	Lactoferrin
LRP	Lipoprotein receptor-related protein
LYZ	Lysozyme
MCP-1	Monocyte chemotactic protein 1
MEK	Mitogen-activated protein kinase kinase
MIP-1	Macrophage inflammatory protein 1
Mmp9	Matrix metalloproteinase 9
mRNA	Messenger ribonucleic acid
MTS	3-(4,5-dimethylthiazol-2-yl)-5-(3-carboxymethoxyphenyl)-2-(4-sulfophenyl)-2H-tetrazolium
MTT	3-(4,5-dimethylthiazol-2-yl)-2,5-diphenyl-2H-tetrazolium bromide
NGF	Nerve growth factor
NMR	Nuclear magnetic resonance
PAA	Polyacrylic acid
PDGF	Platelet-derived growth factor
PEG	Polyethylene glycol
PI3K	Phosphatidylinositol-3-kinase
PKA	Protein kinase A
PLGA	polylactic-co-glycolic acid
PNIPAM	Poly-N-isopropylacrylamide
QRT-PCR	Quantitative reverse transcription polymerase chain reaction
RHAMM	Hyaluronan-mediated motility receptor
RNA	Ribonucleic acid
RT-PCR	Reverse transcription polymerase chain reaction
S. aureus	*Staphylococcus aureus*
SD	Standard deviation
Sol-gel	Solution-to-gel
TGF-α	Transforming growth factor alpha
TGF-β	Transforming growth factor beta
TLRs	Toll-like receptors

TNF-α	Tumor necrosis factor alpha
VEGF	Vascular endothelial growth factor
Wnt4	Wingless-related integration site 4
β-cat	Beta catenin
ΔCT	Difference in cycle threshold

1. INTRODUCTION

The skin provides a protective barrier for the body against environmental threats. A wound is the loss of the integrity of this barrier, caused by an injury or a disease. Wound healing process basically implies immediate closure of the wound and formation of an aesthetically acceptable scar [1] and is a complex process which consists of several biological stages that can be mainly classified in three major phases: Inflammation, proliferation and remodeling [2]. However, cellular and molecular mechanisms lying behind this process are quite complicated. On the other hand, even though the body can activate and regulate these mechanisms in case of an injury by itself, sometimes further assistance might be required for a satisfactory healing process, depending on the type (i.e. chronic wounds) and severity of the wound [3]. As many cytokines, growth factors and other proteins play indispensable roles in this complex process, wound healing studies focus on revealing their native functions, as well as generating effective chemical/biological drug formulations or biopolymers inducing the wound healing stages by promoting or mimicking extracellular matrix (ECM) and providing an antimicrobial environment to prevent infections. Proteins that have effective roles in different healing processes like skin cell proliferation and migration can also be included in these formulations, but one of the leading limitations in protein-based drug delivery systems is the complexity of the maintenance of protein stability especially when the prolonged release is required [4]. However, it is possible to develop hydrogel formulations as sustained protein delivery systems, in which the protein stability and activity can also be preserved [5,6].

One of the leading hydrogels used in skin wound healing studies is formed by a synthetic copolymer called poloxamer, with the commercial name Pluronics®, which itself stimulates wound healing [7], as well as providing a vehicle to the active molecules to be applied on the wound area [8]. Determination of an iron-binding glycoprotein, lactoferrin (LF), for its supportive role in the synthesis of collagen and hyaluronic acid (HA), which are the key components of extracellular matrix, makes it an ideal ingredient for wound healing formulations [9]. On the other hand, lysozyme (LYZ) is a prominent enzyme that is well-known for its antibacterial activity besides having roles in the regulation of inflammation [10]. Therefore, this thesis generally aims at generating a skin wound healing, Pluronic® F127-based hydrogel formulation which contains lactoferrin from human milk and lysozyme

from chicken egg white. Therefore, it was objected to show combinational effects of these two proteins that usually reside together in body fluids on proliferation and migration of mouse fibroblasts *in vitro*. Moreover, it was also aimed to develop a lactoferrin and lysozyme containing hydrogel formulation that is prepared using poloxamer and hyaluronic acid as a carrier for inducing *in vivo* wound healing on cutaneous wound models on rats.

1.1. SKIN WOUND HEALING PROCESS

The skin, which is the largest organ of the body, is made up of three main layers: Epidermis, dermis and hypodermis (Figure 1.1.) [11,12]. Epidermis is the outermost layer mainly consisting of keratin. Melanin pigment is also produced in this layer to give the skin its color [13]. Dermis, where the dermal fibroblasts reside in, is the collagen-rich middle layer bearing the roots of hair follicles and the blood vessels providing nutrients to epidermis [14]. Hypodermis mainly consists of adipose tissue and the connective tissue that connects the skin to the rest of the body through bones and muscles [15]. A skin wound is generally defined as a break in the skin. Although the body has its own wound healing mechanism, in some cases it needs assistance to repair and regenerate the lost tissue which is the main aspect of tissue engineering studies [11].

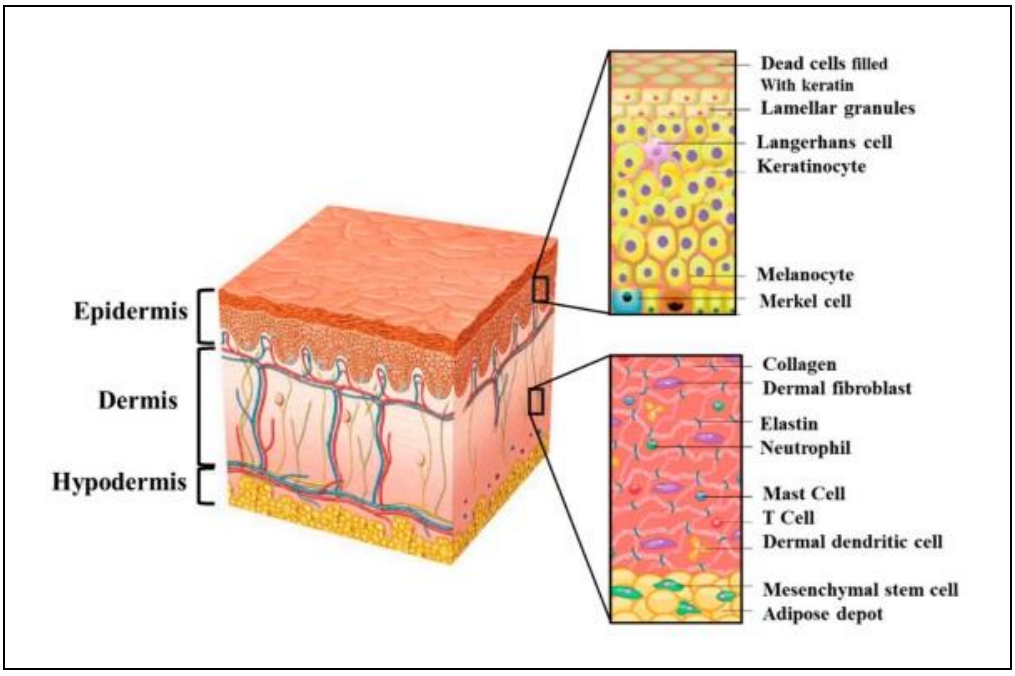

Figure 1.1. The main layers of the skin are epidermis, dermis and hypodermis. The image was derived from the publication by Tavakoli and Klar [11]

More than one classification can be done for wounds, depending on their different features. One of these classifications depends on the healing time, which characterizes wounds as acute or chronic wounds [16,17]. Acute wounds are the ones that can heal in the expected time interval without any complications, while chronic wounds like ulcers, which originate from an internal disorder, diabetes, are unable to heal properly during this predicted time interval and therefore generally end up with some complications [18,19]. Open wounds are the ones in which inner tissue or organs are affected and become exposed to the environment. Incisions, penetration wounds, puncture wounds and surgical wounds are examples to open wounds [20,21]. Full thickness wounds occur when the integrity of the skin is disrupted and reach the subcutaneous (muscle and fat) tissue by going through epidermis and dermis [22,23]. On the other hand, closed wounds are non-penetration wounds such as contusions caused by the accumulation of blood under skin [20,21]. Furthermore, contamination level of a wound can also be considered for classification of wounds. A clean wound is a sterile wound containing no dirt or pathogens, and mostly heals without any complications. However, a contaminated wound is invaded by foreign substances or organisms, and if it gets more serious, an infection may develop turning it into an infected wound. If the contaminated wound contains replicating microorganisms but no infection is observed, then the wound is defined as a colonized wound. Colonized and especially infected wounds undergo delayed healing, causing them to require more attention and special treatment [22,23].

Once a wound is formed, the protective barriers (epidermis and dermis) of the body can be crossed by the outer environment. Therefore, the wound healing process, which is the repair mechanism of the skin, gets activated. It comprises three main overlapping phases: Inflammation, proliferation and remodeling (Figure 1.2.), which is sometimes classified in four stages including hemostasis, as well [22,23]. Inflammation is the stage that lasts about 48 hours post-injury. In this ischemic environment, platelets aggregate and adhere to the endothelium, as a result of which inflammatory cells are attracted by the chemokines released. Then, these cells secrete proinflammatory cytokines, and fibroblasts are activated [2,24]. This stage is followed by proliferation, which spans the first two-to-ten days of wound healing. Granulation tissue (the vascularized connective tissue helping cell migration) is and an eschar (dead tissue adhered to the wound bed) may be formed in this stage. Fibroblasts start to differentiate into myofibroblasts to induce wound contraction. It is

followed by the remodeling stage which may take even years to complete. During this stage fibroblast differentiation continues and as collagen deposition occurs, the granulation tissue disappears [2].

1.1.1. Inflammation

The healing process begins with the inflammatory phase, in which hemostasis, coagulation and inflammation occur. As a consequence of the inflammatory activities, four cardinal signs of inflammation, which are erythema (redness), heat, edema (swelling) and pain, are observed [25].

Following an injury, hemostasis is achieved by the contraction of disrupted blood vessels (vasoconstriction), clotting and coagulation with the help of platelets [26]. Blood clots not only fill the tissue gap and therefore help required growth factors and cytokines to reach the wounded area, but also contain substances like fibrin and fibronectin, helping formation of a provisional matrix that serves as a scaffold promoting migration of leukocytes, keratinocytes, fibroblasts and endothelial cells [27]. The blood vessels are then re-widen (vasodilation), following the release of histamine and serotonin from platelets [28], in order to increase the blood flow which helps required oxygen to be transported to the injured area by erythrocytes and become more permeable. Concomitantly, leukocytes leak into the wound site due to certain chemoattractants originated from platelets; and neutrophils are recruited to the inflammation site and remain there for about two-to-five days to provide sterilization of the wound as well as the removal of necrotic tissue [29]. Tumor necrosis factor α (TNF-α), interleukin 1β (IL-1β) and interleukin 6 (IL-6) are a few examples of the mediators secreted by neutrophils that are involved in the healing process [29,30]. In the later phase of inflammation, macrophages come into play to degrade neutrophils and take over their role of phagocytosis to keep the healing process active. Moreover, these macrophages also release growth factors like fibroblast growth factor (FGF), platelet-derived growth factor (PDGF), transforming growth factor α (TGF-α), transforming growth factor β (TGF-β) and vascular endothelial growth factor (VEGF), leading the proliferative phase of wound healing to get activated [29,31–33].

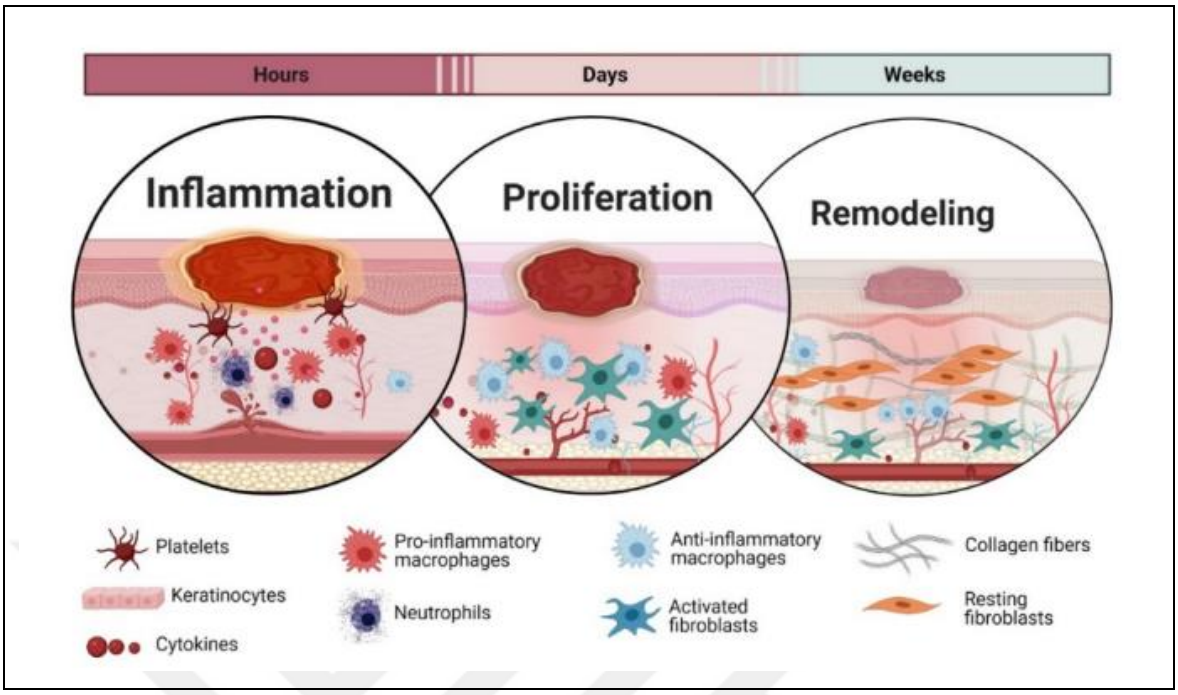

Figure 1.2. The inflammation, proliferation and remodeling stages of wound healing. The image was derived from the publication by Petkovic et. al. [24]

1.1.2. Proliferation

The second major step of wound healing, which is the phase of proliferation, occurs in about two-to-ten days after injury and aims at forming granulation tissue, as well as restoring the vascular system. Following the migration and proliferation of fibroblasts through the fibrin network, re-epithelialization begins and is followed by angiogenesis [29].

Synthesis of type III collagen and fibronectin by fibroblasts increases with the regulatory role of essential cytokines like TGF-β during this phase, which leads to the formation of a provisional ECM closing tissue gaps as well as strengthening the wound [34]. This ECM is then replaced by the granulation tissue, which is essential for reconstruction of the skin and is a highly vascular tissue that also contains fibroblasts, granulocytes, macrophages, endothelial cells and ECM components [34]. Granulation tissue is also required for migration of keratinocytes in full-thickness wounds. Re-epithelization is provided by the keratinocytes migrating from wound edges or from dermal appendages until the cells from both ends meet in the middle. This process is regulated by several cytokines and growth factors like epidermal growth factor (EGF), keratinocyte growth factor (KGF), insulin-like

growth factor 1 (IGF-1) and nerve growth factor (NGF). The faster this migration process is, the less scar is formed [29,35].

The neovascularization/angiogenesis process starts once the specific growth factors including VEGF promote breakdown of basal lamina that is followed by proliferation and migration of endothelial cells of existing blood vessels, which is called “vascular sprouting” [36]. Such angiogenic factors are secreted in low-oxygen conditions (hypoxia) that occur in the wound activating an endothelial transcription factor called hypoxia inducible factor (HIF). Therefore, secretion of VEGF is highly regulated by the stimulation of HIF. Newly formed vessels are then transformed into arteries and venules, which is followed by the initiation of blood flow ending angiogenesis [29].

At the end of this phase, the number of fibroblasts is decreased by differentiating into myofibroblasts which are responsible for wound contraction that continues in the following phase. Adhesive ability of myofibroblasts to ECM and to each other helps reduce the wound size, by contraction of the actin protein found in myofibroblasts causing wound edges to get pulled towards each other [37].

1.1.3. Remodeling

The last phase of the wound healing process is the remodeling phase which may take up to several years to be completed depending on the severity of the injury. The granulation tissue is no longer needed, so the unnecessary cells are removed by apoptosis. One of the most important incidents occurring in this phase is the replacement of type III collagen, which was abundantly secreted by fibroblasts in the previous phase of healing, by type I collagen [3]. With the help of this change, collagen fibers are reoriented into a stronger parallel-bundled structure which is a different fiber composition from the cross-linked collagen originally found in uninjured dermis [38]. On the other hand, in this phase, redundant blood vessels are also eliminated by apoptosis, as fibroblasts are. Therefore, redness of the scar tissue gradually fades as the cellular activity decreases [29].

Unlike fetal wounds, adult dermal wounds heal with a scar, which is directly related to the occurrence of inflammation and the production of collagen [39]. It is important to note that wound repair differs from complete regeneration, in which the injured tissue or organ is

replaced with a new one, structure and function of which are exactly identical to the previous tissue [40]. Even if the wound healing process successfully repairs the epidermis and dermis, sub-epidermal appendages like hair follicles are unable to heal following a serious injury [29]. Therefore, studies on hydrogel-based wound healing treatments sometimes focus on promoting scar-free wound healing and skin regeneration.

1.2. CLASSIFICATION OF HYDROGELS

Hydrogels are three-dimensional, flexible and biocompatible polymeric materials that contain large amounts of water. They are highly utilized in manufacturing contact lenses, as well as providing hygienic properties of several other daily-use products. On the other hand, their high water content, porous structure and biocompatibility make them great choices for drug delivery, wound healing and tissue engineering studies [41].

Hydrogels can be classified in several groups according to their different properties like their source, configuration and type of cross-linking [42]. Depending on the source, they can be classified as natural or synthetic based hydrogels. Natural polymer gels have many odds like biocompatibility and biodegradability, when compared to synthetic polymer gels [43]. Polysaccharides, which are natural polymers, are frequently utilized for designing hydrogels for biomedical applications, as they form hydrophilic hydrogels [44]. Alginate, cellulose, chitosan, dextran, heparin, hyaluronic acid and pullulan are the most commonly used polysaccharides in hydrogel development, especially for protein delivery studies [45]. Among these, hyaluronic acid is the one being interested in this study and will be further discussed in the following sections. Another group of natural polymer-based hydrogels is protein-based hydrogels, which includes collagen, an essential ingredient of the connective tissue, and gelatin, which is produced by its partial hydrolysis [46]. On the other hand, poloxamer (Pluronic®) is the other polymer utilized in this study, which is an example to the mostly utilized synthetic hydrogels [42,47].

Based-on their configuration, hydrogels can be classified in three groups as non-crystalline (amorphous), semi-crystalline and crystalline, while they can also be classified as nonionic (neutral), ionic (anionic or cationic), ampholytic (both acidic and basic) and zwitterionic (both anionic and cationic), depending on the electrical charge of the network [48]. Furthermore, polymeric composition-based classification divides hydrogels into three

groups, which are homopolymeric, co-polymeric and multipolymeric hydrogels. Homopolymeric hydrogels consist of a single type of monomer, while co-polymeric hydrogels contain more than one different type of monomer, at least one of which is hydrophilic. Multipolymeric hydrogels are actually named as “interpenetrating polymer networks (IPNs)”. Unlike co-polymeric hydrogels, in which two or more different monomers generate a single network by polymerizing together, IPNs are developed by inclusion of more than one network [42].

Cross-linking-based classification creates two classes of hydrogels: Chemically cross-linked hydrogel networks and physically cross-linked hydrogel networks. Chemically cross-linked hydrogels have permanent interactions because of the covalent bonding between different polymer chains, while physically cross-linked hydrogels are the ones developed with noncovalent interactions like hydrophobic interactions, ionic interactions or hydrogen bonding, making physical networks more transient. Therefore, physically cross-linked hydrogels are reversible networks that can undergo changes depending on the varying environmental conditions, such as pH and ionic strength [42,49].

The hydrogels that are responsive to environmental stimuli are called “smart hydrogels”. The external stimuli can be physical or chemical, by which swelling behavior, structure or permeability of the hydrogel can be controlled [50]. Such smart hydrogels are great candidates for developing in-situ gelling protein delivery systems. However, effectiveness of a hydrogel-based protein delivery system is determined by properties of both the hydrogel and the protein to be delivered. In such a system, protein release is controlled by various mechanisms like diffusion, swelling and degradation [51], which can further be regulated by physical or chemical stimuli, as mentioned above. Because the porous structure of hydrogels can easily be adjusted, it is possible to classify them based on their porosity into four classes as non-porous, micro-porous, macro-porous and super-porous [52]. Pore and mesh sizes of the hydrogel and size of the protein to be delivered define which mechanism will step in to control release; if the pores of the hydrogel are bigger than the hydrodynamic radius of the protein, the release mechanism will be diffusion-controlled. Diffusion controlled release can be provided by either a reservoir or a matrix system, the former of which consists of a drug-containing center leading to a constant release rate, while the latter contains the drug uniformly dispersed throughout the hydrogel, allowing it to release in a time-dependent manner [41]. On the other hand, if the mesh size is smaller than the protein, hydrogel will

be expected to swell or degrade to be able to release the protein [53]. Once the polymer chains loose as a result of swelling, dispersed drugs can diffuse constantly from hydrogel to the surrounding environment with the help of the gradient between them [47]. However, in hydrogel-based protein delivery systems, stability of the protein should be maintained, not only for preserving the bioactivity of the protein, but also for avoiding immunogenicity that can emerge upon presence of the by-products of protein degradation. As some polymers are not suitable for protein encapsulation, some strategies like addition of protective agents to the network can increase protein stability and bioactivity [54].

1.3. POLYMERIC HYDROGELS USED IN WOUND HEALING STUDIES

Hydrogels used in wound healing studies can be made up of or combined with either natural or synthetic polymeric materials. Natural and synthetic polymers are sometimes formulated together in a hydrogel, in order to compensate for their disadvantages. For example, as natural polymers are generally weaker in mechanical strength than the synthetic ones, they can be combined for increasing the stability of the resulting hydrogel. Similarly, most synthetic polymers are not as biocompatible and biodegradable as natural polymers are. Therefore, a natural polymer can be incorporated into a synthetic polymer-based hydrogel, in order to increase its biocompatibility [48].

Figure 1.3., which was generated by Chen and colleagues to demonstrate the uses of bioactive molecules on wound healing, also represents the possible routes that a biomaterial, like a polymeric hydrogel, with bioactive molecules can be applied on wound repair and regeneration. The bioactive molecules that are sometimes delivered directly to the wound site, can also be carried to the wounds by hydrogels [55]. Another approach is to use the hydrogel as a scaffold for the transplantation of some specific cell types with the bioactive molecules to the wounded area [56].

The characteristics of the polymer chosen for the hydrogel to be developed must be compatible with the needs of the treatment; the polymers that are used in wound care are desired to be biocompatible and to have a non-toxic nature [57]. In addition to these, their individual properties like biodegradability, high oxygen permeability, temperature or pH sensitivity, wound exudate absorption capability, included molecule bioactivity, etc. are considered when selecting the perfect polymer for treating a specific defect.

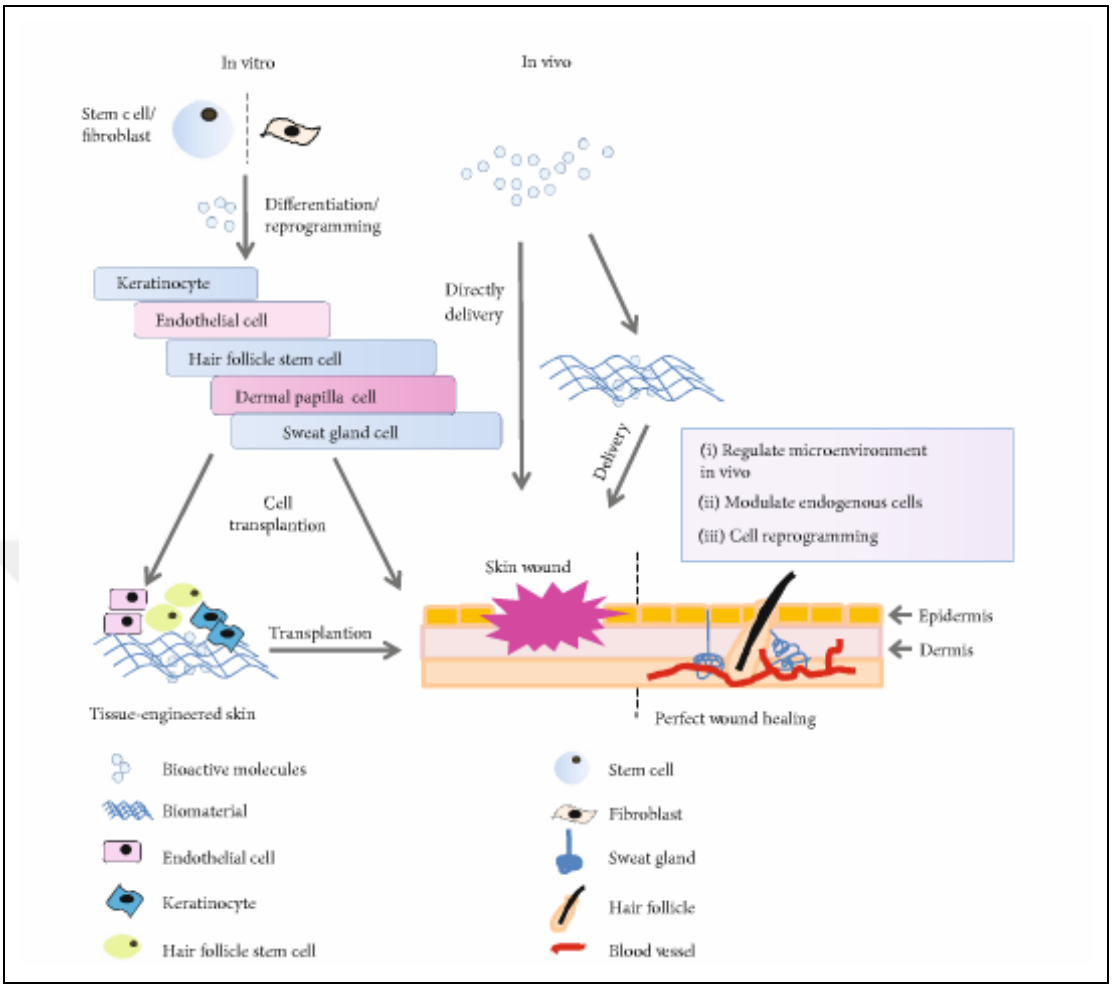

Figure 1.3. Applications of polymeric hydrogels on wound repair and regeneration. The image was derived from the publication by Chen et. al. [55]

Currently, many commercially available polymer-based wound dressings and other formulations are in use on treatments of different types of wounds [11,58]. Polyethylene glycol (PEG), polylactic-co-glycolic acid (PLGA), polyacrylic acid (PAA), poloxamer and poly-N-isopropylacrylamide (PNIPAM) can be given as examples of the most commonly used synthetic polymers in hydrogel-based formulations. PAA is a biodegradable and pH-responsive polymer [59]. On the other hand, PNIPAM is a temperature-sensitive hydrogel [60], when poloxamer also has a thermo-reversible characteristic [61]. PEG is included in hydrogel-based formulations very often and it is generally accepted as non-immunogenic, although some immunological issues have also been reported [62].

On the other hand, natural polymers are highly utilized in wound healing formulations, as they have advantages like higher biodegradability and lower immunogenicity than the

synthetic polymers [63]. Among the natural polymers, chitosan, the only alkaline polysaccharide found in nature, is a polymer with antimicrobial properties, which also promotes wound healing [64]. Collagen and hyaluronic acid are other generally formulated natural polymers that also accelerate wound healing by facilitating cell migration and proliferation [65,66]. Wound healing can also be enhanced by activation of immune cells, which is another role of hyaluronic acid, as well as gelatin and β-glucan [67–69]. Recently, a cytocompatible, bioactive, thermostable and biodegradable protein called silk fibroin has started to get involved in wound healing studies frequently, as it is also permeable to oxygen and water vapor [70].

In this study, one synthetic (poloxamer) and one natural (hyaluronic acid) polymer were combined with each other and with the active proteins lactoferrin and lysozyme when preparing the hydrogel formulation. Their individual roles on wound healing and how they were formulated in previous studies are discussed in the following sections.

1.3.1. Poloxamer-based Hydrogels

Poloxamers are synthetic polymers that consist of triblock copolymers of poly(ethylene oxide)-b-poly(propylene oxide)-b-poly(ethylene oxide) (PEO-PPO-PEO) [71] and they have different commercial names as “Pluronics®”, “Lutrol®”, “Kolliphor®”, “Antarox®” and “Synperonics®” [72]. They are synthesized by adding propylene oxide (PO) and ethylene oxide (EO) monomers sequentially, and different copolymers are obtained according to the number of PO and EO units added. There are several different poloxamers manufactured so far like poloxamer P124 (Pluronic® L44), poloxamer P188 (Pluronic® F68), poloxamer P333 (Pluronic® P103) and poloxamer P407 (Pluronic® F127) which are differentiated from each other by means of their properties like their form, molecular weight, melting temperature and PEO content. The Pluronic®-based nomenclature of these copolymers are also regulated using these properties and the letters mentioned in the names indicate the form of the poloxamer which can be either paste (P), liquid (L) or flake (F) [72].

These copolymers can be used individually or in combination with each other as gelling agents or with other ingredients for various therapeutic applications [73–77]. Among more than twenty poloxamers manufactured so far, poloxamer 407 is one of the mostly utilized one in drug delivery systems because of being thermoreversible, which makes it very useful

for topical, ophthalmic, nasal, vaginal, rectal and intravenous applications [78,79]. In addition to this property, poloxamer 407's low toxicity, high drug solubilizing and sustained release capacities also point it out as an ideal polymer in delivery systems [80–85].

Once dissolved in water at specific concentrations, it shows a thermoreversible solution-to-gel (sol-gel) transition and its block copolymers form micelles that have an inner core and an outer shell formed by hydrophobic blocks and hydrophilic units, respectively. This transition occurs when the concentration of these block copolymers is higher than the critical micelle concentration (CMC). If their concentration is lower than CMC, they remain as molecular solutions in water [82,86]. Hydrogel of poloxamer 407 is generally prepared by dissolving in water at a concentration of 20% (w/w), or higher, and the sol-gel transition occurs when the temperature approaches the physiological temperature (37°C). However, below the room temperature (25°C), poloxamer 407 solutions remain as viscous liquids (Figure 1.4.) [72].

Although poloxamer hydrogels were first introduced as materials utilized in detergent development in the 1950s, they gathered particular interest with the discovery of their being safe polymers for therapeutic applications in the early 1970s. Since then, they have been formulated in many drug delivery systems, in which they can also be combined with other poloxamers or with totally different active molecules [72]. In one of these attempts, for example, puerarin was delivered in the precorneal area by a delivery system consisting of poloxamer 407, poloxamer 188 and carbopol [87]. This was not the only ophthalmic application of these two poloxamers; they were also combined for ocular delivery of ketorolac tromethamine, in which, again, no toxicity or irritation to the eye was observed [88]. Poloxamers sometimes can be cross-linked with other polymers, especially for slowing down the degradation rate which is one of the disadvantages of poloxamers for the sustained delivery of drugs. In one of these, poloxamer 407 cross-linked with carboxymethyl chitosan generated a successful ophthalmic drug delivery system, by which sustained release of nepafenac was provided [89]. Another study focusing on developing a formulation against diabetic retinopathy revealed that, a blend of poloxamers 407 and 188 can be used as a carrier hydrogel for delivering curcumin-loaded albumin nanoparticles to the eye [90].

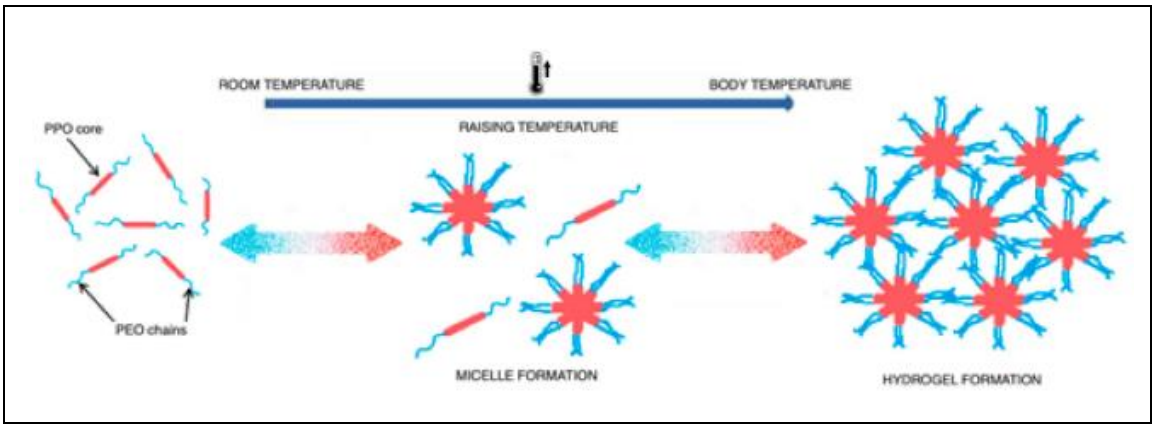

Figure 1.4. Micelle and hydrogel formation of poloxamer. The image was derived from the publication by Russo et. al. [72]

Opthalmic administration, of course, is not the only therapeutic application method for poloxamer hydrogels; there are various poloxamer formulations mentioned in the literature that focus on developing rectal or vaginal formulations, as well. For example; poloxamer 407 combined with hydroxypropylmethylcellulose was utilized in delivery of quinine in 2006 [91], which was followed by the formulations of poloxamer with nimesulide for rectal delivery [78]. In addition to the formulations developed for rectal delivery, poloxamers were also successfully included in the hydrogel formulations for vaginal administration [92,93], which is generally preferred for the drugs poorly absorbed by oral administration [94]. One of the greatest handicaps of using poloxamer in mucosal tissues is that it inhibits surface–tissue adhesion in some cell types [95] and some bioadhesive materials can be added into the poloxamer-based hydrogel formulations under these specific circumstances [72,96].

In addition to the rectal and vaginal administration, some poloxamer hydrogels were also developed as transdermal drug delivery systems for administration of anti-inflammatory, analgesic or anesthetic drugs like tolfenamic acid, fentanyl and lidocaine, respectively [97–99]. In these, the main barrier against delivery is the stratum corneum which in recent years can easily be permeated by microneedles and sustained delivery of the active ingredients can be provided [100].

Poloxamer-based scaffolds are manufactured and used in various tissue engineering applications. They generally are of great interest in bone, cartilage and skin tissue regeneration, even though they are also used for the repair and regeneration of blood vessels, nervous system and some organs like brain and lungs [101]. As aimed in this thesis, many

research groups so far objected to develop poloxamer-containing scaffolds that support and induce skin tissue repair and regeneration. Therefore, various useful poloxamer-based hydrogels were developed for skin wound treatments. An advantage of the poloxamer-based hydrogels is that they can fill the local wound area; they do not need to be manufactured according to the shape of the missing tissue. Moreover, they are biocompatible; and they can even increase the biocompatibility of other biomaterials they are combined with [102]. Inflammatory microenvironment causes wound healing therapeutics like growth factors to be degraded in a short time, when poloxamer can provide suspended release of these drugs by making them stay on the defect for a longer time and also by preventing their hydrolysis [101,103]. Poloxamer hydrogels do not only make good carriers of exogenous anti-inflammatory drugs in wound healing, but can also decrease the secretion of endogenous inflammatory agents and regulate growth factor stimulation [101,104]. They can also support wound healing by means of antimicrobial activity; hydrogel formulations containing poloxamer that were developed by different research groups showed antibacterial effects [104–106].

As a result of the developments in 3D printing technology in recent years, hydrogels were also started to be printed in order to manufacture scaffolds for tissue engineering studies. Poloxamer hydrogels are highly printable because of their thermoreversible sol-gel transition, even though an attempt for 3D printing of poloxamer 407 revealed that it should be improved for being used in long-term cell viability [107–109].

The recently developed poloxamer-based or poloxamer-containing hydrogels for regenerative applications include but are not limited to the development of formulations combining poloxamer with HA. In one of these, for example, scientists designed a HA-poloxamer hydrogel and tested *in vitro* and *in vivo* wound healing effects of it. They didn't only show that this hydrogel is very effective in skin wound healing by allowing high air permeability, having moisturizing activity and leading protein accumulation in the wound area, but also has antibacterial properties [110]. In another recent study, poloxamer was blended with chitosan and HA for being used as a vehicle for delivering vitamins A, D and E and successfully healed burn wounds [111]. In a more recent one, poloxamer 407 was combined with HA again, this time for delivering Ginsenoside Rg3 to the full-thickness skin wounds. Results were not surprising at all; the hydrogel induced wound contraction, collagen

deposition and angiogenesis as well as regulating the expression levels of proteins that have roles in wound healing [112].

Overall these properties of and findings about poloxamer make it a great candidate for being formulated in a wound healing hydrogel, especially when combined with hyaluronic acid, effects of which in wound healing are discussed in below.

1.3.2. Hyaluronic Acid-containing Hydrogels

Hyaluronic acid (HA) is a glycosaminoglycan that consists of D-glucuronic acid and *N*-acetyl-D-glucosamine repeat units [113]. This polysaccharide is elongated with the repetitive addition of glucuronic acid and *N*-acetyl-D-glucosamine to the chain by hyaluronan synthase (HAS) enzymes, which are integral membrane proteins responsible for the synthesis of HA [114]. As HA is one of the main components of the extracellular matrix (ECM), balance between the synthesis and degradation of this polymer is essential for native ECM maintenance and wound healing processes [113], as well as prevention of cancer cell metastasis [115]. Such effects are provided not only by interaction with several ECM proteins like fibronectin and collagen [116,117], but also by binding to a number of cell surface receptors [118]. Among these, cluster of differentiation 44 (CD44), hyaluronan-mediated motility receptor (RHAMM) and toll-like receptors (TLRs) are well-studied hyaluronan receptors, interaction with which regulates some significant signaling pathways, such as phosphatidylinositol-3-kinase and protein kinase B (PI3K/Akt), and mitogen-activated protein kinase kinase/extracellular signal-regulated kinase 1/2 (MEK/ERK1/2), and therefore play important roles in wound healing process by regulating fibroblast and keratinocyte behavior like proliferation, migration and inflammation [114,119–124]. On the other hand, although such interactions of HA and the related signaling are mostly believed to promote wound healing, it is still suspicious whether or not HA affects wound healing or fibrosis via physical interactions [113,120,125].

Although HA hydrogels are considered as useful tools for studying the function of ECM in wound healing process because of imitating native ECM structure, actual environmental conditions may not be fully achieved and additional adhesive proteins like fibronectin may further be included to provide natural interactions [126]. Similarly, a number of hydrogel studies also focuses on integrating HA into collagen or different hydrogels to create a more

realistic ECM environment [120,127], while some others investigate the effects of growth factor-loaded HA-containing hydrogels on wound healing [128].

Effect of HA on wound healing is dependent on its molecular weight. When the high molecular weight HA exerts anti-inflammatory effect, low molecular weight HA depicts pro-inflammatory activity during wound healing [129].

Similar to poloxamer hydrogels, HA-based hydrogels also have good biocompatibility, biodegradability and water absorption capacity [130]; therefore are highly used as carriers for targeted and controlled drug delivery in wound healing treatments. HA can even be conjugated with peptides or proteins and their hydrogels have been used for the prolonged release of protein drugs [131], although cross-linked networks in these systems need to be very-well designed for the sustained release of the protein [130]. Release studies of erythropoietin from HA hydrogels revealed that it can be effectively used for the controlled release of protein drugs [132].

A group of scientists reported the development of an HA-based hydrogel formulated in combination with poloxamer 407 for treating osteoarthritis. The hydrogel was loaded with piroxicam, and the release behavior of this gel was compared with the poloxamer hydrogels containing no HA. As HA increases the mechanical strength and stability of the formulated hydrogel, HA-poloxamer hydrogel showed a slower release of piroxicam [133]. This study was one of the examples depicting the importance of the combinational use of polymers for therapeutic purposes. In addition to the efforts in which HA was mixed with poloxamer that were discussed previously for poloxamer-based hydrogels [110,112], HA was also included in various other hydrogel formulations containing different polymers, recently. In one of these, hybrid hydrogel formulations developed by mixing various concentrations of xanthan gum, HA and silver sulphadiazine were developed and tested for their wound healing activities [134]. HA was physically mixed with chitosan and poloxamer 407 in a different study, and successfully formed a hybrid hydrogel displaying wound healing activity [135]. In the light of these studies revealing the importance of HA in hydrogel-based wound dressings, HA was considered as one of the gelling agents in this proposed study to deliver lysozyme and lactoferrin for inducing wound healing.

1.4. USES OF LACTOFERRIN AND LYSOZYME IN WOUND HEALING FORMULATIONS

Protein contents of milk are indispensable ingredients for nutrition. Two of these proteins, lysozyme and lactoferrin, also play important roles in the regulation of several wound healing stages. Especially lactoferrin has been shown as an effective mediator of skin wound healing [9], while lysozyme has been approved for its anti-inflammatory and anti-microbial activities in earlier studies [136,137]. As wound healing is a very complex process in which many cytokines, growth factors, proteins and signal transduction pathways are involved, such contributors are mostly targeted by wound healing studies in order to develop systems inducing wound healing mechanisms. However, as proteins work collaboratively in the body, cooperation of these mediators in therapeutic applications might also be required to increase the success rate, while decreasing individual concentrations of the proteins in the formulation, which can modulate their toxic effects. Such protein delivery attempts may provide promising therapies for skin wounds, but preservation of the stability and bioactivity of these peptides is another challenge to be considered.

1.4.1. Lactoferrin and Its Use in Wound Healing Formulations

Lactoferrin is one of the members of transferrin family and an iron-binding glycoprotein with a molecular weight of 80 kDa, found abundantly in colostrum (the first milk produced after giving birth) which has about seven times the amount of lactoferrin found in mature milk [138]. It is also secreted into other body fluids like tears, mucus and saliva. Other than being used for treating iron deficiency, diarrhea and bacterial or viral infections, lactoferrin is also known for its promoting role in skin wound healing by regulating inflammatory phase both positively and negatively [9]. However, previous studies conducted on revealing the effects of lactoferrin on several cytokines and growth factors having role in different stages of wound healing showed that lactoferrin does not act only in the inflammatory phase. How lactoferrin gets involved into all stages of a normal wound healing process has been very well summarized by Takayama et. al. As explained in their review, studies demonstrate that levels of cytokines like IL-6, interleukin 8 (IL-8), interleukin 18 (IL-18), macrophage inflammatory protein 1 (MIP-1), monocyte chemotactic protein 1 (MCP-1) and TNF-α are

increased in the wounds treated with talactoferrin, which is a recombinant human lactoferrin [139,140]. This reveals that lactoferrin enhances the expression of proinflammatory cytokines as the positive regulation of the inflammatory phase. On the other hand, lactoferrin also shows anti-inflammatory activity, which is required for avoiding development of a chronic wound as a result of continuous inflammatory response.

In addition to its effects on inflammation, proliferation and migration of fibroblasts are also stimulated by lactoferrin [141]. Both wound healing [142] and transwell migration assays [140,141] demonstrated that lactoferrin promotes fibroblast migration, which requires formation of granulation tissue. Granulation tissue is formed following the release of some growth factors like platelet-derived growth factor (PDGF) and transforming growth factor-b (TGF-b) [35,143]. Lactoferrin can affect the proliferative phase implicitly, not only by regulating these two growth factors for the formation of granulation tissue, but also by promoting the proliferation and migration of keratinocytes [144]. Moreover, following administration of lactoferrin to human dermal fibroblasts, synthesis of HA, which is the major component of ECM and critical for granulation tissue formation, is enhanced as a result of the increased expression of hyaluronan synthase 2 (HAS2) [145]. Lactoferrin can induce synthesis of collagen in fetal rabbit dermal fibroblasts, as well [146], overall which suggest that lactoferrin supports wound healing by leading to matrix formation that further assists fibroblast migration.

In addition to their roles in the granulation tissue formation, growth factors like TGF-β, PDGF and FGF play important roles also in collagen gel contraction, which is promoted by lactoferrin, as well [142]. Moreover, angiogenesis is also induced by apo-human lactoferrin via regulation of VEGF, whereas basic fibroblast growth factor (bFGF) or VEGF-induced proliferation and migration of human umbilical vein endothelial cells (HUVECs) are inhibited by the treatment with bovine lactoferrin [147].

All this information indicates that lactoferrin promotes wound healing in multiple ways, therefore it attracts attention for being used in different pharmaceutical formulations. However, it should be kept in mind that properties of the delivery system must be regulated properly to maintain its stability, especially in long-term delivery systems. Therefore, lactoferrin has been formulated in various hydrogel-based drug delivery systems for tissue repair and regeneration so far.

As very well reviewed by Icriverzi et. al., lactoferrin is especially used in bone tissue healing and regeneration, individually or in combination with other bioactive compounds and it can be integrated within hydrogels, liposomes, microspheres and nanofibers for delivery [148]. In one of these studies, researchers developed an injectable hydrogel for cell delivery from bovine lactoferrin by enzymatic cross-linking, which helps maintain the viability and proliferation of mouse bone marrow-derived stromal cells, as well as affecting growth factor production in them [149]. The same group also generated an enzymatically cross-linked hydrogel using recombinant human lactoferrin and showed that it can be used as a cell delivery vehicle for bone tissue engineering. This hydrogel supported the osteogenic activity of lactoferrin by showing that recombinant lactoferrin can enhance the viability, proliferation and differentiation of pre-osteoblasts. Moreover, it revealed that protein kinase A/lipoprotein receptor protein 6 (PKA/LRP6) signaling is required for the stabilization of β-catenin in these cells [150]. In addition to the studies in which lactoferrin is used as the hydrogel itself, it has also been involved in many other polymeric hydrogels to be utilized in bone tissue studies. For example, lactoferrin combined with hydroxyapatite and incorporated into gellan gum spongy-like hydrogels generated a suitable microenvironment for human adipose-derived stem cells (hASCs) to enhance their viability [151]. Another formulation of lactoferrin as a bioactive molecule in bone regeneration was in a chitin/PLGA-$CaSO_4$ hydrogel, in which lactoferrin has been consolidated with the chemotactic agent substance P, improved stem cell proliferation and migration, therefore it could be a favorable formulation for regeneration of calvarial bone defects [152]. On the other hand, in a very recent study, in which lactoferrin has been formulated in poloxamer to be tested on calvarial defect model on rats, scientists revealed that although the formulation they tested was good enough not to show any cytotoxicity or immune response, it also had no positive activity on inducing bone regeneration in the selected defect model [153]. Therefore, the results of this study also highlights the importance of *in vivo* testing of the developed formulations which were tested for cytotoxicity by *in vitro* assays.

In addition to being highly utilized in the hydrogel formulations for bone tissue repair and regeneration, there are also other hydrogel formulations that lactoferrin got involved in, especially against wound infections. When loaded into gelatin as a bio-nanosilver complex, it showed antibacterial and anti-biofilm effect, while having no diverse effects like cytotoxicity or anti-migratory activities on human dermal fibroblasts *in vitro*, which suggest

the formulation as a promising dressing for chronic and infected wounds [154]. Another hydrogel based on lactoferrin and xylitol was able to improve a commercial silver wound dressing, by reducing biofilm viability upon their combined use [155]. Moreover, even though they have not yet been tested on any wound models *in vitro* or *in vivo*, lactoferrin showed very promising antimicrobial activities when it was combined with lysozyme and loaded into poloxamer to be used against *Mutans streptococci* and *lactobacilli*. Scientists suggested these antibacterial formulations they developed can be utilized in dental treatments [105]. Their study also supports the objective of this thesis by revealing the synergetic activity of lactoferrin and lysozyme against infections.

1.4.2. Lysozyme and Its Use in Wound Healing Formulations

Lysozyme is a 14.3 kDa enzyme secreted by animal tissues and found in tear, breast milk and mucosal body fluids. The commercial and the most abundant source is generally egg white by direct crystallization and it is found in the albumen in a concentration of about 3.5% [156]. Lysozyme is well-known for its role in the innate immunity as it has the ability to lyse the most Gram-positive bacteria by catalyzing the hydrolysis of the β-(1,4) glycosidic bonds of the cell wall peptidoglycan; with the help of which it is highly utilized as an antibacterial agent in therapeutic formulations [157]. Moreover, it shows analgesic activity [158], which also supports its being used as a therapeutic agent. On the other hand, lysozyme have several anti-inflammatory functions including inhibition of some immunological responses like chemotaxis of active leukocytes, mitogen induced lymphoblastogenesis, autologous mixed lymphocyte reaction and haemolytic activity of serum complement [136,159]. The anti-bacterial and analgesic activities of lysozyme cannot be ignored for wound care, and termination of the inflammatory phase is a required mechanism as prolonged inflammation may result in non-healing chronic wounds.

In early studies on identifying the effects of lysozyme on skin wounds conducted by Gasior-Chrzan in 1988, it has been shown that ovalbumin lysozyme induces healing of skin wounds in guinea pigs [160] which has been followed by a clinical trial in which the positive activity of lysozyme on skin wound healing in humans has been revealed [161]. More recently, another group of scientists developed a lysozyme-antimicrobial peptide fusion protein to be tested on diabetic wound models. This protein was not only able to decrease the wound size

in mice, but also induced the expression levels of both PDGF and VEGF as mRNA and protein, which indicates its likely effect on angiogenesis and anti-inflammatory activity [162,163]. In addition to inducing expression of these growth factors, another study showed that egg white lysozyme can increase collagen type 1 alpha 1 (Col1a1), collagen type 3 alpha 1 (Col3a1) and hyaluronan synthase 1 (Has1) levels in mouse fibroblasts, which indicates egg white lysozyme induces the secretion of collagen and hyaluronic acid in dermal fibroblasts [164]. A more recent study showed the two-faced activity of I-type lysozyme, in which it supported migration of fibroblasts and keratinocytes, as well as accelerating epidermal regeneration. On the other hand, it also revealed that I-type lysozyme can prevent excessive scar formation by reducing excessive collagen deposition and fibrosis [165].

As a result of the recent improvements in the use of biomaterials in wound healing formulations, lysozyme has been formulated in many different types of wound dressings in the past decade. One example to these formulations was developed by Charernsriwilaiwat and colleagues, in which they produced lysozyme-loaded chitosan-based fibrous mats by electrospinning and they tested them in rat wound models to show the positive role of lysozyme-loaded biomaterials on skin wound healing [166]. Three years later, they generated lysozyme-immobilized ion exchange nanofibrous mats to be used on wound healing [167]. Fibrous mats were not the only materials developed with lysozyme for promoting healing of wounds. A non-cytotoxic cross-linked hydrogel made up of chitosan and lysozyme showed enhanced cell adhesion and proliferation, while showing antibacterial activity, which makes it a great candidate for being evaluated as an effective wound treatment [168]. Moreover, a lysozyme-loaded polyurethane foam dressing provided the moist environment needed by the wound to accelerate the healing while generating an antibacterial activity at the same time [169]. In addition to these examples, lysozyme was also successfully coupled with hyaluronic acid and PEG recently by two separate research groups, for being used as a wound dressing coacervate [170] and a suturable biohydrogel tissue patch [171], respectively.

Other than being used in development of wound healing formulations, lysozyme is also utilized as a model protein drug in the investigation of appropriate release and delivery of proteins from different biomaterials for several purposes. For example, it has been formulated in a photo-cross-linkable Pluronic® hydrogel to investigate the sustained release of proteins [172]. This was followed by the studies on release of lysozyme from PLGA

[173,174] and gelatin microspheres [175], which focus on investigating the effect of different agents and polymers on the release of proteins. Prevention of protein aggregation has also been tested with the help of lysozyme in two separate studies. The researchers showed that poloxamers are much more preferable than PEG for avoiding aggregation of heat denatured lysozyme [176], which also supports the objective of this current study.

Cooperation of lysozyme with a different agent inducing early inflammatory phase like lactoferrin may help provide a balance between the activation of wound healing cascades and the relief of pain, while preventing formation of chronic wounds. Tonguc-Altin et. al. has previously reported that lactoferrin and lysozyme accompanied with poloxamer 407 are effective against *Streptococcus mutans* and *Lactobacillus acidophilus*, indicating that these formulations can be used for dental care and oral hygiene [105]. Once all these antibacterial, anti-inflammatory and analgesic activities of lysozyme, lactoferrin and poloxamer are being considered, formulating them in such a poloxamer-based hydrogel can be very promising for developing a wound healing formulation, as well.

2. MATERIALS AND METHODS

The materials that were used and the methods that were performed in this study were as follows:

2.1. MATERIALS

All the materials; consumables, chemicals, instruments, cells and primers that were used in the experimental procedures of this study are listed below.

2.1.1. Consumables

Consumable materials that were used in *in vitro* and *in vivo* experiments are listed in Table 2.1.

Table 2.1. Brand names and catalog numbers of the consumables used in the experiments

Brand Name	Item	Catalog Number
Isolab	Microcentrifuge tubes	078.03.021
Axygen	Screw Cap Tubes 15 ml/50 ml	SCT-15ML/50ML
Axygen	Pipet Tips 10 µl, 200 µl, 1000 µl	T-1000-B T-200-Y T-300
Axygen	Filtered Pipet Tips	TF-200-R-S
TPP	Tissue Culture Flasks 25-75-150	90025-90075-90150
Corning Costar	24/96 Well Cell Culture Plate	CLS3524/ CLS3596
SPL	Serological Pipet 5 ml-10 ml- 25 ml	91005-91010-91025

Falcon	Cell Culture Insert	353097
Sartorius AG	Minisart Syringe Filter 0.2-0.45 µm	10410063
TERUMO	20 G Syringe	NN-2025R
Isolab	Petri Plates	120.13.035
Isolab	Inoculation Loops	082.01.003
Isolab	Cell spreader	082.03.001
Corning	Microscope slides	CLS294875X25

2.1.2. Chemical Substances and Experimental Kits

Chemical substances that were used in *in vitro* and *in vivo* experiments were as listed in Table 2.2.

Table 2.2. Brand names and catalog numbers of the chemicals and kits used in the experiments

Brand Name	Item	Catalog No
PAN Biotech	1X Dulbecco's phosphate buffered saline (DPBS)	P04-36500
Gibco	1X Dulbecco's modified eagle medium (DMEM)	41966-029
Gibco	Antibiotic-Antimycotic (100X)	15240-062
Gibco	Fetal Bovine Serum (FBS)	26140079
Gibco	Trypsin-EDTA (0.05%)	25300054
Merck	Giemsa's azur eosin methylene blue solution	1.09204.500
Isolab	Methanol	947.046.2500
Merck	Ethyl alcohol	1.00983.2511
Merck	Xylene	108298
Sigma-Aldrich	Hematoxylin	H3136

Sigma-Aldrich	Eosin Y	230251
Merck	Ammonia	105432
Sigma-Aldrich	Acid Fuchsin	F8129
Merck	Phosphomolybdic acid	100480.0100
Sigma-Aldrich	Light Green SF Yellowish	L1886
Sigma-Aldrich	Acid Alcohol	56694
Sigma-Aldrich	Paraplast®	P3558
BIO-RAD	iTaq Universal SYBR Green Supermix	172-5121
BIO-RAD	iScript cDNA Synthesis Kit	1708890
GeneMark	Total RNA Purification Kit	TR01-150
Merck	Nutrient Agar	105450.0500
Merck	Nutrient Broth	105443.0500
Sigma	Pluronic® F-127	P2443
Acros Organics	Sodium Hyaluronate, 95%	AC251770010
Sigma	Lactoferrin from human milk	L0520
Sigma	Lysozyme from chicken egg white	L6876
Promega	CellTiter96 Aqueous One Solution	G3582
Sigma	Thiazolyl Blue Tetrazolium Bromide	M5655
Oxoid	Oxacillin Antimicrobial Susceptibility Test Disks	CT0159B
Oxoid	Ciprofloxacin Antimicrobial Susceptibility Test Disks	CT0425B

2.1.3. Instruments

Devices and machines that are stated in Table 2.3. were used as the instrumental equipment for performing the experiments:

Table 2.3. Brand names and catalog numbers of the instruments used in the experiments

Brand Name	Item	Model/Catalog No
Arçelik	Fridge (+4°C /-18°C)	N/A
VWR	-80°C Freezer	N/A
New Brunswick	CO_2 Incubator	Galaxy 170R
JSR	Shaker Incubator	JSSI-300
Beckman Coulter	Allegra X-30R Centrifuge	B06320
WiseBath	Water Bath	DHWB000106
Thermo Scientific	Varioskan Flash Plate Reader	N06354
Precisa	Precision Balance	EP 220 A
ALP	Autoclave	CLG-32L
Dragon Lab	Vortex Mixer	MX-S
Eppendorf	Thermomixer	Compact 5350
Thermo Scientific	Nanodrop 2000 Spectrophotometer	ND-2000
BIO-RAD	TC20 Automated Cell Counter	1450102
HP	Desktop PC	8200/P201
Labconco	Biosafety Cabinet	Logic+
Biobase	Sterile Cabinet	PCR-01
Roche	Light Cycler 96	05815916001
Eppendorf Research	Micropipettes 0.5 - 10 ul, 2 - 20 ul, 20 - 200 ul, 100 - 1000 ul	2231300006
OLYMPUS	Phase Conntrast Microscope	CKX41
MSHOT	Microscope Camera	CMOS MD50
VARIAN	NMR Spectrometer	Anova Unity 500 MHz

2.1.4. Bacterial and Animal Cells

Bacterial strains and the animal cell line used in the study are shown in Table 2.4.

Table 2.4. Bacterial strains and the fibroblast cell line used in cell culture experiments

Brand Name	Item	Catalogue Number
ATCC	Mouse Embryonic Fibroblast Cells (NIH/3T3)	CRL-1658
ATCC	*Escherichia coli*	8739
ATCC	*Staphylococcus aureus*	6538

2.1.5. Primers

Primers used in quantitative RT-PCR experiments were kind gifts from Assist. Prof. Dr. Yuk Yin Ng. Nucleotide sequences of the primers were as shown in Table 2.5.

Table 2.5. Sequences of forward and reverse primers used in QRT-PCR assays

Gene	Primer Sequence
Mmp9	Forward: 5'- gagacgggtatcccttcgac -3' Reverse: 5'- acgatgacgagttgtggtcc -3'
Wnt4	Forward: 5'- tgtacctggccaagctgtc -3' Reverse: 5'- gaaactcaagggcctgatcc -3'
β-cat	Forward: 5'- agctgaccagctctctcttca -3' Reverse: 5'- gctgatcttggacttgatattgg -3'
Abl	Forward: 5'- tggagataacactctaagcataactaaaggt -3' Reverse: 5'- gatgtagttgcttgggaccca -3'

2.2. *IN VITRO* EXPERIMENTS

The methods that were followed in the *in vitro* experiments are explained below:

2.2.1. Cell Culture

NIH/3T3 cells (mouse embryonic fibroblast cells, ATCC, CRL-1658) were cultured with 4.5 g/L glucose DMEM (Gibco) supplemented with 10% FBS and 1% Penicillin/Streptomycin. Culture media is changed in every 2 days and cells were regularly subcultured to a new flask when they reached 80-90% confluency.

2.2.2. MTS Assay

Stock solutions of Lactoferrin and Lysozyme were prepared by dissolving in complete DMEM at a concentration of 3.2 mg/mL. After being filtered through a 0.2 μm filter (Sartorius AG, Göttingen, Germany), further dilutions (400 μg/mL, 200 μg/mL) of both lactoferrin and lysozyme were prepared in complete DMEM. Optimal concentrations for combining lactoferrin and lysozyme on viability of NIH/3T3 cells were investigated by the MTS assay (CellTiter96 Aqueous One Solution; Promega, Southampton, UK) according to the manufacturer's instructions. Briefly, NIH/3T3 cells were seeded in 96-well plates (Costar Corning, Rochester, NY) at a concentration of 5×103 cells/well and incubated overnight at 37 ºC with 5% CO_2. The old media was replaced by complete DMEM (100 μl/well) containing freshly prepared reagents at different concentrations and cells were incubated at 37 ºC with 5% CO_2 for 24 hours. 20 μl of MTS reagent was placed in each well and a further 3 hours incubation at 37 ºC with 5% CO_2 was performed. Then, the absorbance values at 490 nm were measured using a 96-well plate reader.

2.2.3. MTT Assay

Stock solutions of Lactoferrin and Lysozyme were freshly prepared by dissolving in complete DMEM at a concentration of 3.2 mg/mL. After being filtered through a 0.2 μm filter (Sartorius AG, Göttingen, Germany), further dilutions (800, 400 and 200 μg/mL) of

both Lactoferrin and Lysozyme were prepared in complete DMEM. Optimal concentrations for combining Lactoferrin and Lysozyme on viability of NIH/3T3 cells were investigated by the MTT assay according to the manufacturer's instructions. Briefly, NIH/3T3 cells were plated on a 96-well plate (Costar Corning, Rochester, NY) as 100 µl/well, at a concentration of 5×103 cells/well and incubated overnight at 37 ºC with 5% CO_2. The next day, freshly prepared reagents at different concentrations were added to the cells (100 µl/well) and incubated at 37 ºC with 5% CO_2 for 24 hours. The next day, 100 µl of media was removed and 10 µl of MTT reagent (5 mg/ml) was placed in each well and a further 3 hours incubation at 37 ºC with 5% CO_2 was performed. Then, 50 µl was removed and 100 µl DMSO was added to dissolve MTT. Plate was incubated at room temperature for 45 minutes by shaking at 400 rpm in the dark and the absorbance values at 570 nm were measured using a 96-well plate reader.

2.2.4. Transwell Migration Assay

For transwell migration assay, NIH/3T3 cells (mouse embryonic fibroblast cells, ATCC, CRL1658) were trypsinized and resuspended in complete DMEM. After centrifugation, cells were washed once with serum-free DMEM and centrifuged again. Then, the cells were resuspended in serum-free DMEM and seeded on 24-well cell culture inserts placed in 24-well cell culture plates at a confluency of $5x10^4$ cells/insert in 100µl DMEM. Lactoferrin from human milk and chicken egg white lysozyme were dissolved freshly in complete growth media (4.5 g/L glucose DMEM (Gibco) supplemented with 10% FBS and 1% Penicillin/Streptomycin) as 2 mg/ml and filtered through 0.2µm filters prior to use. Further dilutions of lactoferrin and lysozyme solutions were prepared by serial dilution. 400µg/ml and 200µg/ml of lactoferrin and lysozyme respectively, and their combinations placed in the lower chambers of the 24-well plate. As control, DMEM with 10% FBS was used in the lower chamber. All samples were prepared in triplicates. For migration, the cells were incubated at 37º with 5% CO_2 for 6 or for 18 hours. Then, cell culture inserts were washed once with PBS and both migrated and non-migrated cells were fixed with 100% ice-cold methanol for 15 minutes at -20ºC. Then, insert membranes were air dried and the cells were stained with 10% Giemsa staining solution for 1 hour at room temperature. Membranes were washed twice with distilled water and the non-migrated cells on the upper sides of the membranes were removed using cotton swabs.

Inserts were placed on microscope slides and migrated cells were counted at 200X magnification in 5 random fields/insert (Fields were chosen from the upper, lower, left, right and the middle parts of each insert) and pictures were taken at 100X or 200X magnification.

2.2.5. Scratch Wound Healing Assay

Stock solutions of lactoferrin from human milk and chicken egg white lysozyme were freshly prepared by being dissolved in high glucose DMEM with 1% FBS at a concentration of 1.6 mg/ml. After being filtered through a 0.2 μm filter (Sartorius AG, Göttingen, Germany), further dilutions (400 and 200 μg/ml respectively) of lactoferrin and lysozyme were prepared in DMEM with 5% FBS. Previously determined active concentrations of lactoferrin and lysozyme were tested on NIH/3T3 cells by scratch assay. Briefly, NIH/3T3 cells were plated on a 24-well plate (Costar Corning, Rochester, NY) in triplicates as 500 μl/well, at a concentration of 5×10^4 cells/well and incubated overnight at 37 ºC with 5% CO_2. The next day, a scratch was made on each well using a 10 μl pipette tip. Then, the wells were washed once with PBS and the media was changed with the media containing freshly prepared reagents at different concentrations (500 μl/well) and incubated at 37 ºC with 5% CO_2 for 24 hours. Pictures of the scratches were taken by MShot CMOS microscope camera at 0, 16, 20 and 24 hours of incubation (only 0 and 24 hours are shown in the results). The images were analyzed by ImageJ software.

2.2.6. Quantitative RT-PCR

Firstly, NIH/3T3 cells were seeded on 6 well plates with a confluency of $2x10^5$ cells and treated with 400 μg/ml of lactoferrin and/or 200 μg/ml lysozyme dissolved in complete DMEM. After 24 hours of incubation, total RNA was purified from each experimental group using a commercial kit (GeneMark) according to the manufacturer's instructions. Shortly, cells were lysed in lysis solution and an equal volume of 70% ethanol was added. Then, the mixture was transferred into an RNA Spin Column and centrifuged at top speed for one minute. The membrane was washed with RNA wash solutions I and II respectively, and residual ethanol was removed by an additional one minute spin. The column was placed in a fresh microcentrifuge tube and 40 μl of RNase-free water was used for elution.

Concentrations of the RNA samples were determined by NanoDrop. iScript cDNA Synthesis Kit (BIO-RAD) was used for cDNA synthesis before quantitative RT-PCR. 1 µg of total RNA was added to 4 µl reaction mix and 1 µl reverse transcriptase enzyme. Total volume was completed to 20 µl with nuclease-free water. The mixture was incubated in a thermal cycler according to the protocol given in Table 2.6.

Table 2.6. Protocol used for cDNA synthesis

Priming	5 min at 25ºC
Reverse transcription	20 min at 46ºC
RT inactivation	1 min at 95ºC
Optional step	Hold at 4ºC

Synthesized cDNAs were used in quantitative RT-PCR with iTaq Universal SYBR Green Supermix (BIO-RAD). According to the manufacturer's instructions, 10 µl of 2X Supermix was mixed with 1 µl of each primer (forward and reverse primers with a 10 µM of working concentration), 5 µl of cDNA and 3 µl dH_2O for each reaction. Reaction mixtures were prepared in duplicates for each of matrix metalloproteinase 9 (Mmp9), wingless-related integration site 4 (Wnt4), β catenin (β –cat) genes and also for abelson tyrosine-protein kinase (Abl) as the housekeeping gene. The following PCR protocol (see Table 2.7.) was run on Roche Light Cycler for quantitative analysis of the mRNA expression levels of the respective genes. All materials and primers used in quantitative RT-PCR were provided by Assist. Prof. Dr. Yuk Yin Ng from Istanbul Bilgi University as a kind gift. :

Table 2.7. Reverse transcription PCR protocol

Preincubation	50ºC for 120 s	1 Cycle
	95ºC for 600 s	
2 Step Amplification	95ºC for 15 s	40 Cycles
	60ºC for 60 s	

After PCR, mRNA expression levels were normalized to Abl as an internal reference and graphs were generated.

2.3. HYDROGEL PREPARATION

For preparing 20% (w/v) poloxamer hydrogel, Poloxamer 407 (Pluronic® F-127, Sigma) was dissolved in dH_2O in a beaker. It was dissolved by incubating first at -20 ºC for 1-2 hours, then it was placed at 4 ºC and left overnight to form a solution (Figure 2.1.). On the experiment day, 3% (w/v) sodium hyaluronate was prepared by dissolving in poloxamer hydrogel with vortexing shortly to prepare poloxamer-HA hydrogel. Depending on the experimental groups, 2% (w/v) lactoferrin or 1% (w/v) lysozyme were prepared freshly by dissolving in this poloxamer-HA gel.

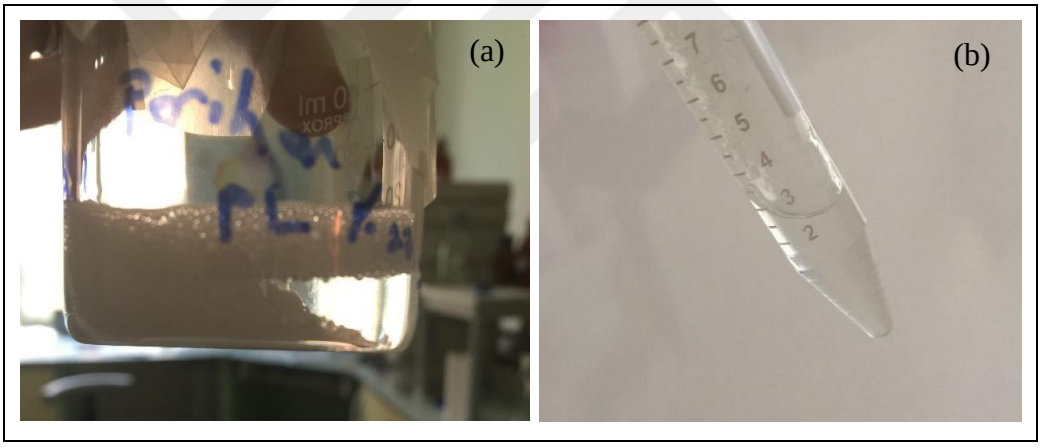

Figure 2.1. The images of poloxamer 407 (a) before and (b) after incubations at -20 ºC respectively

2.4. AGAR DISK DIFFUSION ASSAY

Bacterial strains *Escherichia coli* (*E. coli*) (ATCC, 8739) and *Staphylococcus aureus* (*S. aureus*) (ATCC, 6538) were kind gifts from Assist. Prof. Dr. Özgür Gül from Istanbul Bilgi University. Antimicrobial activity tests were performed by inoculating 100 µl of bacterial suspension containing 10^8 CFU/ml of bacteria on nutrient agar. Whatman filter paper disks with a diameter of 6 mm were prepared under aseptic conditions by adding 20 µl of 20% Pluronic® F127 hydrogels with or without lactoferrin/lysozyme on each disk. When the

disks were dried, they were placed on agar plates that were inoculated with either *E. coli* or *S. aureus*. 5µg ciprofloxacin or 1 µg oxacillin-containing ready-to-use disks were positioned at the center of the plates as controls for *E. coli* or *S. aureus* cultures, respectively. The inoculated plates were then incubated at 37 °C for 24 h. Antibacterial activity of the hydrogels and controls were observed and pictures of the plates were taken.

2.5. *IN VIVO* EXPERIMENTS

The methods that were followed in *in vivo* experiments were as follows:

2.5.1. Animal Care

Approval for the use of animals and the protocol was obtained from Yeditepe University Ethics Committee of Experimental Animal Use (YÜDHEK) (See Appendix A for the approval). Female Spraque-Dawley rats (8-12 weeks old, n=36) were fed ad libitum in a 12 hours light/dark cycle at room temperature during the experiment.

2.5.2. Excisional Wound Healing

For the creation of excisional wound models, rats were anesthetized by intraperitoneal xylazine hydrochloride (10 mg/kg) and ketamine hydrochloride (75 mg/kg) injection. Then, the dorsal hairs of the rats were shaved and cleaned with 70% ethanol and iodine solution. Full thickness excisional wounds were created using a 6 mm punch biopsy tool (Figure 2.2.). The wounds created were either left untreated, or treated with 30 µl of vehicle hydrogel (20% Pluronic® F127 with 3% Hyaluronic Acid), hydrogel containing lactoferrin (2%), hydrogel containing lysozyme (1%), hydrogel containing both lactoferrin (2%) and lysozyme (1%), or Madecassol® (Bayer) as control for 8 days (Figure 2.3.). Dimensions of the wounds were measured by a caliper as seen in Figure 2.4. and the pictures of the wounds were taken on days 0, 3, 5, 7 and 8. On day 8, animals were sacrificed and wound tissue samples were dissected for histopathological assessment.

Figure 2.2. Two rats with the wounds created on day 0

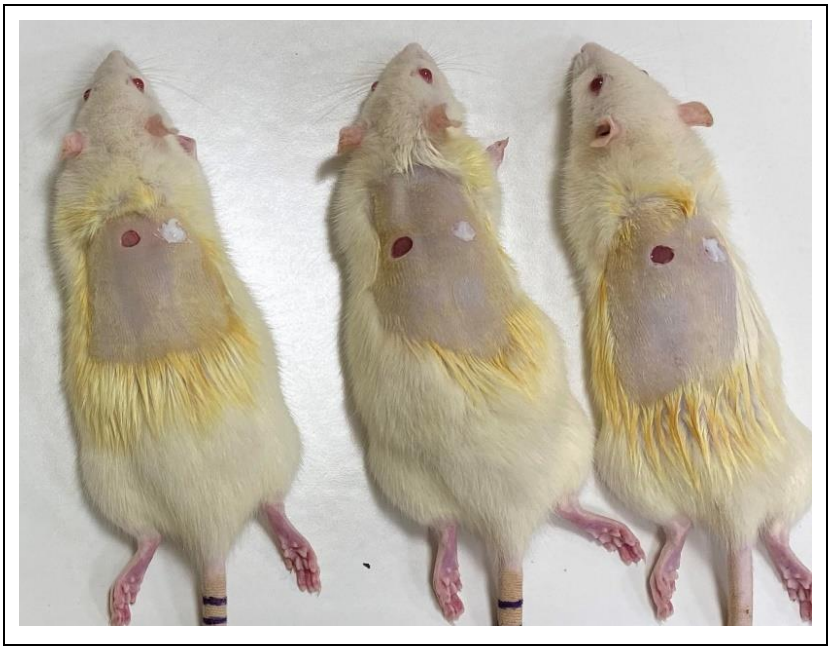

Figure 2.3. Rats with topically applied Madecassol® on one side on day 0

Figure 2.4. Measurement of wound dimensions by a caliper

2.6. HISTOPATHOLOGY

After excisional wound healing experiments, tissue samples dissected from each wound were further examined at Embryology Department at Yeditepe University for histopathological analysis.

2.6.1. Tissue Sampling, Fixation and Processing

After dissection, tissue samples were dipped into 10% neutral formalin at 4°C. Then, tissues were transferred to the tissue processor after being washed under running water for 1 hour. After following the tissue processing steps listed in Table 2.8., tissue samples were embedded in paraffin blocks (Paraplast®, Sigma-Aldrich).

Table 2.8. Experimental protocol followed for tissue processing

Step	Duration	Chemical
1	1 h	70 % ethyl alcohol
2	1 h	80 % ethyl alcohol
3	1 h.	90 % ethyl alcohol
4	1 h.	96 % ethyl alcohol
5	30 min	96 % ethyl alcohol
6	30 min	96 % ethyl alcohol
7	1.5 h	100 % ethyl alcohol
8	1.5 h	100 % ethyl alcohol
9	1 h	Xylene
10	1 h	Xylene
11	30 sec	Paraplast® (70 °C)
12	30 sec	Paraplast® (70 °C)

2.6.2. Tissue Sectioning and Staining

Tissue samples from each wound were sectioned with a 5 μm thickness and placed on microscope slides. Then, sectioned tissues were stained following the hematoxylin and eosin (HE) and Masson's trichrome staining methods indicated in Table 2.9 and Table 2.10.

Table 2.9. Hematoxylin and eosin staining protocol

Step	Duration	Chemical
Oven	15 min	
	3 min	Xylene
	3 min	Xylene
	5 min	Xylene
	2 min	100 % Ethyl alcohol
	2 min	96 % Ethyl alcohol
	2 min	96% Ethyl alcohol

Washing	2 min	
	1 min	Distilled water
	1.10 sec	Hematoxylin
Washing	1 min	
Washing	1 min	
	1 min	Acid Alcohol
Washing	1 min	
	0.10 sec	Ammonia
Washing	1 min	
	30 sec	96 % Ethyl alcohol
	1.20 sec	Eosin Y
	30 sec	96 % Ethyl alcohol
	30 sec	96 % Ethyl alcohol
	1 min	96 % Ethyl alcohol
	1 min	100 % Ethyl alcohol
	3 min	Xylene
	3 min	Xylene
	4 min	Xylene

Table 2.10. Masson’s trichrome staining protocol

Step	Duration	Chemical
Oven	15 min	
	3 min	Xylene
	3 min	Xylene
	5 min	Xylene
	2 min	100 % Ethyl Alcohol
	2 min	96 % Ethyl Alcohol
	2 min	70 % Ethyl Alcohol
	1 min	Distilled water

	4 min	Hematoxylin
	1 min	1 % Acid Alcohol
Washing	1 min	
	5 min	Acid Fuchsin
	1 min	Distilled water
	5 min	Phosphomolybdic acid
	6 min	Light Green SF Yellowish
	1 min	Distilled water
	2 min	1 % Acid Alcohol
	1 min	70 % Ethyl Alcohol
	1 min	80 % Ethyl Alcohol
	1 min	96 % Ethyl Alcohol
	1 min	100 % Ethyl Alcohol
	5 min	Xylene
	5 min	Xylene

2.6.3. Histopathological Analysis

Histopathological analysis was performed by determining damage and healing scores of the wound tissue samples under light microscopy, according to the parameters indicated in Table 2.11. and the pictures of tissue samples were taken.

Table 2.11. Parameters used for histopathological analysis

Healing Score	Damage Score
Absent: 0	Severe: 0
Mild: 1	Moderate: 1

Moderate: 2 Severe: 3				Mild: 2 Absent: 3	
Edema	Degeneration of Epithelium	Congestion	Mononuclear Cell Infiltration	Fiber Regeneration	Tissue Regeneration

2.7. NUCLEAR MAGNETIC RESONANCE (NMR) SPECTROSCOPY

In the study carried out by research group, poloxamer 407 hydrogel (20%) containing lactoferrin (2%) and lysozyme (1%) was prepared by dissolution as explained above. ^{1}H NMR was used to determine the interaction of proteins in the hydrogel formulation. Spectra were recorded at 500 MHz on a Varian spectrometer. Different spectra were obtained at various temperatures from 22 ºC to 37ºC and the analysis was repeated the next day with the same sample.

2.8. STATISTICAL ANALYSIS

GraphPad Prism software version 9.3.1 was used for the generation of the graphs and the statistical analysis of the results, which are shown as mean ± standard deviation (SD). One-way analysis of variance (ANOVA) test followed by Tukey's post-hoc test was performed for the analysis of the *in vivo* assays. For the analysis of *in vitro* assays, either t-test or one-way ANOVA (with Tukey's) was done and mentioned in the figure captions. P values less than 0.05 were accepted as significant.

3. RESULTS

Results obtained from *in vitro* and *in vivo* assays are explained below:

3.1. RESULTS OF *IN VITRO* EXPERIMENTS

MTS and MTT assays, transwell migration assay, scratch wound healing assay and quantitative RT-PCR were the *in vitro* experiments performed in this study and the results were as follows:

3.1.1. MTS and MTT Assays

In the very first attempts of evaluating effects of lactoferrin and lysozyme with Pluronic® F127 on viability of NIH/3T3 fibroblasts, various concentrations of lactoferrin and lysozyme were prepared in 20% Pluronic® F127. Then, wells of a 96-well plate were coated with lactoferrin or lysozyme containing F127 hydrogel or blank F127 hydrogel as control. A non-coated well was also used as a negative control. However, at the end of one-day incubation, MTS assay did not give consistent results (data not shown), which indicates that such an experimental setup with gelation of F127 is not suitable for evaluating effects of these molecules on cell viability *in vitro*.

Therefore, effect of various concentrations (400 μg/ml, 200 μg/ml, 100 μg/ml and 50 μg/ml) of lactoferrin and lysozyme on NIH/3T3 cell viability were examined separately for defining optimal concentrations that do not show any cytotoxicity, while having a positive effect on cell proliferation. As a result of MTS assay performed after 24 hours of treatment, viability of the cells treated with 400 μg/ml lactoferrin, 200 μg/ml lysozyme and 100 μg/ml lysozyme slightly increased, while other concentrations of lactoferrin and lysozyme having no significant effect on viability of NIH/3T3 cells (Figure 3.1.), indicating none of the tested concentrations show cytotoxic effect on these cells.

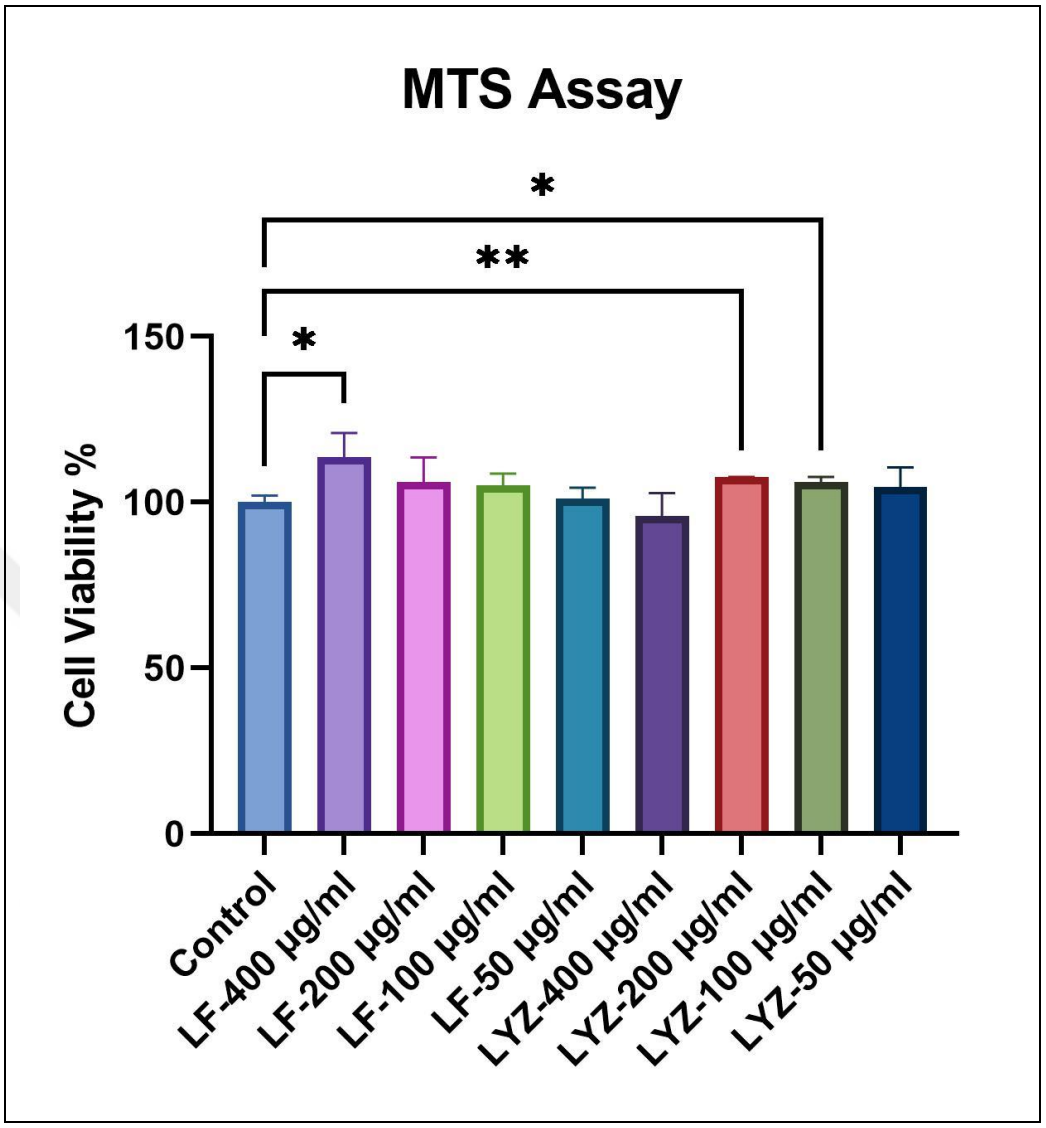

Figure 3.1. The effect of different concentrations of lactoferrin, lysozyme and their combinations on NIH/3T3 cell viability measured by MTS assay. Data represent the mean values±SD. Comparisons were performed by t-test. *p<0.05, **p<0.01

In order to double-check the results obtained by MTS, an MTT assay was also performed to reveal the effect of different concentrations of lactoferrin and lysozyme, and their combinations on the viability of NIH/3T3 fibroblasts. Consistent with the results obtained by the previous MTS assay, 200 µg/ml of lysozyme caused a significant increase in the viability of NIH/3T3 cells. Moreover, none of the tested concentrations of lactoferrin showed any cytotoxicity even though 400 µg/ml of lactoferrin failed in significantly inducing cell viability this time. (Figure 3.2.). In addition, although 800 µg/ml was the most and the only significantly effective concentration of lactoferrin in increasing cell viability individually, it

was not as much effective when combined with 200 µg/ml of lysozyme. Therefore, combination of 400 µg/ml of lactoferrin with 200 µg/ml lysozyme, which promoted cell viability significantly, was selected as the concentration to be tested in the following transwell migration assays.

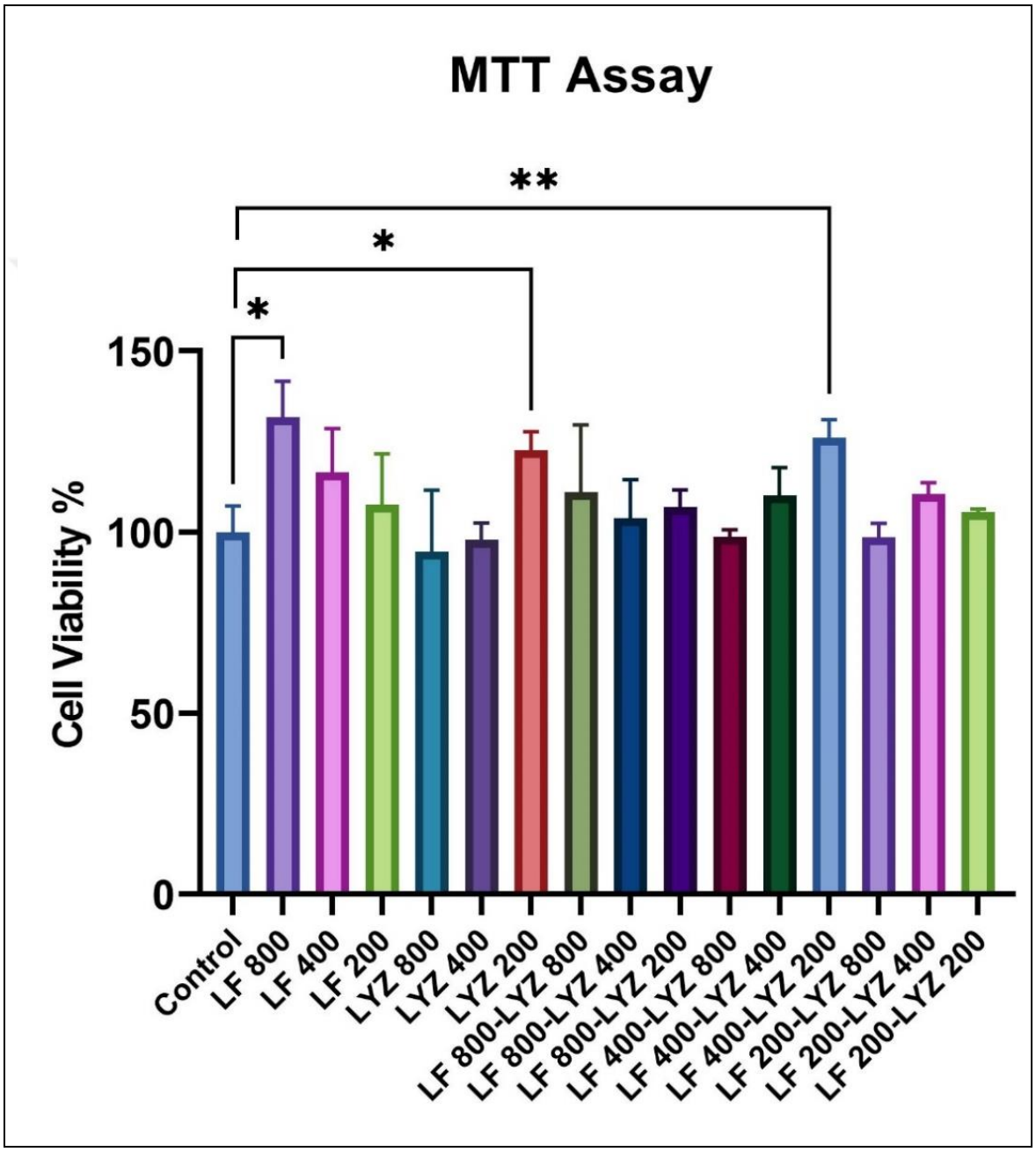

Figure 3.2. The effect of different concentrations of lactoferrin, lysozyme and their combinations on NIH/3T3 cell viability measured by MTT assay. Data represent the mean values±SD. Comparisons were performed by t-test. *p<0.05, **p<0.01

3.1.2. Transwell Migration Assays

In the first attempts of transwell migration assay, NIH/3T3 cells were seeded on the upper compartments of the transwell membranes at a confluency of $5x10^4$ cells/insert and they were allowed to migrate towards lactoferrin and/or lysozyme-containing DMEM in the lower compartments without addition of FBS. However, when there was no or low concentration (1%) of FBS in the lower compartments, the cells failed to migrate and no difference was observed between the experimental groups (data not shown). Therefore, lactoferrin and/or lysozyme were added into the lower compartments with the presence of 10% FBS in culture medium, in order to observe cell migration. At first, cells were incubated under these conditions for 6 hours. Although some cells migrated towards lactoferrin and lysozyme-containing wells, the number of the migratory cells was very low to evaluate the results (Figure 3.3.). Therefore, incubation time was increased to 18 hours in the next attempt.

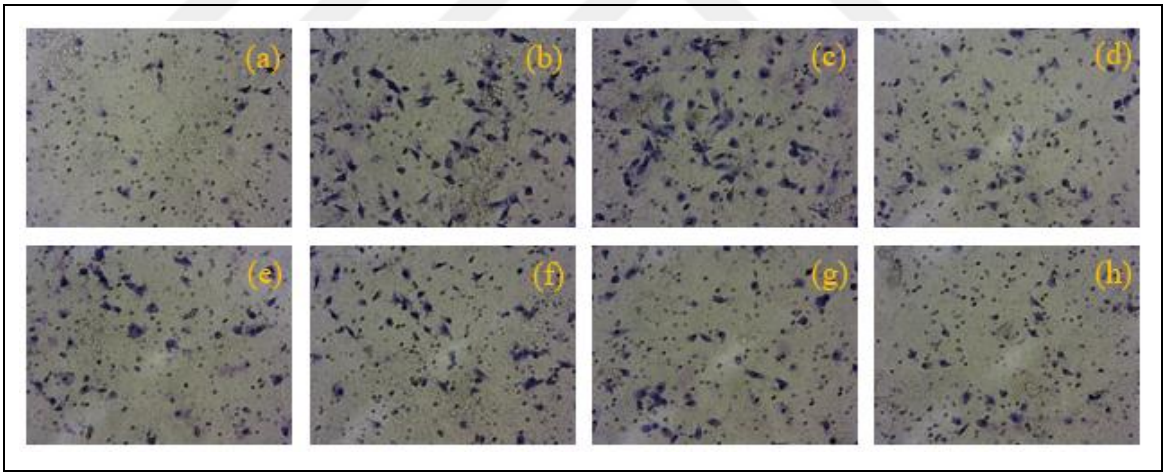

Figure 3.3. Representative images of transwell inserts after 6 hours of migration. Cells migrated towards (a) 10% FBS as control, (b) LF 400 µg/ml, (c) LF 200 µg/ml, (d) LYZ 400 µg/ml, (e) LYZ 200 µg/ml, (f) LF 200 µg/ml with LYZ 200 µg/ml, (g) LF 400 µg/ml with LYZ 200 µg/ml, (h) LF 200 µg/ml with LYZ 400 µg/ml. Images were captured at 200X magnification

As mentioned previously, treating cells with the combination of 400 µg/ml of lactoferrin and 200 µg/ml lysozyme resulted with the highest increase in cell viability (Figure 3.2.). Therefore, the effect of this combination on the migration of NIH/3T3 cells was tested

following 18 hours of incubation. This time, more cells migrated from upper compartments to the lower ones, which generated more consistent results. Although combined lactoferrin and lysozyme showed a slight chemotactic activity on NIH/3T3 fibroblasts, 200 µg/ml of lysozyme was more effective when applied individually. More interestingly, lactoferrin attenuated fibroblast migration slightly, but it was not a significant decrease when compared to the number of the cells that migrated towards the control medium. In other words, when transwell migration assay revealed that chicken egg white lysozyme has a chemoattraction effect on mouse fibroblasts, lactoferrin failed in showing such an activity. Moreover, lactoferrin modulated the effect of lysozyme when applied in combination with the selected concentrations (Figure 3.4. and Figure 3.5.).

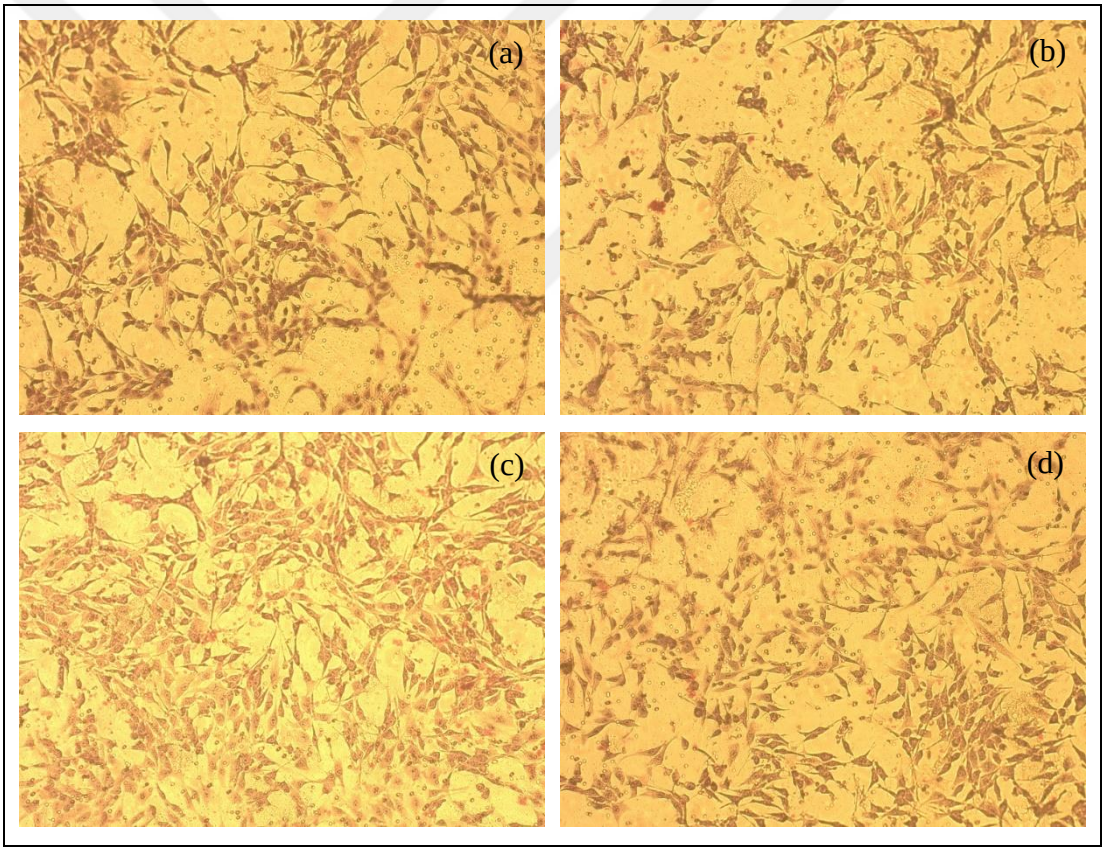

Figure 3.4. Representative images of transwell inserts after 18 hours of migration. Cells migrated towards (a) 10% FBS as control, (b) LF 400 µg/ml, (c) LYZ 200 µg/ml, (d) LF 400 µg/ml with LYZ 200 µg/ml. Images were captured at 100X magnification

In addition to the chemotactic activity, in order to reveal how migration of fibroblasts is affected following lactoferrin and/or lysozyme treatments, NIH/3T3 cells were also

incubated with lactoferrin and/or lysozyme in the upper compartment of the transwell membrane in the absence or presence of 1% FBS, when the lower compartment was containing culture medium with 10% FBS. However, under these conditions, cells failed to migrate through the transwell membrane and no difference was obtained between the experimental groups. Therefore, *in vitro* scratch wound healing assay was further utilized in order to analyze how fibroblast migration is affected when the cells are treated directly with the selected concentrations of lactoferrin and/or lysozyme.

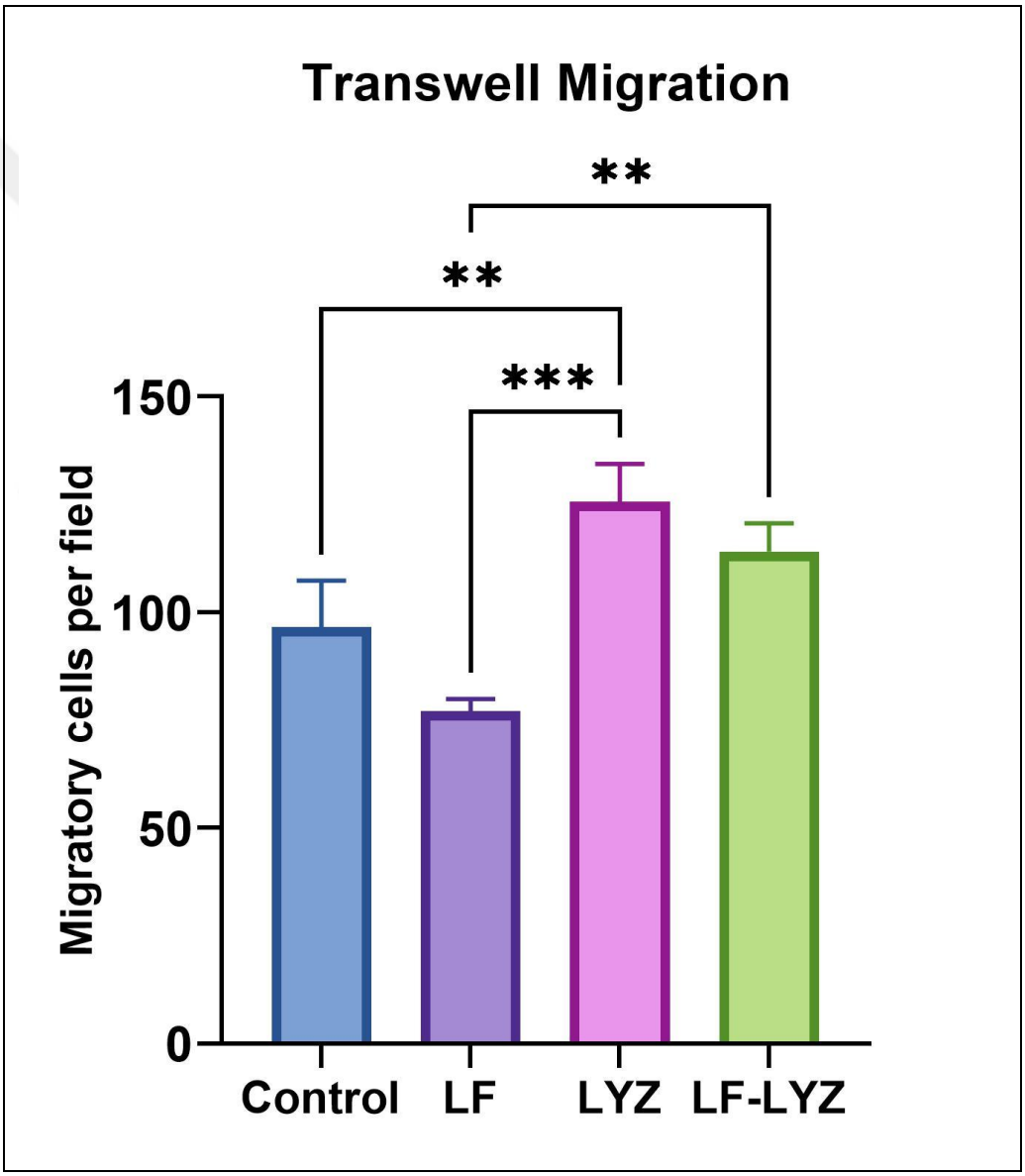

Figure 3.5. The number of NIH/3T3 fibroblast cells migrated towards lactoferrin, lysozyme, and their combinations determined by transwell migration assay. Data represent the mean values±SD. Comparisons were performed by one-way ANOVA followed by Tukey's post-hoc test. *p<0.05, **p<0.01, ***p<0.001

3.1.3. Scratch Wound Healing Assays

In order to test the effects of selected concentrations of 400 µg/ml lactoferrin and 200 µg/ml lysozyme on the migration of fibroblasts, a scratch wound healing assay was performed on NIH/3T3 cells. According to the results, both lactoferrin and lysozyme were able to induce migration of fibroblasts during 6, 18 and 24 hours of incubation. Although the LF-LYZ combination was the most effective and the only one with the significant effect during the first 6 hours, interestingly, it could not show the same effect at 18 and 24 hours when compared with the activity of lactoferrin and lysozyme individually. On the other hand, at the end of 24 hours of incubation, it was observed that individually applied lactoferrin and lysozyme significantly induced scratch wound healing of NIH/3T3 fibroblasts.

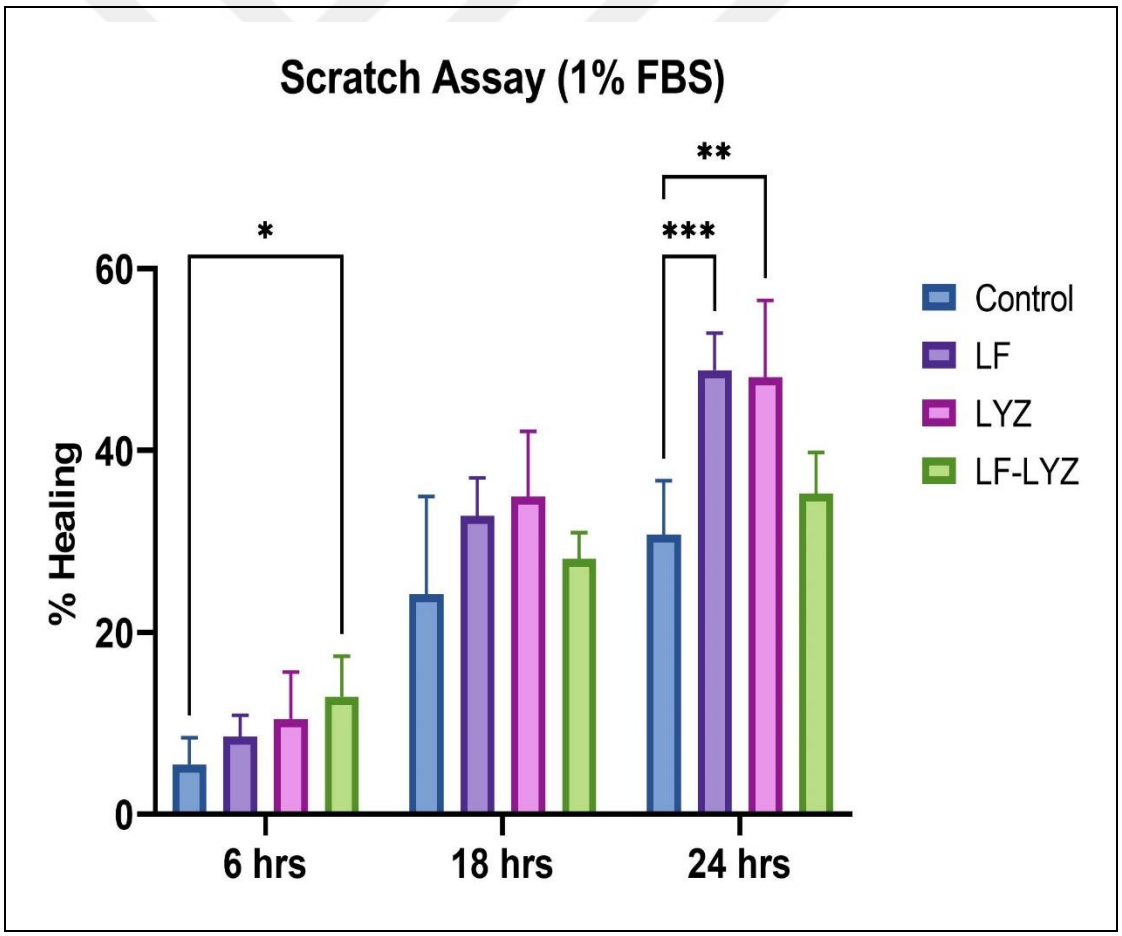

Figure 3.6. The effect of lactoferrin and/or lysozyme with 1% FBS on scratch wound healing of NIH/3T3 cells at different time intervals. Data represent the mean values±SD. Comparisons were performed by one-way ANOVA followed by Tukey's post-hoc test. *p<0.05, **p<0.01, ***p<0.001

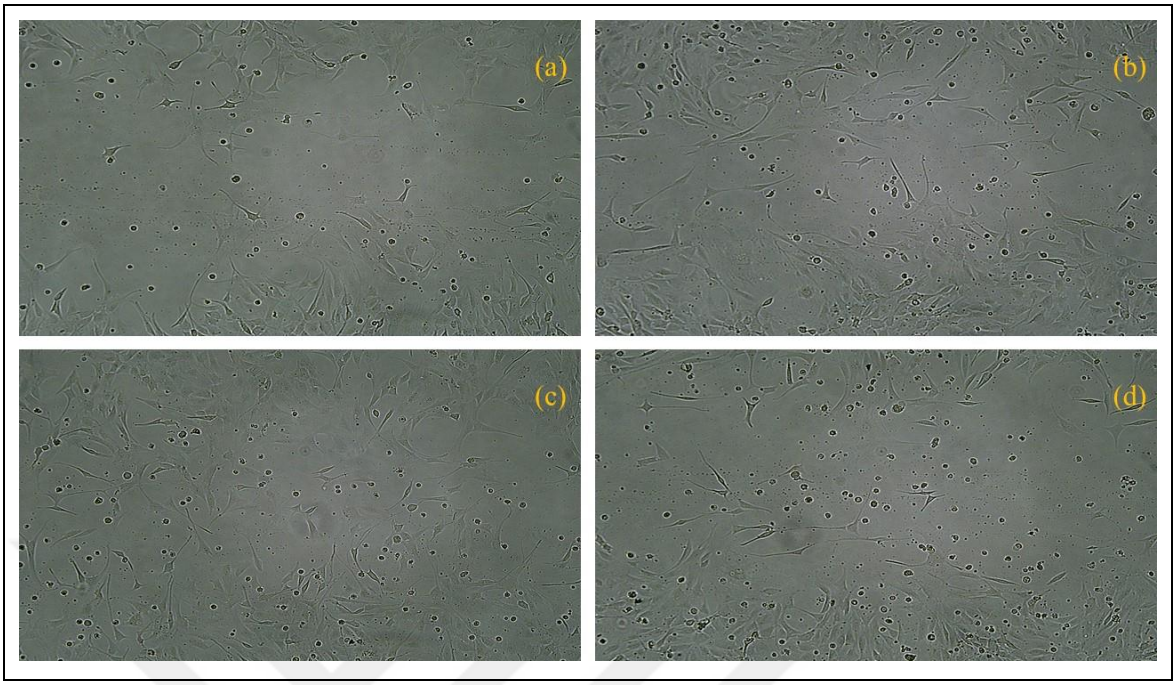

Figure 3.7. Dead cells floating on the scratches treated with (a) culture medium containing 1% FBS as control, (b) lactoferrin, (c) lysozyme, (d) both lactoferrin and lysozyme in culture medium containing 1% FBS

The cells were incubated until the scratch wounds were completely healed and it took at least 48 hours. However, measurements obtained from 48 hours of treatment were not included in Figure 3.6., which summarizes the results of this first scratch assay. As the cells were almost unable to survive with 1% FBS until the scratches heal completely (Figure 3.7.), the experiment was repeated with 5% FBS and more consistent results were obtained (Figure 3.8. and Figure 3.9.).

Although pictures of the scratches were taken at different time points (6 hours, 18 hours and 24 hours), as it took 24 hours for the scratches to heal and to show significant differences among experimental groups, only the images that were obtained after 24 hours were used for the analysis of percent healing (Figure 3.8.). According to these results, lysozyme was able to induce migration of fibroblasts individually or in combination with lactoferrin during 24 hours of incubation, even though lactoferrin could not increase fibroblast migration significantly. Moreover, the lactoferrin-lysozyme combination was the most effective one by almost doubling the healing rate when compared to the control (Figure 3.9.).

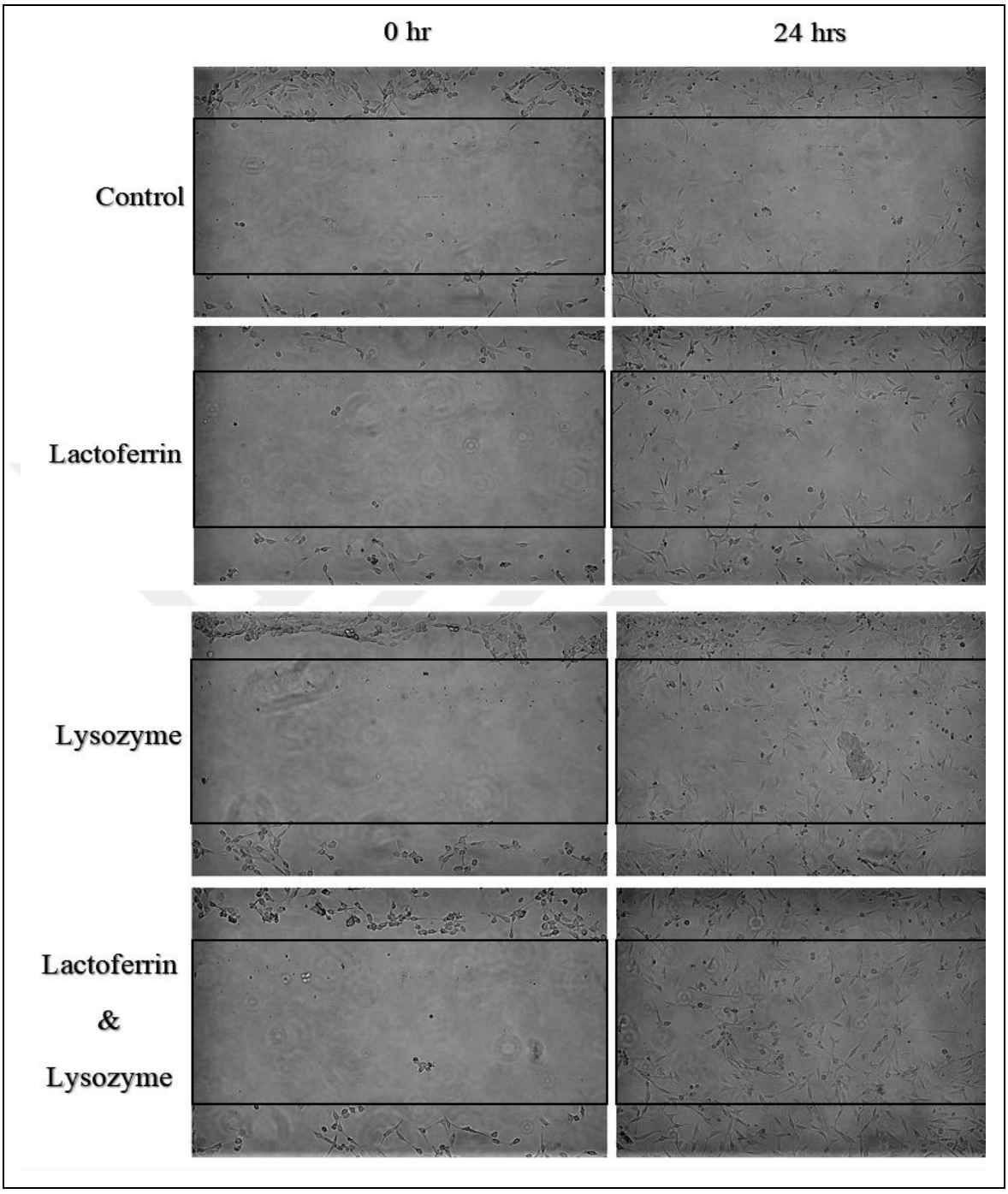

Figure 3.8. The effect of lactoferrin and/or lysozyme with 5% FBS on scratch wound healing of NIH/3T3 cells at different time intervals

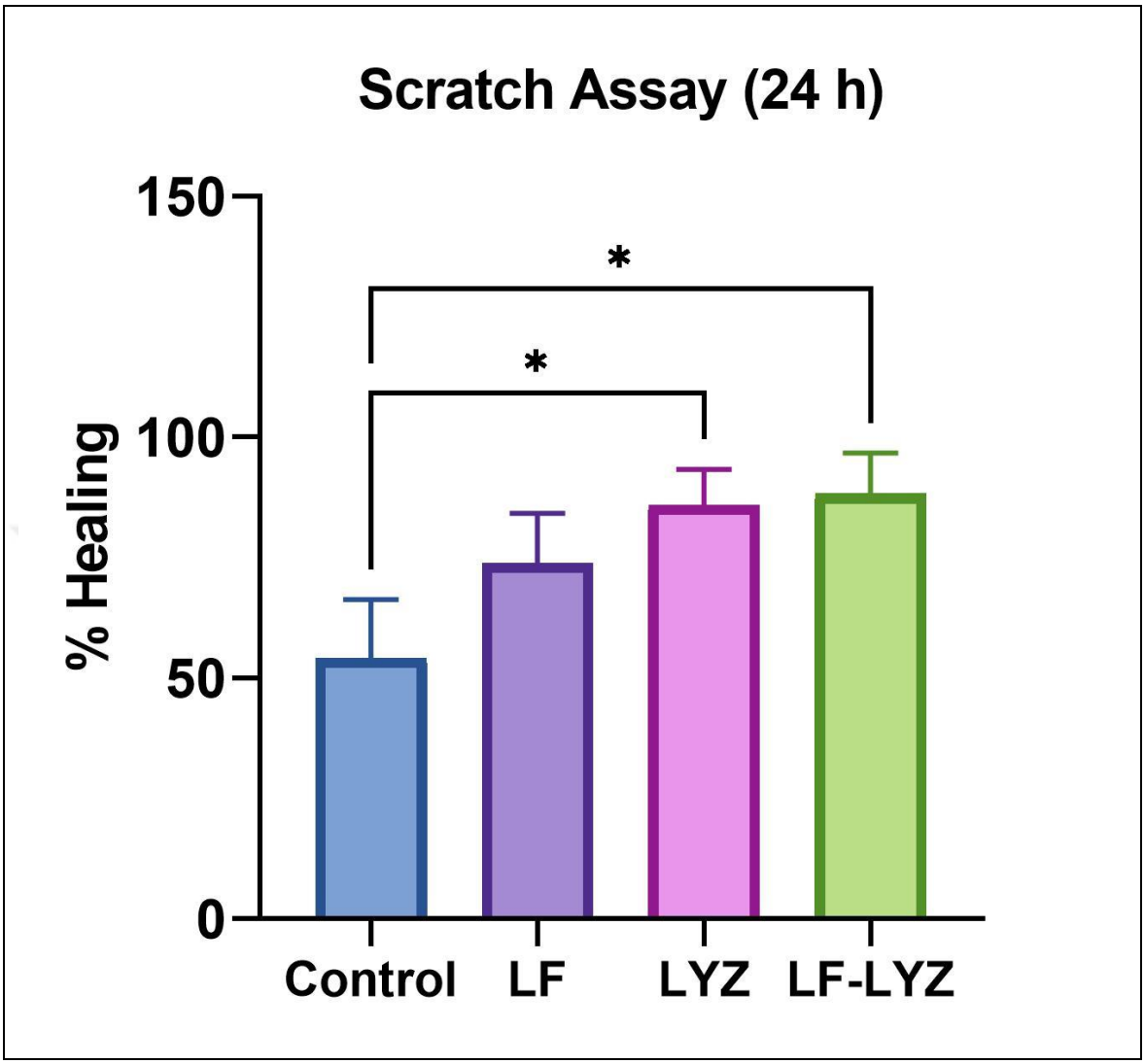

Figure 3.9. The effect of lactoferrin and/or lysozyme with 5% FBS on scratch wound healing of NIH/3T3 cells after 24 hours. Data represent the mean values±SD. Comparisons were performed by t-test. *p<0.05

3.1.4. Quantitative RT-PCR Results

NIH/3T3 fibroblast cells were treated with or without lactoferrin and/or lysozyme and QRT-PCR was performed to analyze how mRNA levels of Mmp9, Wnt4 and β-cat are affected by treatment with these two proteins. It was observed that lactoferrin was able to induce Mmp9 levels individually, while it failed to induce it when combined with lysozyme. By contrast, Wnt4 and β-cat levels have been increased the most, when lactoferrin and lysozyme were applied in combination. Interestingly, lysozyme showed a higher effect on β-cat than

lactoferrin, which may support the previous results obtained in scratch wound healing assay, in which lysozyme-treated cells showed a higher healing rate than the ones treated with lactoferrin.

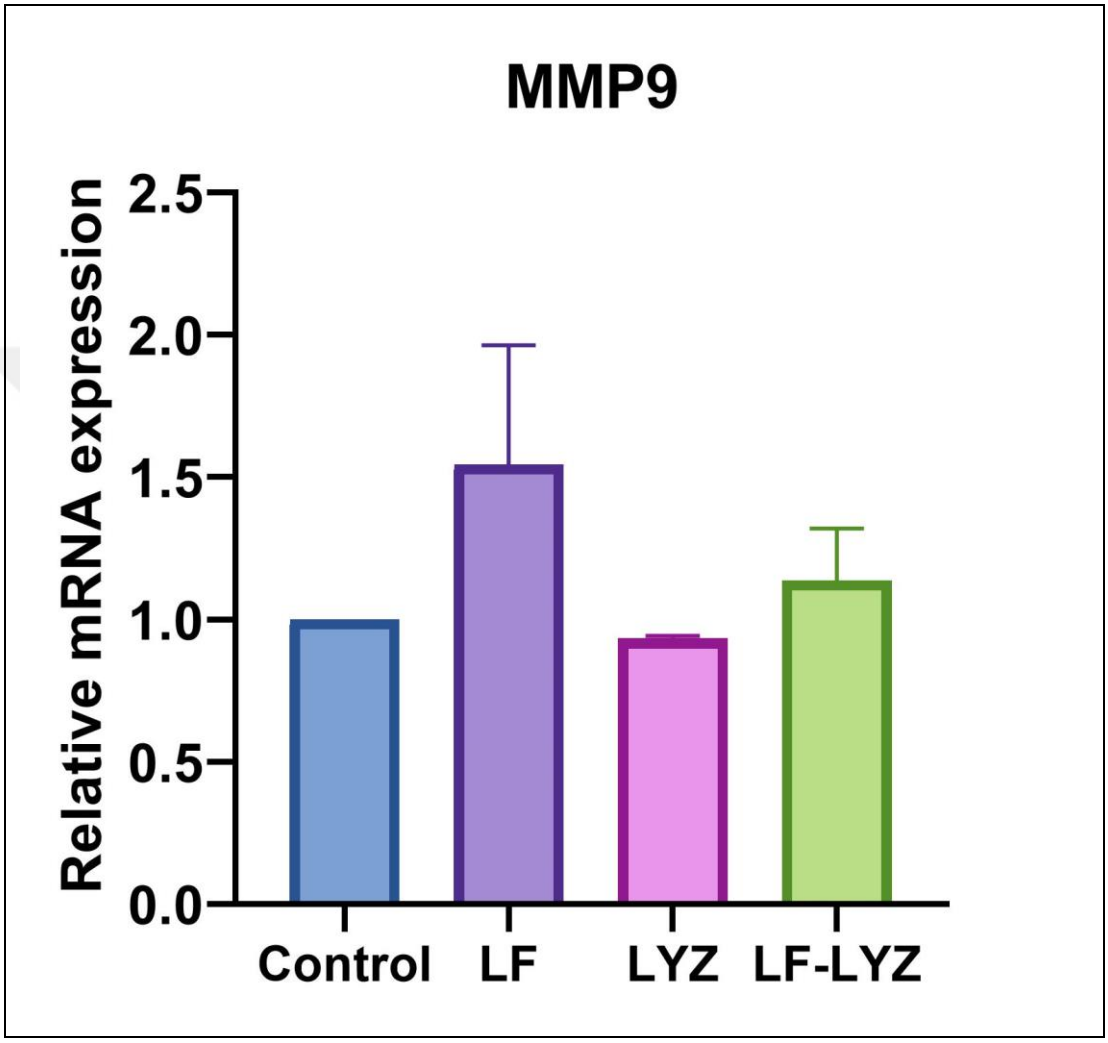

Figure 3.10. Relative mRNA expressions of Mmp9 in fibroblasts treated with lactoferrin and/or lysozyme

QRT-PCR results were statistically analyzed applying t-tests. However, only the increase in mRNA expression of Wnt4 in the cells treated with both lactoferrin and lysozyme, which was about 4.5-fold, was statistically significant when compared to the control (Figure 3.11.). On the other hand, no statistically significant increase or decrease in any of the tested mRNA levels were observed following the treatments with or without lactoferrin and/or lysozyme (Figures 3.10., 3.11. and 3.12.).

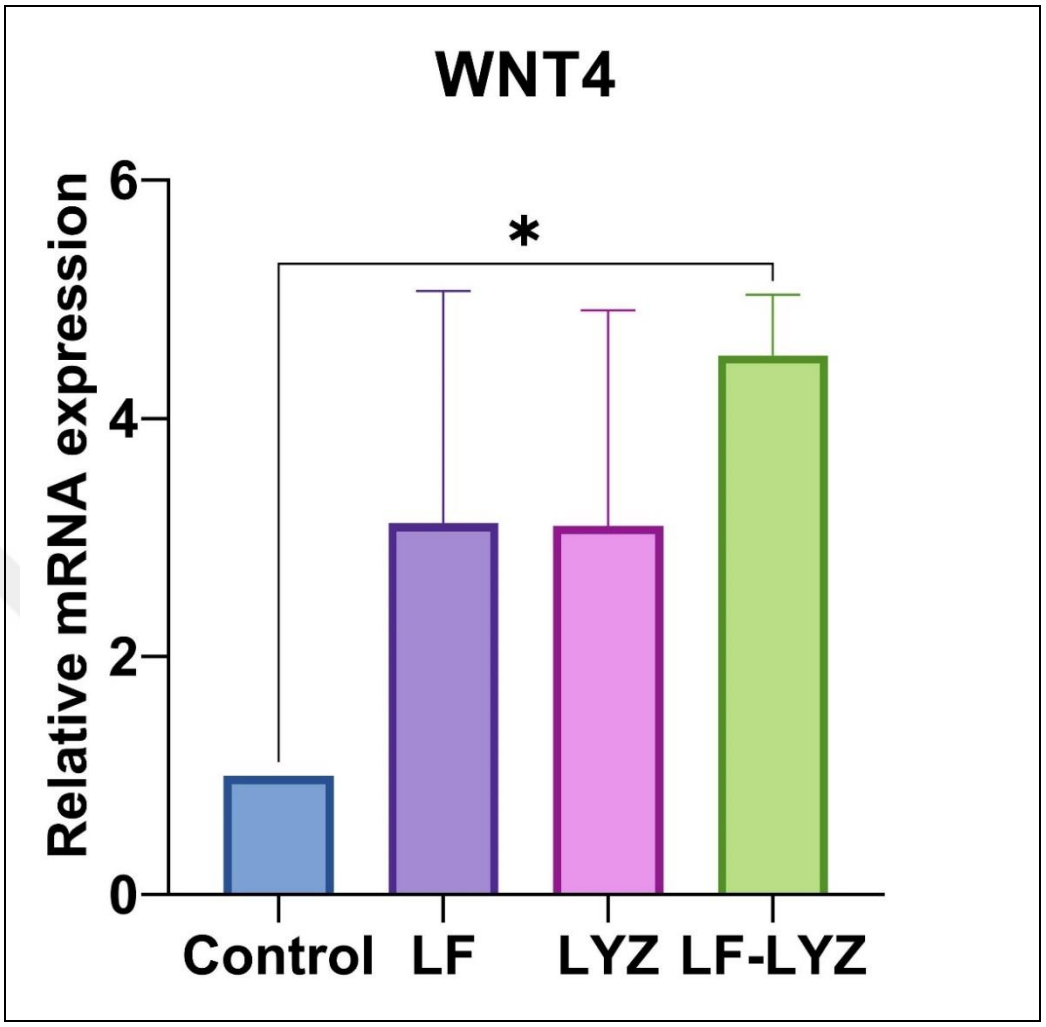

Figure 3.11. Relative mRNA expressions of Wnt4 in fibroblasts treated with lactoferrin and/or lysozyme. Data represent the mean values±SD. Comparisons were performed by t-test. *$p<0.05$

Even though QRT-PCR experiments were repeated for Mmp9, Wnt4 and β-cat, obtained results were not consistent with the results of the first trial. Therefore, results were not combined and only the mRNA levels obtained from the first duplicate results were used for the development of graphical images.

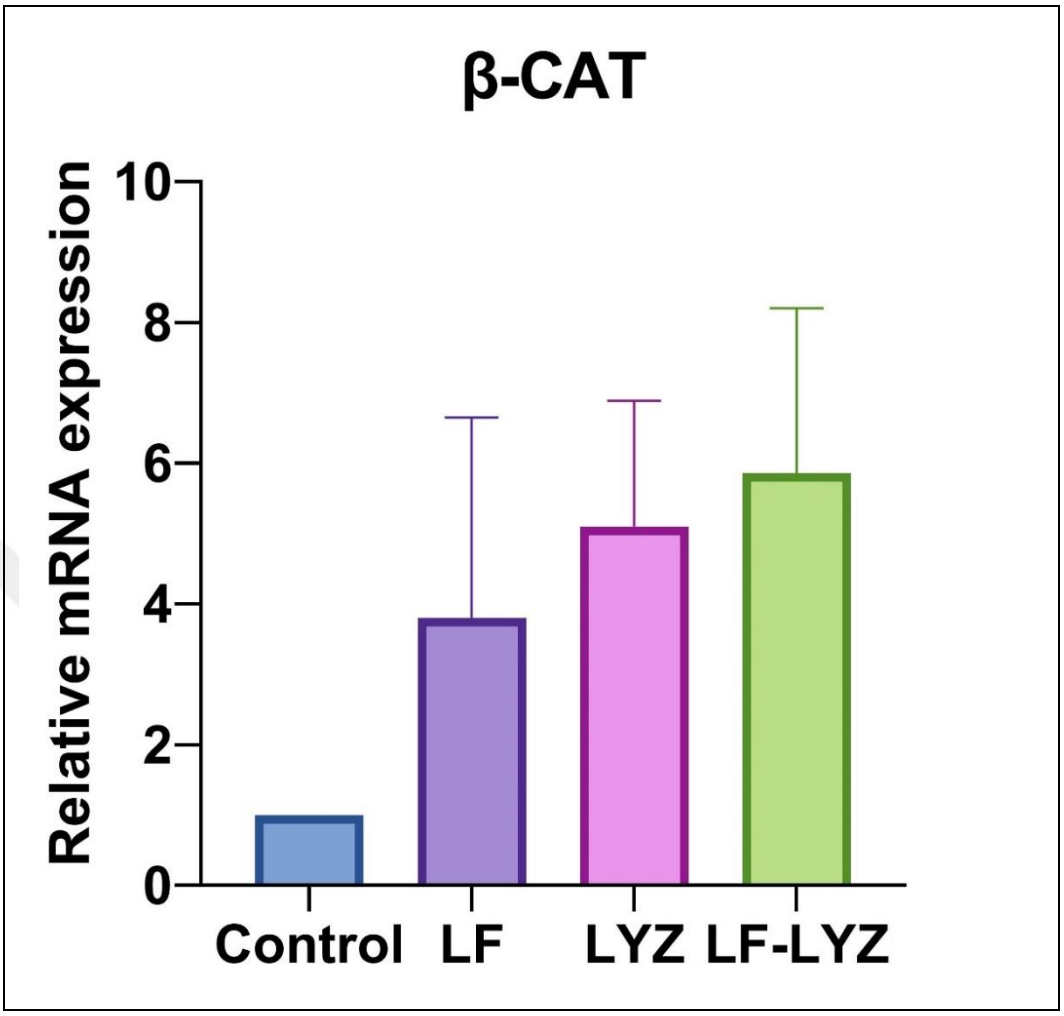

Figure 3.12. Relative mRNA expressions of β-cat in fibroblasts treated with lactoferrin and/or lysozyme

3.2. RESULTS OF DISK DIFFUSION ASSAY

Antibacterial activity of lactoferrin and lysozyme-containing Pluronic® F127 hydrogels were tested against *E. coli* and *S. aureus* by agar-well diffusion assay. Firstly, formulations were prepared in 20% Pluronic® hydrogel by dissolving lactoferrin and lysozyme having final concentrations of 400 µl/ml and 200 µl/ml respectively. However, as none of these formulations showed inhibitory activity against bacteria, experiment was repeated with 10% hydrogel concentration. Unfortunately, similar results were obtained, in which only the positive control (tetracycline hydrochloride) had an inhibition zone which was about 2 cm (Figure 3.13.).

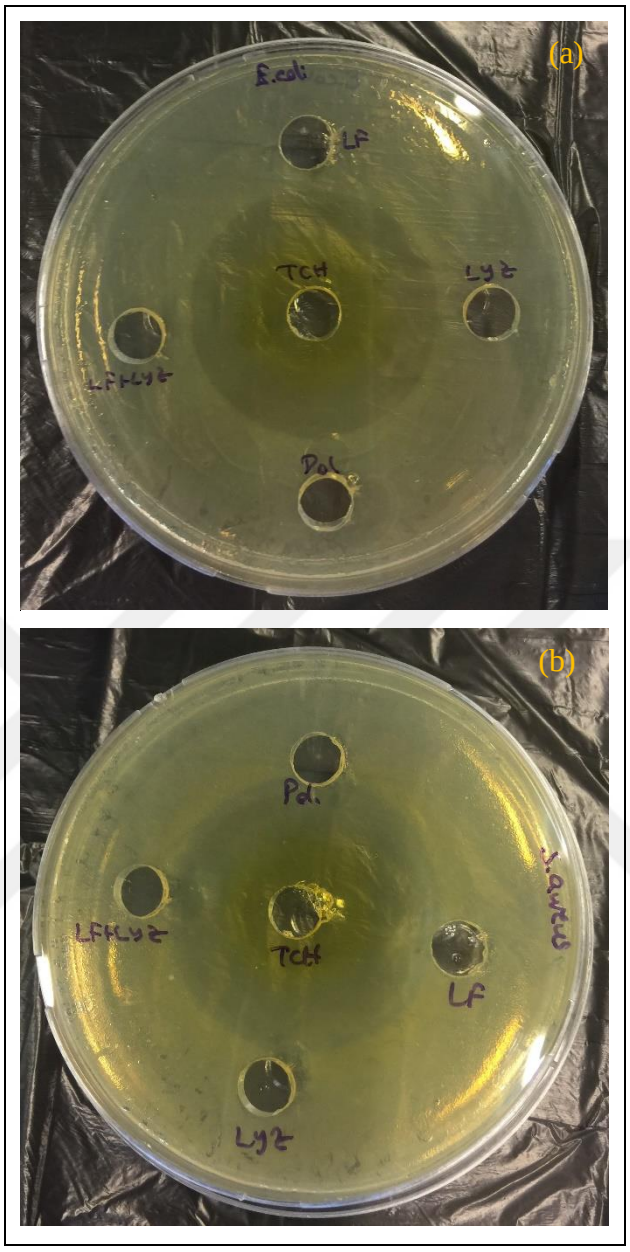

Figure 3.13. Agar well diffusion assay results showing the effects of blank hydrogel or hydrogel with lactoferrin and/or lysozyme against (a) *E. coli* and (b) *S. aureus*

Therefore, instead of an agar-well diffusion assay, disk diffusion assay was performed by preparing whatman paper disks containing 20% poloxamer-3% HA hydrogels with or without 2% lactoferrin and/or 1% lysozyme, in order to disclose the antibacterial activity of the hydrogels with the selected concentrations against *E. coli* and *S. aureus* bacteria, which are gram-negative and gram-positive respectively. As a result, unfortunately, it was observed that only the hydrogels not containing lysozyme were able to inhibit bacterial growth

slightly. Inhibition zones, however, were too small to be measured and analyzed, but images of the plates show the differences between groups clearly (Figure 3.14. and Figure 3.15.).

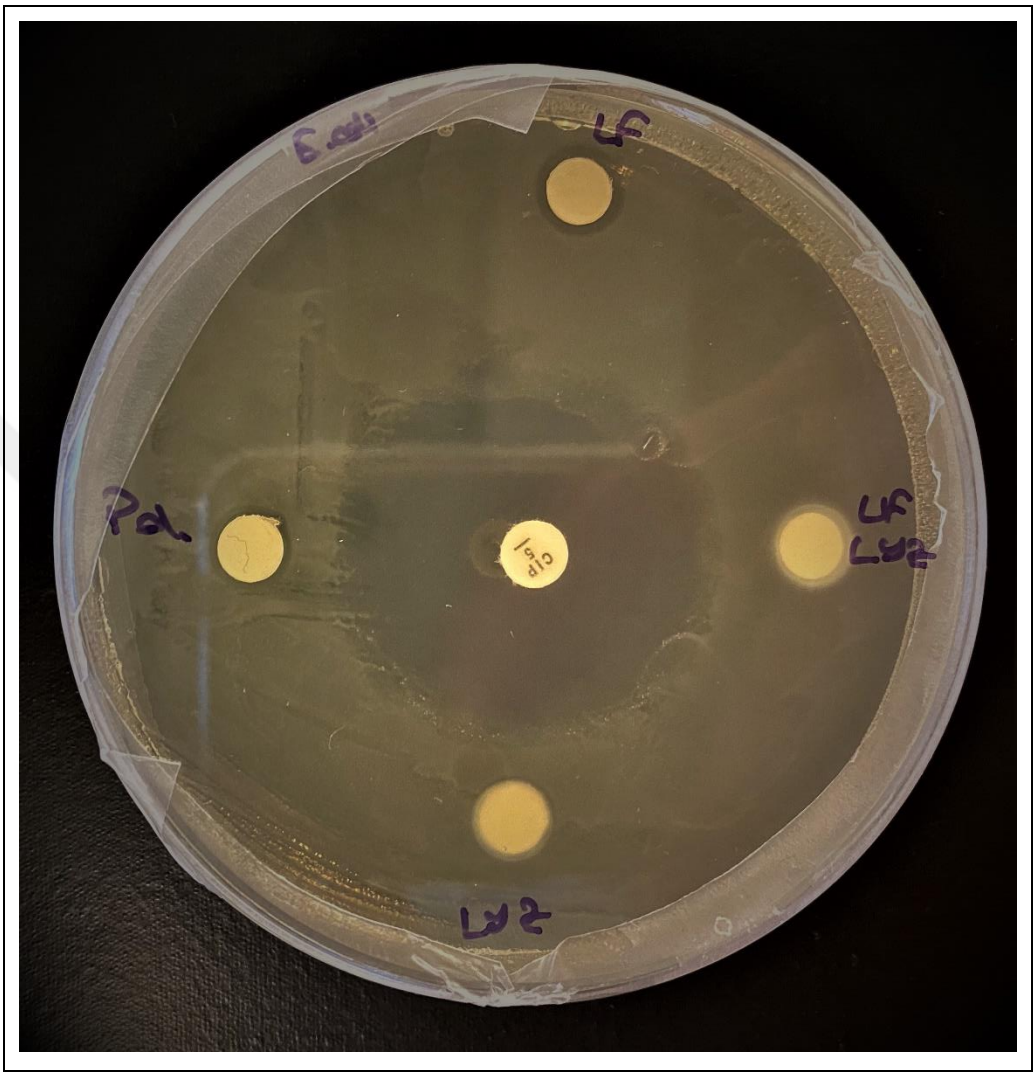

Figure 3.14. Disk diffusion assay result showing the effects of blank hydrogel or hydrogel with lactoferrin and/or lysozyme against *E. coli*

Interestingly, no antibacterial activity was observed with the disks containing only lysozyme or both lactoferrin and lysozyme, which indicates that all the antibacterial activity of the gel itself and the gel with lactoferrin are wiped out with the presence of lysozyme in the hydrogel.

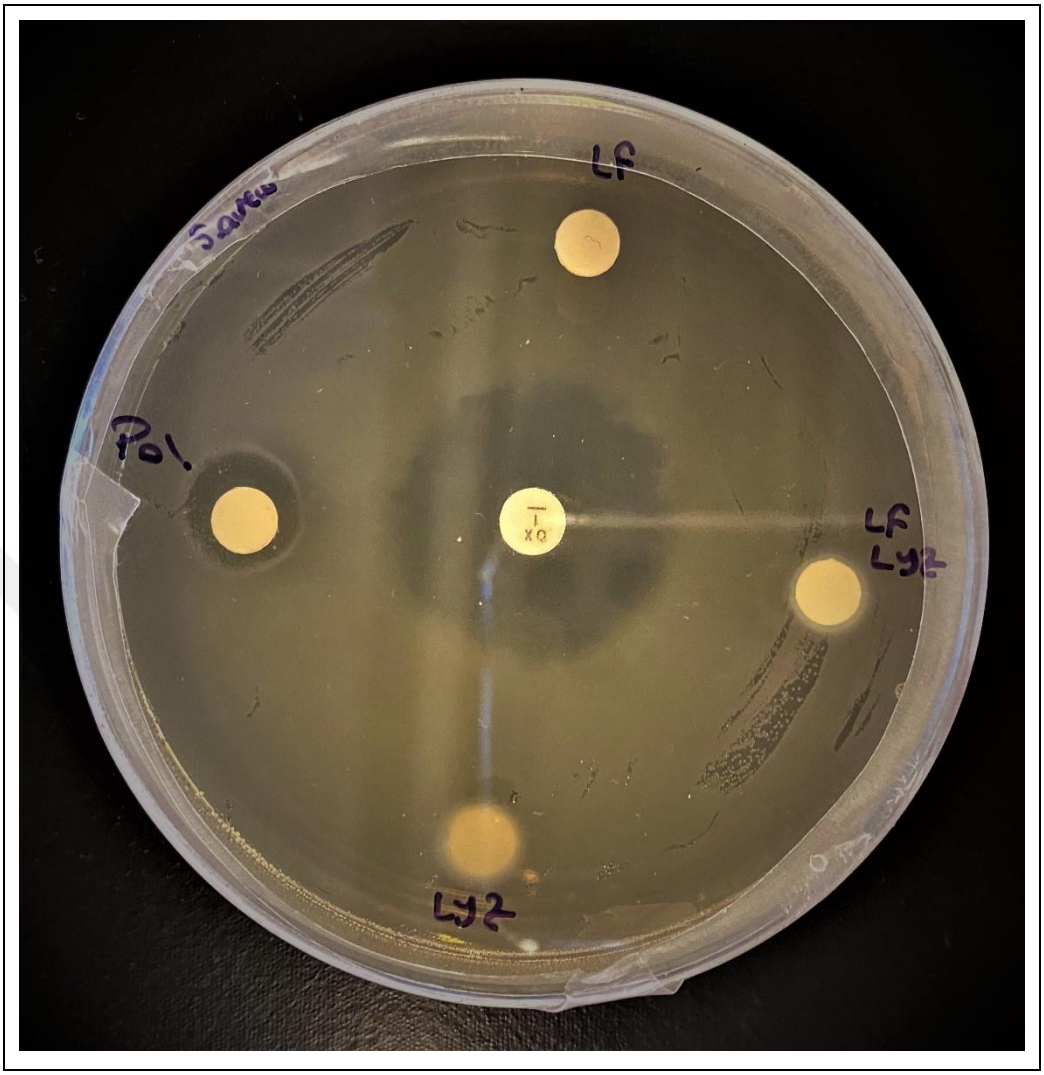

Figure 3.15. Disk diffusion assay result showing the effects of blank hydrogel or hydrogel with lactoferrin and/or lysozyme against *S. aureus*

3.3. RESULTS OF *IN VIVO* EXPERIMENTS

As *in vitro* experiments with fibroblasts revealed that the combinational application of lactoferrin and lysozyme may induce wound healing, poloxamer-HA hydrogel formulations containing either lactoferrin or lysozyme and their combination were developed and tested on rat excisional wound models. As expected, all the gel formulations, including the vehicle itself, induced wound healing from day 1 to day 8. Among these gel formulations, the one containing both lactoferrin and lysozyme was the most effective one when compared to the untreated control on day 8 (Figure 3.20.).

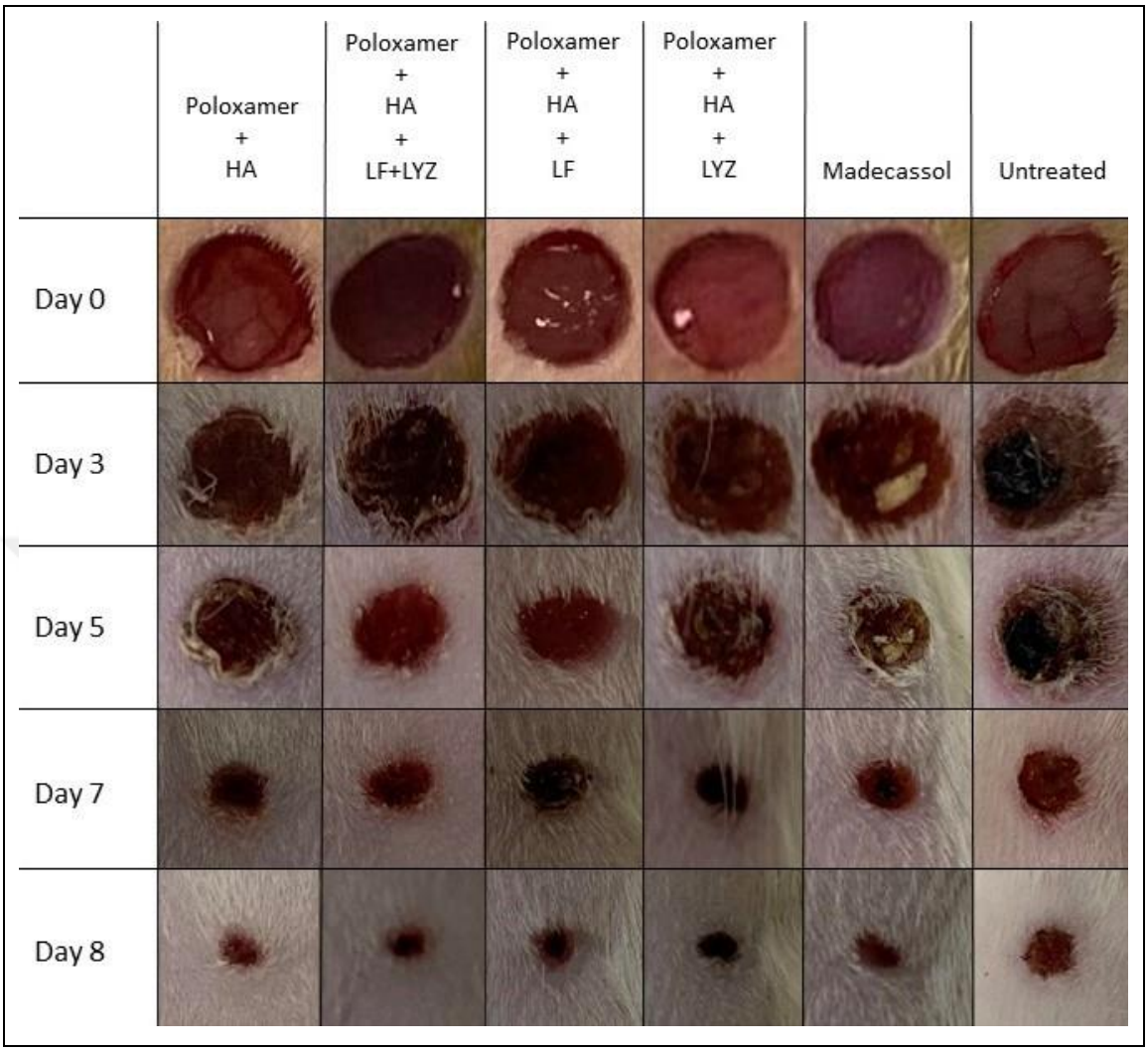

Figure 3.16. Representative images of wounds left untreated or treated with Madecassol®, blank hydrogel or hydrogel with lactoferrin and/or lysozyme at different time points

Wounds were treated with the hydrogels daily, and the dimensions of the wounds were measured before the pictures were taken on days 0, 3, 5, 7 and 8 (Figure 3.16.). Differences between the wound sizes of the experimental groups are graphically shown below as the wound area at different time points. On day 3, blank hydrogel showed the highest healing by means of the wound size. Even though the other treated wounds were also smaller than the untreated control, they were not statistically significant (Figure 3.17.).

On day 5, all treated wounds, except for the ones treated with hydrogel containing only lysozyme, showed better healing than the untreated control. However, interestingly, none of the hydrogels containing lactoferrin and/or lysozyme were able to significantly induce wound closure better than the blank hydrogel (Figure 3.18.).

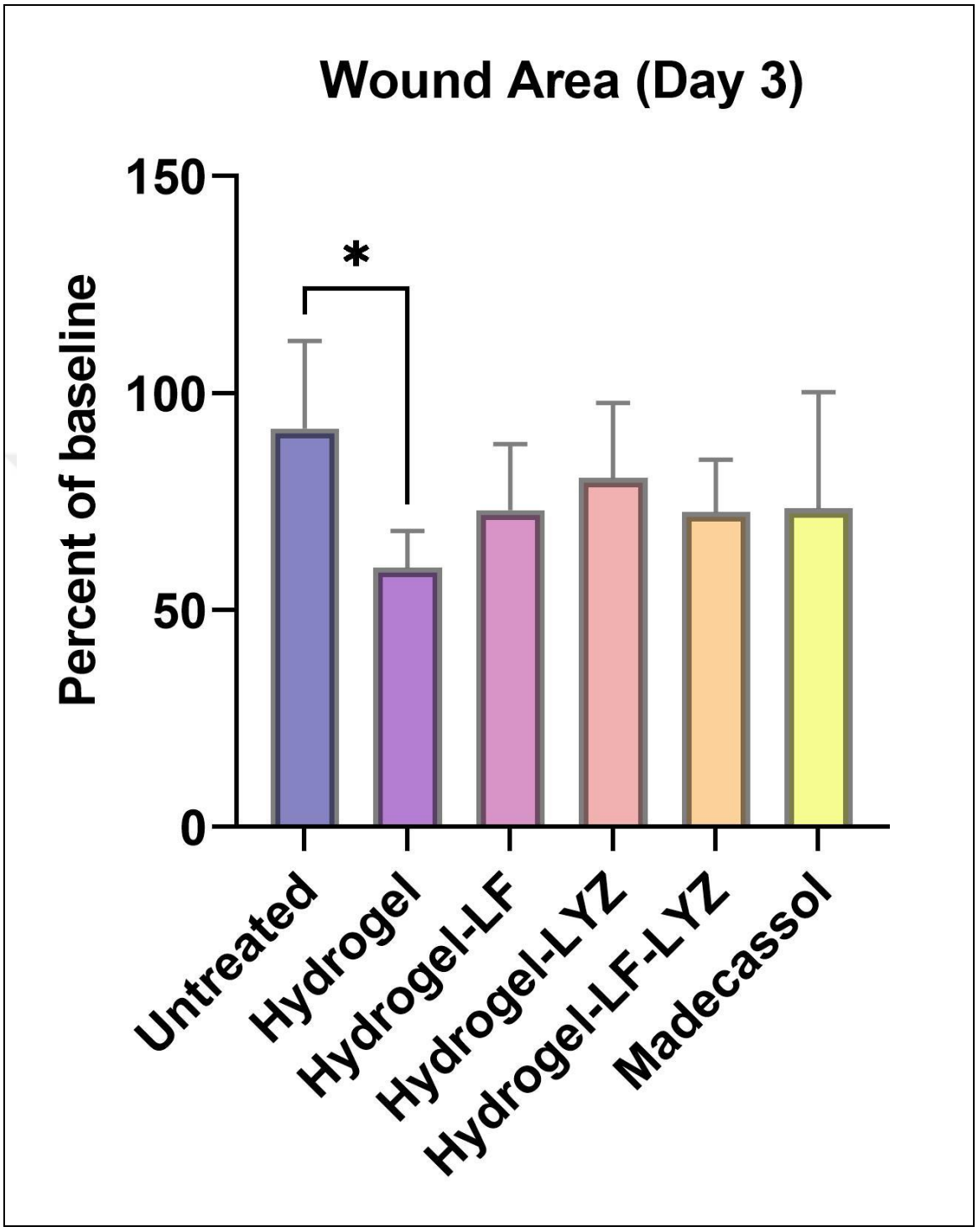

Figure 3.17. Healing of wounds left untreated or treated with Madecassol®, hydrogel or hydrogel with lactoferrin and/or lysozyme on day 3. Data represent the mean values±SD. Comparisons were performed by one-way ANOVA followed by Tukey's post-hoc test. *$p<0.05$

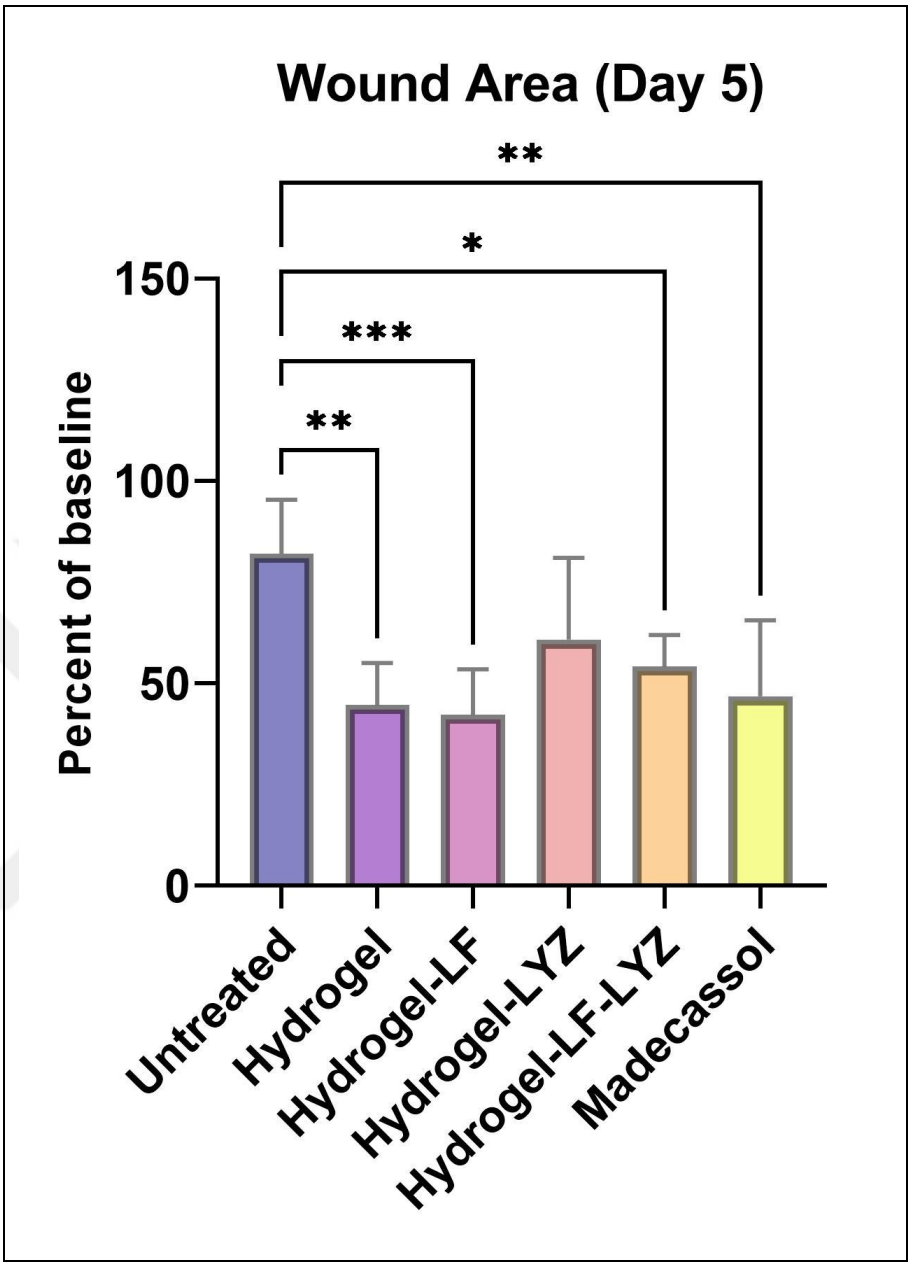

Figure 3.18. Healing of wounds left untreated or treated with Madecassol®, hydrogel or hydrogel with lactoferrin and/or lysozyme on day 5. Data represent the mean values±SD. Comparisons were performed by one-way ANOVA followed by Tukey's post-hoc test. *p<0.05, **p<0.01, ***p<0.001

When the dimensions of the wound areas were measured and compared on day 7, interesting results were obtained again. When compared to the untreated control, only the wounds treated with the blank hydrogel and with the hydrogel containing both lactoferrin and lysozyme were able to induce wound contraction significantly. On the other hand, there was

no significant difference between blank hydrogel and hydrogel-LF-LYZ groups. Surprisingly, Madecassol® also failed in decreasing the wound area, when compared to the other treated groups and the untreated control (Figure 3.19.).

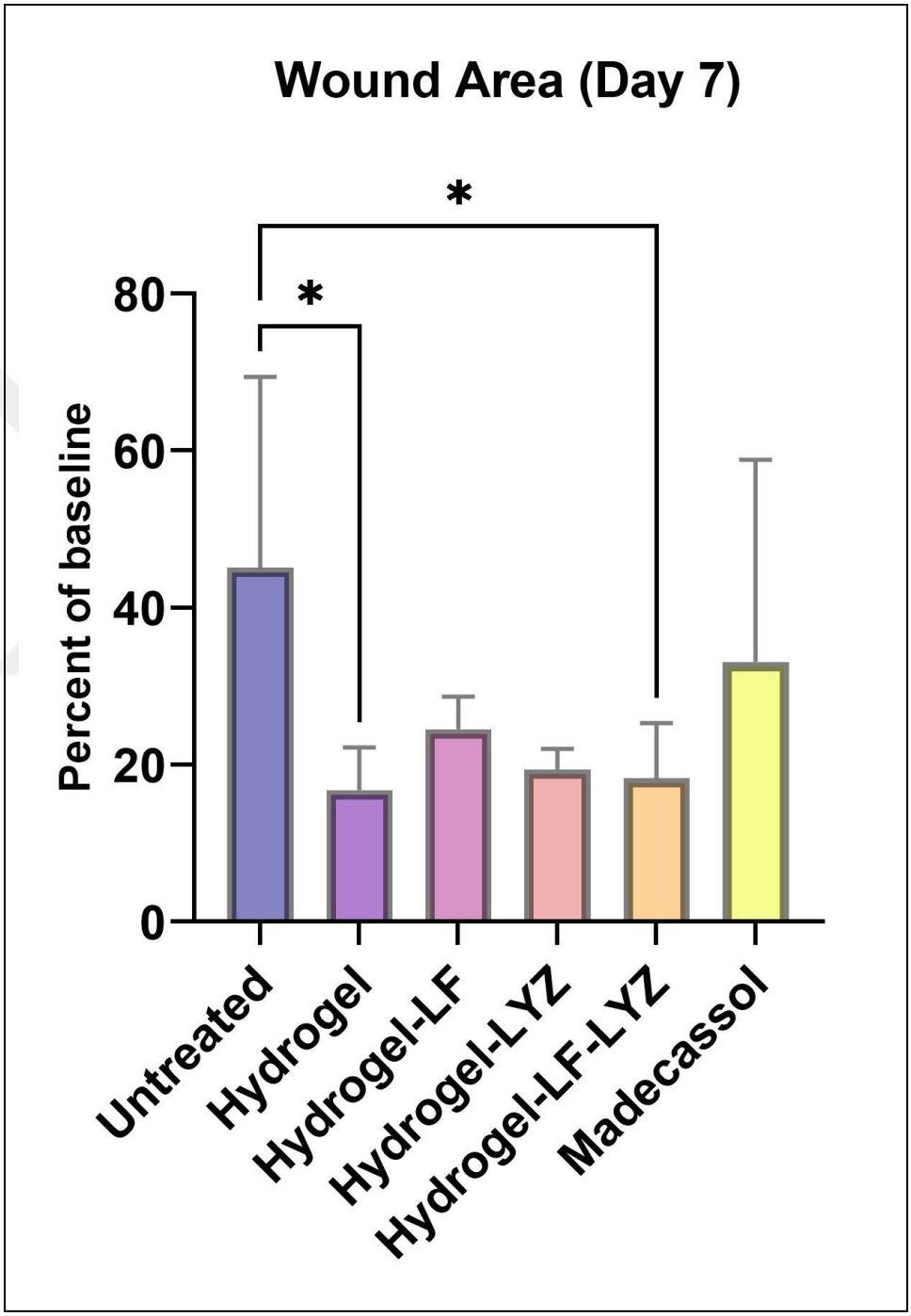

Figure 3.19. Healing of wounds left untreated or treated with Madecassol®, hydrogel or hydrogel with lactoferrin and/or lysozyme on day 7. Data represent the mean values±SD. Comparisons were performed by one-way ANOVA followed by Tukey's post-hoc test. *$p<0.05$

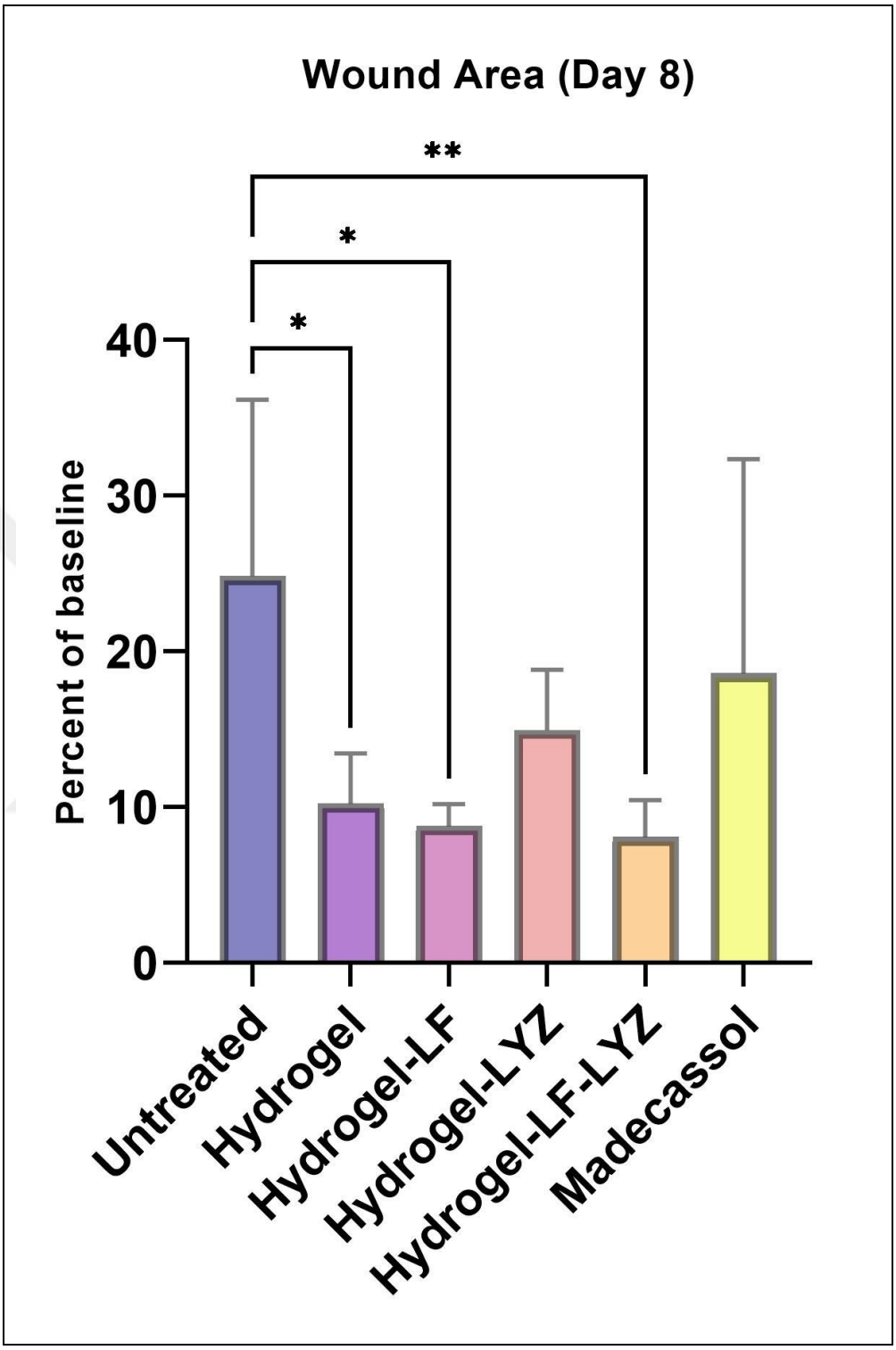

Figure 3.20. Healing of wounds left untreated or treated with Madecassol®, hydrogel or hydrogel with lactoferrin and/or lysozyme on day 8. Data represent the mean values±SD. Comparisons were performed by one-way ANOVA followed by Tukey's post-hoc test. *p<0.05, **p<0.01

Finally, on day 8, the wound dimensions were measured for the last time and wound tissues were collected for being evaluated in histopathological analysis after tissue sectioning and stainings. These last measurements and observations revealed that the groups treated with either blank hydrogel, hydrogel-LF, or hydrogel-LF-LYZ were the only ones that showed a significant decrease in the wound sizes when compared to the untreated wounds. However, neither hydrogel-LF, nor hydrogel-LF-LYZ had a better effect on wound contraction than the hydrogel itself, even though the wounds treated with the hydrogel-LF-LYZ were the ones with the smallest wound size on day 8 (Figure 3.20.). As obtained in the previous time points, according to the mean values, Madecassol again was not as good as expected on wound contraction, and the wounds treated with it were unable to reach a significantly smaller size than the untreated control, even though some animals in this experimental group showed very good healing rate (Figure 3.21.). Overall healing of the wounds at different time points were also summarized in Figure 3.22.

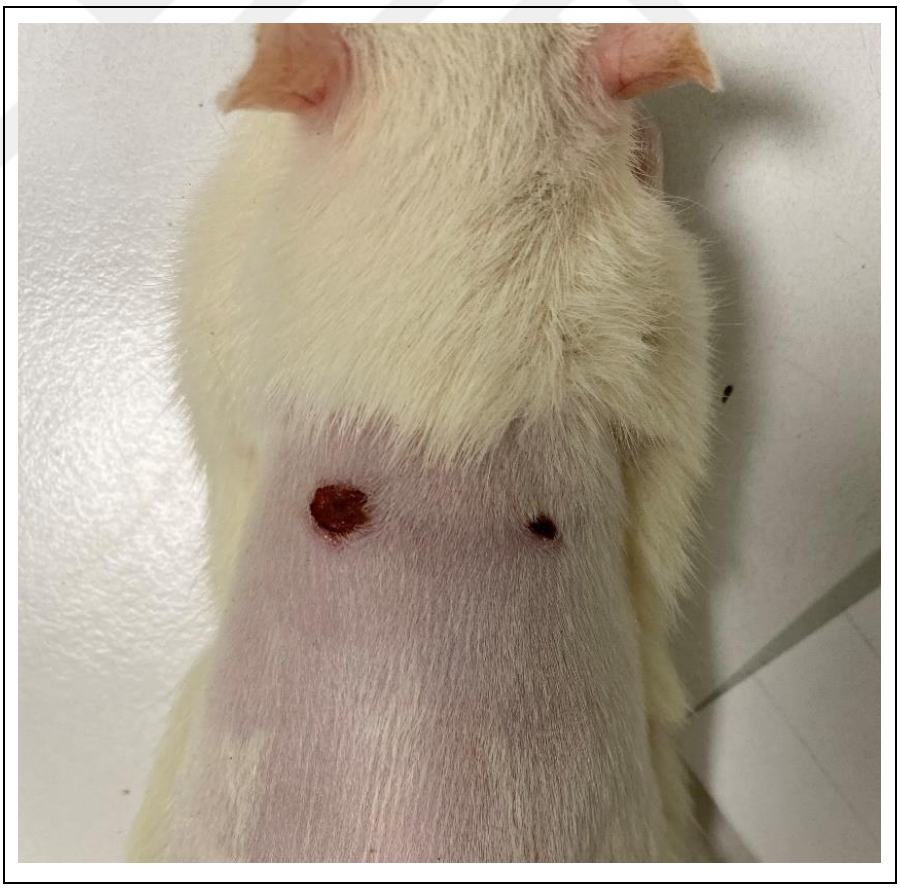

Figure 3.21. One of the animals treated with Madecassol® on the right wound and left untreated on the left wound on day 7

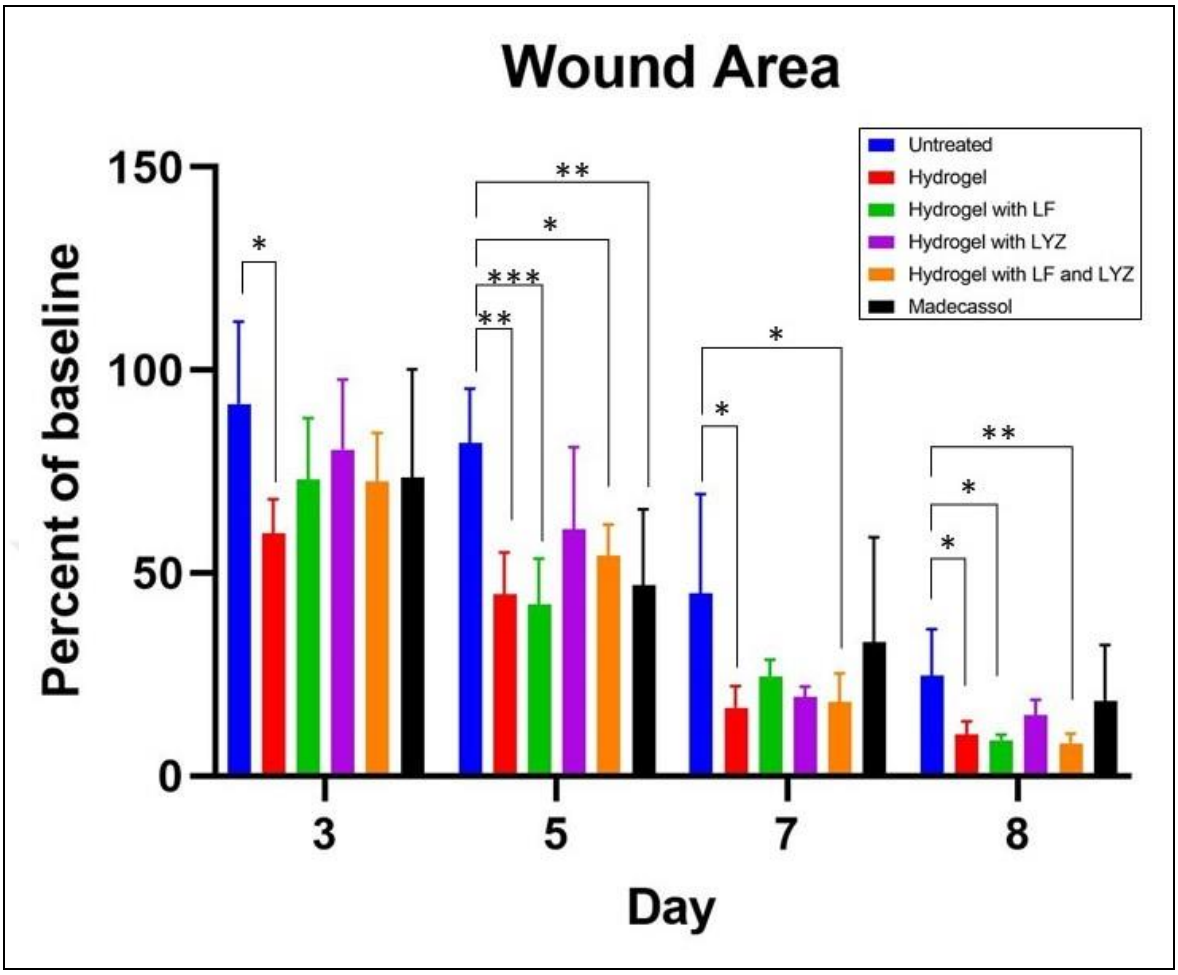

Figure 3.22. Summary of the wound contraction at different time points. Data represent the mean values±SD. Comparisons were performed by one-way ANOVA followed by Tukey's post-hoc test. *p<0.05, **p<0.01, ***p<0.001

3.4. RESULTS OF HISTOPATHOLOGICAL ANALYSIS

According to the histopathological scoring performed on the sections stained with hematoxylin-eosin (Figure 3.23.) and Masson's trichrome staining (Figure 3.24.) results, hydrogel containing lactoferrin and lysozyme had the highest healing activity. Masson's trichrome staining of the tissues were not as good as hematoxylin-eosin stainings, but they were still utilized in evaluation of histopathological findings. Interestingly, hydrogel with lysozyme showed better activity than hydrogel itself, which is contrary to the findings obtained from the wound sizes, in which wounds treated with hydrogel containing lysozyme showed a slower healing than the ones treated with the blank hydrogel.

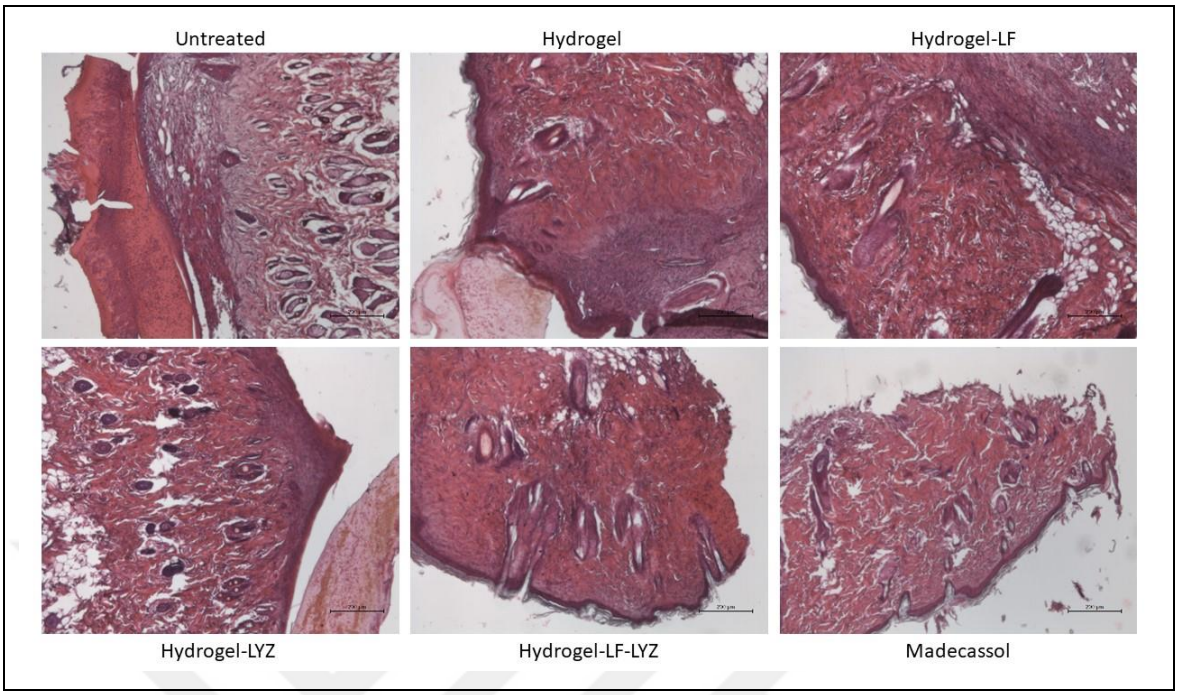

Figure 3.23. Representative images of the tissue sections after hematoxylin-eosin staining

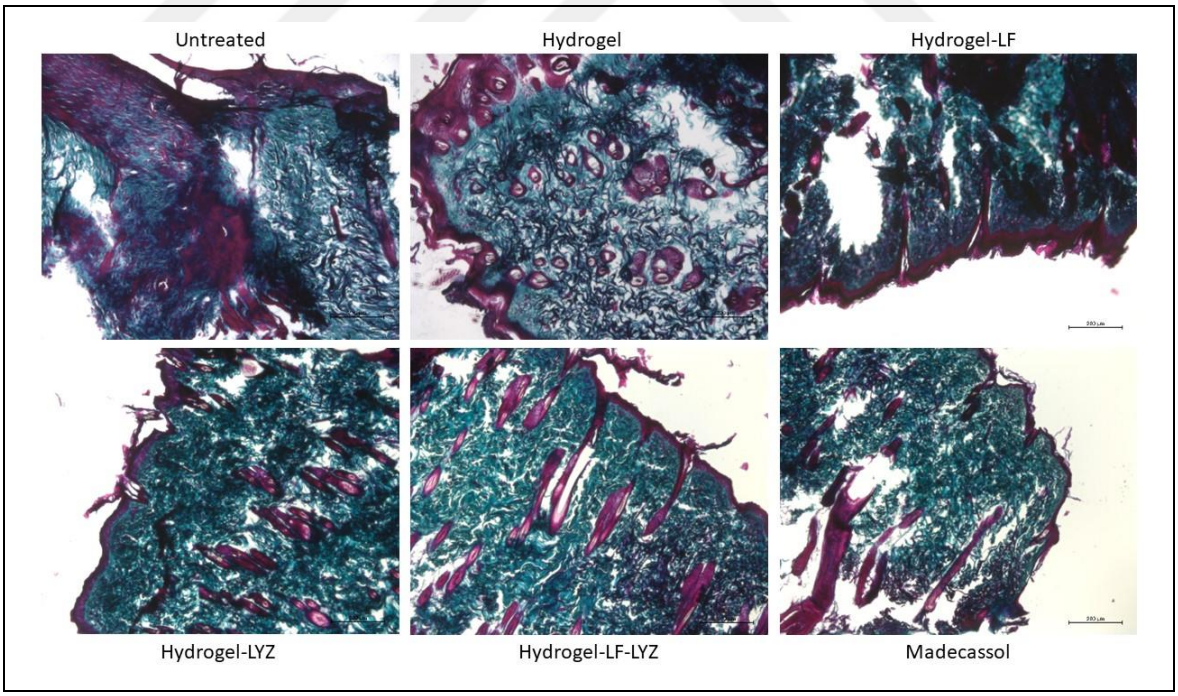

Figure 3.24. Representative images of the tissue sections after Masson's trichrome staining

It was observed in the stained tissue sections that all formulations prepared with poloxamer hydrogel led to a better healing by means of fiber and tissue regeneration on cutaneous wounds than the wounds left untreated. Similarly, wounds treated with any of the tested

hydrogel formulations had less tissue damage by means of edema, degeneration of epithelium, congestion and mononuclear cell infiltration, when compared to the untreated wounds (Figures 3.25. and 3.26.).

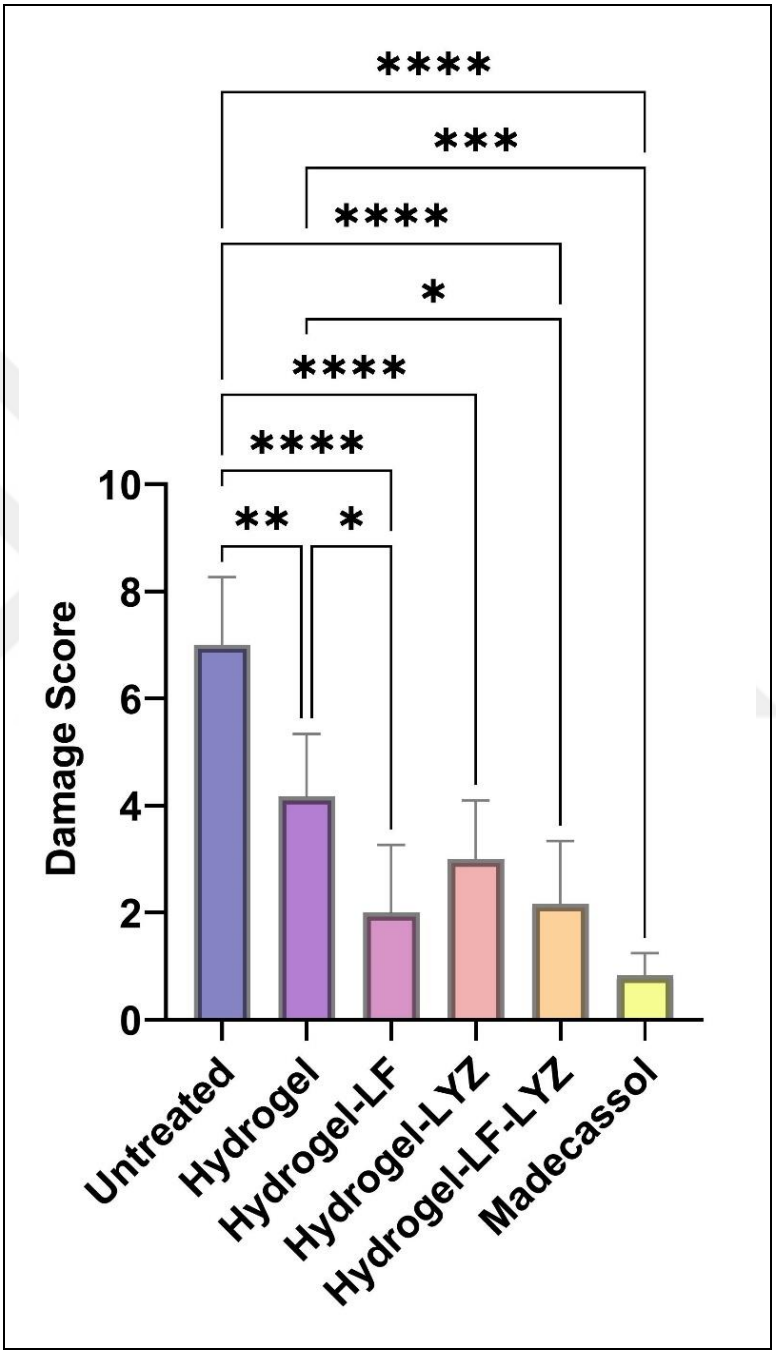

Figure 3.25. Damage scores obtained by the histopathological analysis. Data represent the mean values±SD. Comparisons were performed by one-way ANOVA followed by Tukey's post-hoc test. *p<0.05, **p<0.01, ***p<0.001, ****p<0.0001

On the other hand, among the hydrogels prepared with or without lactoferrin and/or lysozyme, hydrogel containing both lactoferrin and lysozyme had the highest wound healing effect, even though it was not significantly higher than the effect of hydrogel containing only lactoferrin. This result is consistent with the findings of the wound contraction and verifies the literature reporting the superior effect of lactoferrin in wound healing (Figures 3.22. and 3.23.).

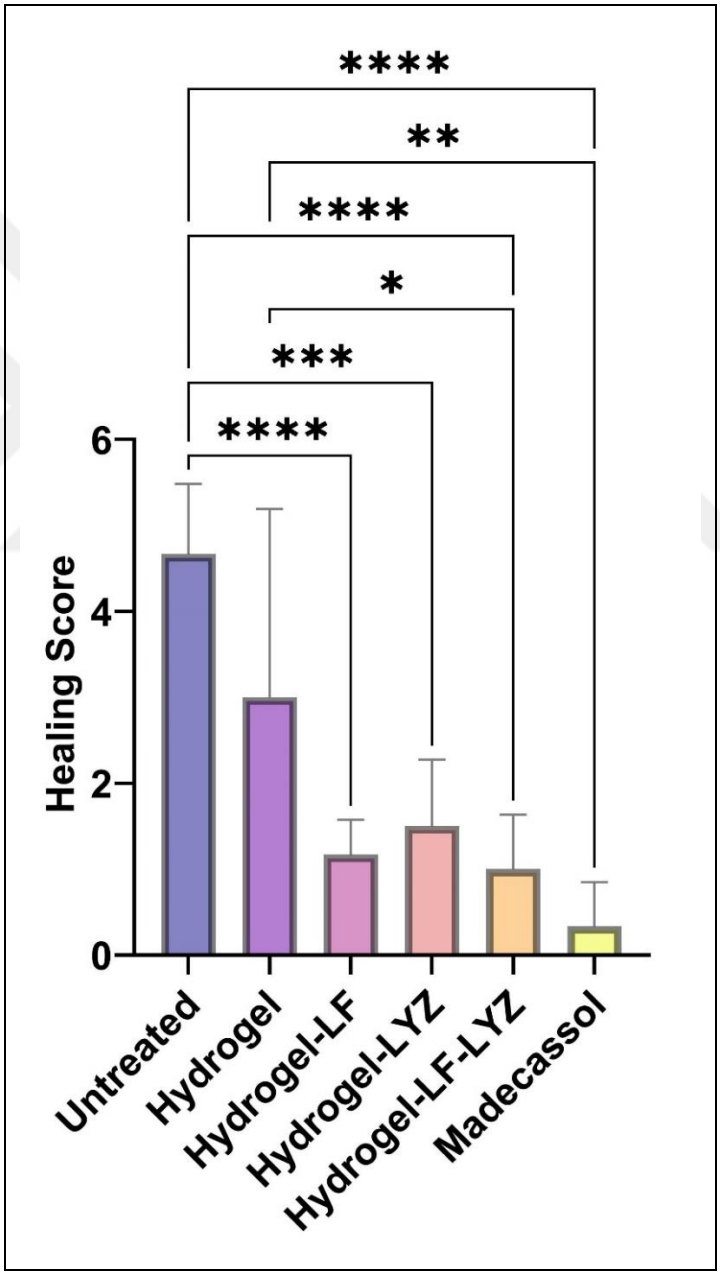

Figure 3.26. Healing scores obtained by the histopathological analysis. Data represent the mean values±SD. Comparisons were performed by one-way ANOVA followed by Tukey's post-hoc test. *p<0.05, **p<0.01, ***p<0.001, ****p<0.0001

3.5. NMR SPECTROSCOPY RESULTS

NMR spectroscopy was performed with the hydrogel containing both lactoferrin and lysozyme at various temperatures in order to investigate how their stability is affected by the state of the poloxamer. Lactoferrin and lysozyme had the best stability when the poloxamer was in gel state at 37ºC. Once the temperature of the hydrogel was dropped to 22 ºC, which turns it back into the solution state, protein stability evidently decreased. Moreover, the spectra obtained with the same sample at 22 ºC the next day showed that the lactoferrin and lysozyme lost their stability and started to be degraded when stored as a solution (Figure 3.27.).

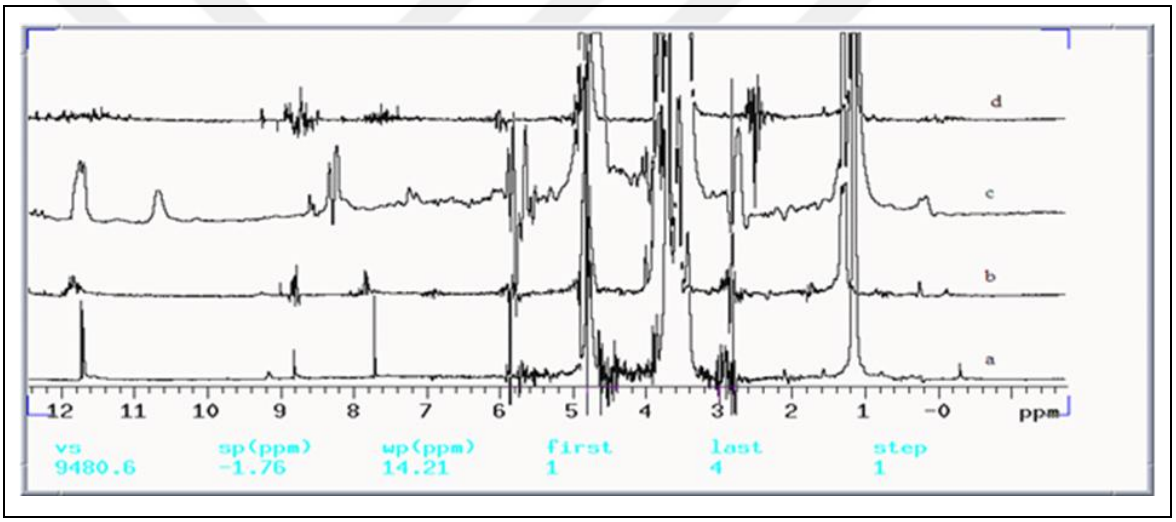

Figure 3.27. ^{1}H NMR spectra of lactoferrin and lysozyme-containing poloxamer at (a) room temperature, (b) 37°C, (c) 22ºC again after heating to 37°C, (d) 22°C the next day

4. DISCUSSION

In this study, it was aimed to develop a hydrogel consisting of poloxamer 407 and hyaluronic acid, in which two proteins, lactoferrin from human milk and lysozyme from chicken egg white, are formulated in combination for inducing cutaneous wound healing. As a 20% poloxamer hydrogel is thermoreversible and has rapid degradation property [177], it was not compatible for being tested by the proposed *in vitro* assays. Therefore, only the effects of lactoferrin and lysozyme by being dissolved directly in the culture medium were tested. For this purpose, first of all, the non-cytotoxic concentrations of lactoferrin and lysozyme that may promote fibroblast proliferation and migration were tried to be determined *in vitro*. Even though MTT assay can be utilized in examining biocompatibility of poloxamer, the following assessments like scratch wound healing are not compatible with the thermoreversible property of this hydrogel. To that aim, cytotoxicity assays were also performed in the absence of poloxamer and HA.

It was first proposed in this study that lactoferrin and lysozyme can show synergistic effects which were previously reported by means of a bactericidal effect against some bacteria in the literature [105,178]. Therefore, MTS assay was first performed to determine the concentrations that are not toxic to the NIH/3T3 cell line and can even increase the cell viability. NIH/3T3 is a mouse embryonic fibroblast cell line, which is a highly utilized model in *in vitro* wound healing studies. MTS assay is a colorimetric assay used for evaluating cell viability and relative cell proliferation, which was developed by modifying MTT assay. It is generally called the “one-step MTT assay”, in which the reagent is added to the cultured cells directly, therefore it does not need the step used for solubilization of formazan crystals in MTT [179].

The concentration ranges selected to be tested in cell viability assays were determined by a literature search considering the studies used lactoferrin and lysozyme for similar attempts. Their effects on cell viability were examined after 24 hours of treatments, as none of the following assays require treatments that take any longer than 24 hours. The results obtained following the MTS assay performed after 24 hours of incubation demonstrated that cells treated with 400 µg/ml of lactoferrin and the ones treated with 200 µg/ml and 100 µg/ml of lysozyme slightly increased the viability of fibroblasts, where none of the tested concentrations of lactoferrin and lysozyme showed any cytotoxicity on this specific cell type

in vitro. This assay was repeated several times resulting in the shortage in MTS reagent. Thus, effects of the combined concentrations of lactoferrin and lysozyme were tested by a regular MTT assay that was also performed after 24 hours of incubation with the proteins. As a result, among the individually applied concentrations, the cells treated with 800 μg/ml of lactoferrin and 200 μg/ml of lysozyme showed a higher viability when compared to the untreated control cells. Similar to the results obtained by MTS assay, none of the treatments caused any cytotoxicity on the fibroblasts. Among the concentrations of combinationally applied lactoferrin and lysozyme, only 400 μg/ml of lactoferrin and 200 μg/ml of lysozyme mixture resulted in an increase in cell viability. Even though it failed inducing the viability of the fibroblasts according to the results obtained from MTT assay, as 400 μg/ml of lactoferrin individually didn't show any cytotoxicity by MTS assay, it was selected as the concentration to be combined with 200 μg/ml lysozyme in the following transwell migration and scratch wound healing assays. Moreover, as the aim was to decrease the individual concentrations of lactoferrin and lysozyme in the formulation, any one of the concentrations bearing 800 μg/ml of lactoferrin was not selected for further testing for wound healing, although none of them had a cytotoxic activity on NIH/3T3 fibroblasts.

The cell viability assays were followed by transwell migration assay in order to reveal the effects of selected lactoferrin and lysozyme concentrations on fibroblast migration. Transwell migration assay is a method first introduced by Boyden, which is also known by his own name. This assay is frequently utilized for investigating cell migration and invasion, specifically towards a defined chemoattractant. Basically, cells are placed on top of a microporous membrane and the chemoattractant is placed below [180]. However, it is a complicated method and there are several parameters to be considered and optimized, such as; cell seeding density, incubation time, serum concentration, where to apply agents (upper or lower compartments), cell fixation and staining, etc. Therefore, there is no standard protocol for this assay and every research group optimizes these parameters depending on the cell line and the active molecules that they are using. On account of this, various methods were tried on transwell migration assays in this study.

First of all, NIH/3T3 fibroblasts were seeded on the upper parts of the transwell insert in a serum-free medium and lactoferrin and/or lysozyme were added into the lower compartments containing complete culture medium. The cells were allowed to migrate through the pores of the transwell membrane towards the lower compartment for 6 hours

which was followed by the fixation and staining of the migratory cells. It was resulted with a migration of some cells, number of which was too less to come to a reliable conclusion. To be more specific, for example, in average around 200 cells per insert migrated towards the medium containing 200 μg/ml of lysozyme which was the most chemoattractant concentration among the tested ones, when around 50 cells per insert migrated towards the control. Therefore, the assay was repeated with a longer incubation time, 18 hours, this time which resulted with the migration of more cells like around 100 cells per area.

The results were interesting; lactoferrin failed in showing a promoting role in the migration of NIH/3T3s, although its positive effect on the fibroblast migration is very-well defined in the literature [9]. On the other hand, lysozyme caused the highest and the only significant increase in the number of migrated cells when compared to the control, which was modulated by the inclusion of lactoferrin in the lower compartment. Instead of an expected synergistic activity of lactoferrin and lysozyme on the migration of fibroblasts, they showed an antagonistic effect, when the proteins were added into the lower compartment in combination.

These unexpected results were attributed to the inclusion of 10% FBS in the lower compartments of the transwell inserts in which lactoferrin and lysozyme were added. Moreover, it was thought that in order to demonstrate the effect of lactoferrin and lysozyme on the intrinsic factors regulating fibroblast migration, cells should be treated with lactoferrin and/or lysozyme in the upper compartments in the absence of high FBS concentration. Therefore, the transwell migration experiment was repeated with no FBS or 1% FBS in the upper part that also contained lactoferrin and/or lysozyme and the cells were allowed to migrate towards the culture medium with 10% FBS in the lower part. However, fibroblasts failed in migrating through the membrane.

As no migration could be observed by the direct treatment of the fibroblasts with lactoferrin and/or lysozyme, scratch wound healing assay was performed by treating the cells bearing a scratch formed with the tip of a micropipette in the presence or absence of the proteins in the medium supplemented with 1% FBS. Scratch assay is a method used in wound healing studies, which is another method used in *in vitro* determination of cell migration, in addition to transwell migration assay. In scratch assay, an artificial wound is created on the cell monolayer, closure of which is measured and evaluated over time, following the addition of migration agents [181].

It was preferred to prepare the desired concentrations of lactoferrin and lysozyme in a culture medium having 1% of FBS, because addition of high concentrations of FBS in the medium may mask the real effects of the tested drugs or proteins on the migration of the cells by inducing cell proliferation [182]. Pictures of the scratch wounds were taken at different time points (6, 18, 24 and 48 hours) following the treatments and the images were analyzed by ImageJ for the area measurement. Although the scratch on the cells treated with lactoferrin and lysozyme simultaneously healed significantly after six hours of treatment, further treatment of the cells with the protein cocktail failed to induce scratch wound healing. Furthermore, the scratch healing was so slow that even after 24 hours of incubation, only about 50% of the scratch wound areas were closed. Moreover, even in the control group, many dead cells were observed at 24^{th} hour, number of which increased gradually until 48^{th} hour when the scratch wounds were still not completely closed in any of the experimental groups. Therefore, it was realized that the tested concentration of the lactoferrin and lysozyme mixture may exert a toxic effect on 3T3 fibroblasts when incubated for any longer than 12 hours in a medium containing low concentration of FBS (1%).

In order to reveal a more realistic result for the scratch wound healing assay, it was repeated in the presence of 5% FBS in the medium containing lactoferrin and/or lysozyme. As a result, the wounds that were treated with both lactoferrin and lysozyme were almost completely healed after 24 hours of incubation and the healing rate was significantly higher than it was observed in the control. Similar to the result obtained from transwell migration assay, lactoferrin itself failed to induce scratch wound healing, even though it did not inhibit it either. On the other hand, sole lysozyme promoted the cell migration, effect of which however, was not attenuated by the inclusion of lactoferrin this time; but instead depicted a supportive activity.

Overall these findings unveiled that 400 μg/ml of lactoferrin and 200 μg/ml of lysozyme can be formulated together for inducing the viability of NIH/3T3 fibroblasts. According to the results obtained from the scratch wound healing assay, mixture of the same concentrations of these two proteins can also promote fibroblast migration to the wound size, although the cells should be treated with the proteins in the presence of 5% FBS in the culture medium. Results of the transwell migration assay also revealed that the experiment can be repeated by dissolving the proteins placed into the upper compartment in a culture medium containing

5% FBS, as that concentration was high enough for preserving cell viability while not affecting migration.

The effects of lactoferrin activity [162,163] and lysozyme activity [162,163] on the expressions of some extracellular matrix proteins like hyaluronic acid and collagen, as well as the growth factors such as PDGF, FGF and VEGF being regulated in wound healing stages, are clear in the literature. Therefore, how the expression levels of different genes that are also regulated during wound healing stages are affected by lactoferrin and/or lysozyme treatment was aimed to be investigated in this study. Moniri and colleagues investigated the genes that are regulated the most during wound healing; Mmp9, Wnt4 and β-cat were found among them [183]. How the expressions of these genes are regulated upon treatment with lactoferrin and/or lysozyme is not yet clear in the literature. Therefore, how their mRNA expression levels are affected by lactoferrin and/or lysozyme was analyzed in this study by quantitative RT-PCR analysis. It is known that Mmp9, which is a type IV collagenase, needs to be expressed during wound healing. However, its overexpression is observed in chronic wounds and may lead to delayed healing [184]. For example, Mmp9 is highly expressed in diabetic foot ulcers and can be targeted in the drug formulations developed for supporting the healing of these chronic wounds [185]. As no significant change was observed in the mRNA levels of Mmp9 following the treatment with lactoferrin and/or lysozyme, it can be concluded that it is possible to apply them safely on chronic wounds as well, even though further investigation is needed. On the other hand, previous studies revealed that various Wnt proteins are expressed in skin wounds, and Wnt4, which is expressed in the dermis and localized to hair follicles, are found in mouse full-thickness wounds for even up to seven days [2]. Furthermore, Wnt4 is a mediator of myofibroblast differentiation [186] and regulates skin cell proliferation and migration by stimulating the nuclear translocation of β-cat [187]. The only significant change was observed in the expression level of Wnt4, when the cells were treated with 400 μg/ml of lactoferrin and 200 μg/ml of lysozyme in combination. This finding supports the results obtained from MTT and migration assays showing increased fibroblast proliferation and viability. There was no significant change in the mRNA levels of β-cat upon lactoferrin and/or lysozyme treatment and the standard deviations were pretty high. Even if a change was observed, as stabilization and nuclear translocation of β-cat are the key factors in β-cat-regulated wound healing [188,189], it would not be possible to come to a conclusion by analyzing only the mRNA levels and

western blot analysis is also required. Moreover, the experiment could only be performed in duplicates and needs to be repeated with more replicates, in order to get more reliable results.

Agar well diffusion assay is one of the best methods that can be used in revealing the antimicrobial effects of poloxamer-based hydrogel formulations, as the wells created on an agar plate can be filled with the hydrogel when it is in the liquid phase and transform into gel phase upon incubation at 37°C for bacterial growth. Therefore, it was utilized also in this study for investigating if the generated thermoreversible poloxamer-HA hydrogel including lactoferrin and lysozyme show any antibacterial activity against *E. coli* and *S. aureus*, which are among the most abundant bacteria found in the infected wounds [190]. Unfortunately, neither blank hydrogel, nor lactoferrin and/or lysozyme-including hydrogels demonstrated any bacteriostatic activity against *E.coli* or *S.aureus*, because 400 µg/ml of lactoferrin and 200 µg/ml of lysozyme were used in the preparation of the hydrogels. However, these were the concentrations used for direct dissolution of lactoferrin and lysozyme in the culture medium previously. It is known that lactoferrin shows antibacterial effects on *E. coli* [191] and *S. aureus* [192,193]. On the other hand, as *E.coli* is a gram-negative bacteria, it was not surprising to observe that the hydrogel bearing lysozyme was not effective against *E. coli*. Moreover, it is known that pathogenic staphylococci are resistant to lysozyme as well [194,195]. However, as there are studies in the literature reporting synergistic effects of lactoferrin and lysozyme against various bacteria, it still deserved a try. Even in one of these, Tonguç-Altın and colleagues reported the effects of lactoferrin and lysozyme-containing poloxamer-based hydrogels against *Streptococcus mutans* and *Lactobacillus acidophilus* [105]. Therefore, when no effect could be observed in any of the tested formulations with agar-well diffusion assay against *E.coli* and *S.aureus*, the hydrogels were then tested by Bauer-Kirby disk diffusion assay with the concentrations similar to the ones reported in the mentioned study. It could be better if the hydrogels containing 2% lactoferrin and/or 1% lysozyme were tested against bacterial growth by agar well diffusion assay. However, it needs hundreds of microliters of hydrogel to fill the wells up, whereas the disks used in disk diffusion assay can be prepared by only 20 µl of sample.

Kirby-Bauer disk diffusion method is a susceptibility test used for determining the antibiotic sensitivity or resistance of bacteria [196], and utilized in this study to reveal the prospective antibacterial effects of the developed hydrogel. Oxacillin and ciprofloxacin were used as the controls in this test against *S.aureus* and *E.coli* respectively, as they are effective antibiotics

used in treating infections of these bacteria [197]. Whatman paper disks containing 20% poloxamer-3% HA hydrogels with or without lactoferrin and/or lysozyme were prepared by loading each disk with 20 µl of hydrogel. The dried disks were placed on the agar plates inoculated with either *E.coli* or *S.aureus* and incubated at 37°C for 24 hours. It was not surprising to obtain results indicating that only the hydrogels not containing lysozyme were able to show bacteriostatic activity against both strains, which were, however, too slight to be measured as inhibition zones. On the other hand, there was no significant difference between the inhibition zones obtained from the blank hydrogel and the hydrogel containing lactoferrin, indicating that the bacteriostatic activity was provided by the hydrogel itself and not by the lactoferrin. As the disks containing the hydrogels with sole lysozyme or with both lactoferrin and lysozyme failed to inhibit bacterial growth, it was concluded that lysozyme showed antagonistic effects on the antibacterial activity of the gel itself and the gel with lactoferrin. This antagonistic effect of lysozyme and failure of these two proteins in showing antibacterial activities can be attributed to lysozyme's known non-effectiveness against these bacterial strains, as well as to the possibly insufficient concentration of lactoferrin. Moreover, as this study only focuses on the characterization of these hydrogels by means of wound contraction and histopathological analysis, it could not unveil the properties like release time and behavior, as well as the physical interactions between the molecules included in the hydrogels. Therefore, further investigation on these is needed in order to come to a conclusion about the results obtained from the disk diffusion assay.

NMR spectroscopy revealed the importance of preparing the solutions of lactoferrin and lysozyme freshly before using. It also indicated that the stabilities of lactoferrin and lysozyme are better preserved in the poloxamer when it is in the gel state. However, thermoreversing the gel into solution led to a decrease in the stability. On the other hand, the spectra recorded the next day with the same sample showed that lactoferrin and lysozyme can be easily degraded when in solution. This situation can explain the inconsistency of the results obtained from in vitro assays, in which lactoferrin and lysozyme were directly dissolved in the culture media, even though they were prepared freshly.

One of the main aims in this study was to investigate the effect of the generated poloxamer-HA hydrogel containing lactoferrin and lysozyme on promoting healing of cutaneous wounds on rats. To this end, full-thickness wounds were created on rats and they were treated with or without hydrogels carrying lactoferrin and/or lysozyme for 8 days. Dimensions of

the wounds were measured and recorded every two days, in order to demonstrate the effects of the gels on wound contraction. Wound contraction is an important process, by which the size of a wound is reduced. However, if the wound contraction is not sufficient, a non-healing wound may arise, when excessive contraction is another problem leading to a scar contracture [198]. As a result, the hydrogel containing both lactoferrin and lysozyme was the one promoting the wound contraction the most on day 8, although it did not show any better effect than the blank hydrogel. Moreover, the proposed and expected synergistic effect could not be observed for lactoferrin and lysozyme, even though there was either no antagonism. This was again attributed to the insufficient concentrations of lactoferrin and lysozyme formulated, which were determined by a literature search and according to the physiological concentrations of lactoferrin and lysozyme. The same non-toxic concentrations determined by *in vitro* assays could not be used in this *in vivo* experiment, because the active proteins were not directly applied on the wounds; but instead, they were delivered by the poloxamer-HA hydrogel. However, as mentioned previously in the discussion of disk diffusion results, release properties of the formulated hydrogel should have been examined for lactoferrin and lysozyme, in order to understand whether the proteins can successfully reach the wound area, or not.

On the other hand, the hydrogel containing sole lysozyme was the least effective one in wound contraction; it even failed to generate a better healing effect than the untreated control at any time points measured. However, the remaining areas of the wounds did not significantly differ from the ones treated with other hydrogels, as well. Two of the animals in this group unfortunately died on days 3 and 5, as they could not stand to be anesthetized repeatedly. Therefore, the insignificance of the results regarding the lysozyme-bearing hydrogels can also be attributed to this issue.

Madecassol® is a commercially available, topical wound healing agent with proven efficacy, which was used in this study as the control for comparing the improvements observed in the wounds. Results revealed that the experimental groups treated with a hydrogel showed wound contraction similar to the Madecassol®-treated wounds from day 0 to day 5. However, on days 7 and 8, it was interestingly observed that Madecassol®, on average, was not able to induce closure of the wounds in contrast to what was expected. Six animals were included in each experimental group (n=6), and some of the animals, wounds of which were treated with Madecassol®, showed very significant wound contraction when compared with

the untreated wounds on days 7 and 8 (Figure 3.19). Such results can even be due to the behavior of the animals; for example, they sometimes lick the therapeutics applied on others' wounds leading to the incomplete treatment of them.

Although wound contraction results proved that the developed hydrogel containing both lactoferrin and lysozyme has no toxic effect and can be used as a cutaneous wound dressing safely, it was not any more effective than the blank hydrogel in accelerating the wound closure. Moreover, the healing of a wound is not only measured by how fast the wound is closed, but also by checking various other factors having a role in wound healing. Therefore, histopathological analysis was performed following the sectioning and staining of the wound tissues collected on day 8. HE and Masson's trichrome stainings were preferred as they are the most common stains preferred in wound tissue evaluation. Although images obtained from Masson's trichrome staining were not very good at distinguishing the differences among the experimental groups, they still were included in the results part. The total damage scores were determined by evaluating edema, degeneration of epithelium, congestion and mononuclear cell infiltration separately. Collagen fiber formation and tissue regeneration were also scored and used for calculating total healing scores.

The results were very promising; significant differences between the groups treated with the hydrogels carrying lactoferrin and/or lysozyme and the group that had blank hydrogel treatment were observed. Moderate to severe edema was observed in the untreated control tissues, while it was absent to mild in the other experimental groups. Epithelium degeneration was not as severe as the edema in the untreated control and it was absent or mild in the groups treated with hydrogel containing lactoferrin and/or lysozyme. However, moderate epithelium degeneration was present in some of the tissues obtained from the group treated with blank hydrogel. By means of congestion, Madecassol® was the one healing the best with almost no signs of it. On the other hand, mild or no congestion was observed for the wounds treated with the hydrogels delivering the proteins, when the blank hydrogel groups ended up with a moderate congestion which was similar to the untreated controls. There was also moderate mononuclear cell infiltration in the untreated control groups and hydrogel containing both lactoferrin and lysozyme caused minimum infiltration among other treatments, except for the Madecassol®, which resulted with almost no infiltration in the wound tissues.

Collagen fiber formation and tissue regeneration were considered when grading the healing scores of the experimental groups. A graphical demonstration similar to the one generated for damage scores was observed, as the Madecassol®-treated group showed the best healing with almost complete fiber development and regeneration. On the other hand, the wounds treated with the hydrogel bearing both lactoferrin and lysozyme healed very-well by means of collagen amount and tissue regeneration, which was significantly better than the healing of the wounds treated with blank hydrogel. However, sole lysozyme in the hydrogel failed in generating an effect significantly better than the blank hydrogel, as consistent with the wound contraction results. Moreover, the hydrogel with lactoferrin was able to generate a significant difference from the blank hydrogel, as demonstrated by the damage scoring.

Overall these data obtained from histopathological observations revealed that healing of a cutaneous wound cannot be interpreted only by considering the time required for the closure. Madecassol®, for example, was not good enough in inducing wound contraction, which was then contradicted by the histopathological observations. Similarly, the blank hydrogel and the hydrogel containing both lactoferrin and lysozyme depicted similar effects on wound contraction, although the blank hydrogel could not show healing activities as good as the hydrogel containing both proteins. In the light of these findings, it can be concluded that the expected synergistic effect of lactoferrin and lysozyme could not be obtained, as the effect of the hydrogel containing both lactoferrin and lysozyme was not significantly higher than the effect of hydrogel containing lactoferrin or lysozyme solely, verifying the reports indicating the superior effect of lactoferrin in wound healing. Moreover, as lactoferrin-bearing hydrogels ended up with better results than the ones containing sole lysozyme, the reports indicating the superior effect of lactoferrin on wound healing were verified, as well.

5. CONCLUSIONS

In conclusion, *in vitro* assays performed in this study represented that lactoferrin from human milk and chicken egg white lysozyme can be formulated together in skin wound therapeutics, although a synergistic effect of them with the tested concentrations could not be observed on the proliferation and migration of fibroblasts. However, combinational effects of various other concentrations of these two proteins can be further investigated for fibroblast proliferation and migration with more replicates. Furthermore, their activities on the proliferation and migration of keratinocytes can be demonstrated *in vitro* by the same assays performed with a keratinocyte cell line such as HaCaT. As how combinational use of lactoferrin and lysozyme can affect vascularization during wound healing could not be shown in this study, a tube formation assay with HUVECs can also reveal it.

Quantitative RT-PCR utilized in this study was only for displaying how mRNA expression levels of some genes regulated in wound healing are affected. However, further assessment can be made by checking the mRNA levels of some growth factors taking roles at different stages of wound healing like FGF, VEGF and HAS, in order to have a better understanding about the combinational effects of lactoferrin and lysozyme during these phases. Furthermore, as mRNA expression is not always representative of the protein levels, western blot analysis can demonstrate how protein expressions of these genes are regulated when lactoferrin and lysozyme are combined as therapeutic agents in wound healing. In addition, protein expression can also be investigated by immunohistochemistry assay applied on the wound tissues collected after hydrogel treatments.

In vivo testing of the hydrogels generated on full thickness skin wounds on rats indicated that lactoferrin and lysozyme can be formulated together in such a poloxamer-based hydrogel containing HA for being used as a wound dressing. Histopathological analysis also revealed the importance of such active molecules in a wound healing formulation; the wounds treated with lactoferrin and lysozyme-containing hydrogel showed less pathology than the ones treated with blank hydrogel, although no significant difference was observed between their contraction. As recently represented by Park and colleagues, transwell migration inserts can be utilized in *in vitro* characterization of poloxamer-based thermoreversible hydrogels [153] . Therefore, effective concentrations of lactoferrin and

lysozyme included in the poloxamer-HA hydrogels can be better defined by *in vitro* assays to be tested on animal wound models.

Above all, the hydrogels that were developed in this study need further characterization, as the questions regarding their chemical and physical properties, their degradation time, their release behavior, stability of the proteins being delivered, etc. were left unanswered. Moreover, as the poloxamer-based hydrogels tend to be degraded rapidly in physiological media, it can be partnered with a different polymer, other than HA, in order to prolong the elimination of the hydrogel for providing a more controlled and sustained release of the proteins. The hydrogel formulation reported in this study was the first to bring lactoferrin and lysozyme together in a hydrogel made up of poloxamer 407 and HA, which was evaluated for its *in vivo* wound healing activity. Further characterization may help concentrations of the ingredients to be better regulated and even clinical use of the developed hydrogel formulation might be possible eventually. Finally, in order to develop a more innovative hydrogel, 3D printer technology, which has gained a lot of importance in recent years and successfully used for printing poloxamer 407 disks previously [199], can also be used in the future for manufacturing this wound healing formulation.

REFERENCES

1. Kujath P, Michelsen A. Wounds – From Physiology to Wound Dressing. *Deutsches Ärzteblatt international*. 2008;105(13): 239–248.

2. Houschyar KS, Momeni A, Pyles MN, Maan ZN, Whittam AJ, Siemers F. Wnt signaling induces epithelial differentiation during cutaneous wound healing. *Organogenesis*. 2015;11(3):95–104.

3. Nourian Dehkordi A, Mirahmadi Babaheydari F, Chehelgerdi M, Raeisi Dehkordi S. Skin tissue engineering: wound healing based on stem-cell-based therapeutic strategies. *Stem Cell Res Ther*. 2019;10(1):111.

4. Raza F, Zafar H, Zhu Y, Ren Y, -Ullah A, Khan A, et al. A Review on Recent Advances in Stabilizing Peptides/Proteins upon Fabrication in Hydrogels from Biodegradable Polymers. *Pharmaceutics*. 2018;10(1):16.

5. Sakr O, Jordan O, Borchard G. Sustained protein release from hydrogel microparticles using layer-by-layer (LbL) technology. *Drug Delivery*. 2016;23(8):2747–55.

6. Erfani A, Flynn N, Aichele C, Ramsey J. Encapsulation and delivery of protein from within poly(sulfobetaine) hydrogel beads. *Journal of Applied Polymer Science*. 2020;137(40):49550.

7. Kant V, Gopal A, Kumar D, Gopalkrishnan A, Pathak N, Kurade N, et al. Topical pluronic F-127 gel application enhances cutaneous wound healing in rats. *Acta Histochemica*. 2014;116(1):5–13.

8. Feng P, Qiu H, Luo Y, Hu J, Cao Y, Pang Q, et al. Development of Poloxamer Hydrogels Containing Antibacterial Guanidine-Based Polymers for Healing of Full-Thickness Skin Wound. *ACS Biomaterials Science & Engineering*. 2021;7(9):4557–68.

9. Takayama Y, Aoki R. Roles of lactoferrin on skin wound healing. *Biochem Cell Biol*. 2012;90(3):497–503.

10. Ferraboschi P, Ciceri S, Grisenti P. Applications of Lysozyme, an Innate Immune Defense Factor, as an Alternative Antibiotic. *Antibiotics*. 2021;10(12):1534.

11. Tavakoli S, Klar AS. Advanced Hydrogels as Wound Dressings. *Biomolecules.* 2020;10(8).

12. Vig K, Chaudhari A, Tripathi S, Dixit S, Sahu R, Pillai S, et al. Advances in Skin Regeneration Using Tissue Engineering. *Int J Mol Sci*. 2017;18(4).

13. &NA; Anatomy and Physiology of the Skin. *Journal of the Dermatology Nurses' Association*. 2011;3(6):366.

14. Rittié L. Cellular mechanisms of skin repair in humans and other mammals. *Journal of Cell Communication and Signaling*. 2016;10(2):103–20.

15. Pereira R, Sousa A, Barrias C, Bayat A, Granja P, Bártolo P. Advances in bioprinted cell-laden hydrogels for skin tissue engineering. *Biomanufacturing Reviews*. 2017;2(1).

16. Zhao X, Wu H, Guo B, Dong R, Qiu Y, Ma P. Antibacterial anti-oxidant electroactive injectable hydrogel as self-healing wound dressing with hemostasis and adhesiveness for cutaneous wound healing. *Biomaterials*. 2017;122:34–47.

17. Saleh B, Dhaliwal H, Portillo-Lara R, Sani E, Abdi R, Amiji M, et al. Local Immunomodulation Using an Adhesive Hydrogel Loaded with miRNA-Laden Nanoparticles Promotes Wound Healing. *Small*. 2019;15(36):1902232.

18. Da Silva L, Reis R, Correlo V, Marques A. Hydrogel-Based Strategies to Advance Therapies for Chronic Skin Wounds. *Annual Review of Biomedical Engineering*. 2019;21(1):145–69.

19. Wang J, Chen X-YY, Zhao Y, Yang Y, Wang W, Wu C, et al. pH-Switchable Antimicrobial Nanofiber Networks of Hydrogel Eradicate Biofilm and Rescue Stalled Healing in Chronic Wounds. *ACS Nano*. 2019;13(10):11686–97.

20. Degreef H. How To Heal A Wound Fast. *Dermatologic Clinics*. 1998;16(2):365–75.

21. Attinger C, Janis J, Steinberg J, Schwartz J, Al-Attar A, Couch K. Clinical Approach to Wounds: Debridement and Wound Bed Preparation Including the Use of Dressings

and Wound-Healing Adjuvants. *Plastic and Reconstructive Surgery*. 2006;117:72S–109S.

22. Su J, Li J, Liang J, Zhang K, Li J. Hydrogel Preparation Methods and Biomaterials for Wound Dressing. *Life*. 2021;11(10):1016.

23. Chhabra S, Chhabra N, Kaur A, Gupta N. Wound Healing Concepts in Clinical Practice of OMFS. *Journal of Maxillofacial and Oral Surgery*. 2017;16(4):403–23.

24. Petkovic M, Mouritzen MV, Mojsoska B, Jenssen H. Immunomodulatory Properties of Host Defence Peptides in Skin Wound Healing. *Biomolecules*. 2021;11(7).

25. Punchard NA, Whelan CJ, Adcock I. The Journal of Inflammation. *J Inflamm (Lond)*. 2004;1(1):1.

26. Periayah MH, Halim AS, Mat Saad AZ. Mechanism Action of Platelets and Crucial Blood Coagulation Pathways in Hemostasis. *Int J Hematol Oncol Stem Cell Res*. 2017;11(4):319–27.

27. Clark RA, Ghosh K, Tonnesen MG. Tissue engineering for cutaneous wounds. *J Invest Dermatol*. 2007;127(5):1018–29.

28. Stadelmann WK, Digenis AG, Tobin GR. Physiology and healing dynamics of chronic cutaneous wounds. *Am J Surg*. 1998;176(2A Suppl):26S–38S.

29. Reinke JM, Sorg H. Wound repair and regeneration. *Eur Surg Res*. 2012;49(1):35–43.

30. Eming SA, Krieg T, Davidson JM. Inflammation in wound repair: molecular and cellular mechanisms. *J Invest Dermatol*. 2007;127(3):514–25.

31. Tziotzios C, Profyris C, Sterling J. Cutaneous scarring: Pathophysiology, molecular mechanisms, and scar reduction therapeutics Part II. Strategies to reduce scar formation after dermatologic procedures. *J Am Acad Dermatol*. 2012;66(1):13–24.

32. Profyris C, Tziotzios C, Do Vale I. Cutaneous scarring: Pathophysiology, molecular mechanisms, and scar reduction therapeutics Part I. The molecular basis of scar formation. *J Am Acad Dermatol*. 2012;66(1):1–10.

33. Koh TJ, DiPietro LA. Inflammation and wound healing: the role of the macrophage. *Expert Rev Mol Med.* 2011;13:e23.

34. Olczyk P, Mencner Ł, Komosinska-Vassev K. The role of the extracellular matrix components in cutaneous wound healing. *Biomed Res Int*. 2014;2014:747584.

35. Werner S, Grose R. Regulation of wound healing by growth factors and cytokines. *Physiol Rev*. 2003;83(3):835–70.

36. Senger DR, Davis GE. Angiogenesis. *Cold Spring Harb Perspect Biol*. 2011;3(8):a005090.

37. Hinz B. Formation and function of the myofibroblast during tissue repair. *J Invest Dermatol*. 2007;127(3):526–37.

38. Gurtner GC, Evans GR. Advances in head and neck reconstruction. *Plast Reconstr Surg*. 2000;106(3):672–82; quiz 683.

39. Yates CC, Hebda P, Wells A. Skin wound healing and scarring: fetal wounds and regenerative restitution. *Birth Defects Res C Embryo Today.* 2012;96(4):325–33.

40. Robson MC, Steed DL, Franz MG. Wound healing: biologic features and approaches to maximize healing trajectories. *Curr Probl Surg*. 2001;38(2):72–140.

41. Caló E, Khutoryanskiy V. Biomedical applications of hydrogels: A review of patents and commercial products. *European Polymer Journal*. 2015;65:252–67.

42. Ahmed EM. Hydrogel: Preparation, characterization, and applications: A review. *J Adv Res*. 2015;6(2):105–21.

43. Catoira MC, Fusaro L, Di Francesco D, Ramella M, Boccafoschi F. Overview of natural hydrogels for regenerative medicine applications. *J Mater Sci Mater Med*. 2019;30(10):115.

44. Pushpamalar J, Meganathan P, Tan H, Dahlan N, Ooi L-T, Neerooa B, et al. Development of a Polysaccharide-Based Hydrogel Drug Delivery System (DDS): An Update. *Gels*. 2021;7(4):153.

45. Dragan E, Dinu M. Polysaccharides constructed hydrogels as vehicles for proteins and peptides. A review. *Carbohydrate Polymers*. 2019;225:115210.

46. Davari N, Bakhtiary N, Khajehmohammadi M, Sarkari S, Tolabi H, Ghorbani F, et al. Protein-Based Hydrogels: Promising Materials for Tissue Engineering. *Polymers*. 2022;14(5):986.

47. Vermonden T, Censi R, Hennink WE. Hydrogels for protein delivery. *Chem Rev*. 2012;112(5):2853–88.

48. Ho T-C, Chang C-C, Chan H-P, Chung T-W, Shu C-W, Chuang K-P, et al. Hydrogels: Properties and Applications in Biomedicine. *Molecules*. 2022;27(9):2902.

49. Caló E, Khutoryanskiy V. Biomedical applications of hydrogels: A review of patents and commercial products. *European Polymer Journal*. 2015;65:252–67.

50. Bordbar-Khiabani A, Gasik M. Smart Hydrogels for Advanced Drug Delivery Systems. *International Journal of Molecular Sciences*. 2022;23(7):3665.

51. Li J, Mooney D. Designing hydrogels for controlled drug delivery. *Nature Reviews* Materials. 2016;1(12).

52. Naik E, Reddy V, Swetha N. Super Porous Hydrogels. *Research Journal of Pharmacy and Technology*. 2019;12(1):434.

53. Zustiak S, Leach J. Characterization of protein release from hydrolytically degradable poly(ethylene glycol) hydrogels. *Biotechnology and Bioengineering*. 2011;108(1):197–206.

54. Lin C-C, Anseth K. PEG Hydrogels for the Controlled Release of Biomolecules in Regenerative Medicine. *Pharmaceutical Research*. 2009;26(3):631–43.

55. Chen D, Hou Q, Zhong L, Zhao Y, Li M, Fu X. Bioactive Molecules for Skin Repair and Regeneration: Progress and Perspectives. *Stem Cells Int*. 2019;2019:1–13.

56. El-Sherbiny IM, Yacoub MH. Hydrogel scaffolds for tissue engineering: Progress and challenges. *Glob Cardiol Sci Pract*. 2013;2013(3):316–42.

57. Birajdar MS, Joo H, Koh W-GG, Park H. Natural bio-based monomers for biomedical applications: a review. *Biomater Res*. 2021;25(1):8.

58. Aswathy SH, Narendrakumar U, Manjubala I. Commercial hydrogels for biomedical applications. *Heliyon*. 2020;6(4):e03719.

59. Swift T, Swanson L, Geoghegan M, Rimmer S. The pH-responsive behaviour of poly(acrylic acid) in aqueous solution is dependent on molar mass. *Soft Matter*. 2016;12(9):2542–9.

60. Xu X, Liu Y, Fu W, Yao M, Ding Z, Xuan J, et al. Poly(N-isopropylacrylamide)-Based Thermoresponsive Composite Hydrogels for Biomedical Applications. *Polymers*. 2020;12(3):580.

61. Fakhari A, Corcoran M, Schwarz A. Thermogelling properties of purified poloxamer 407. *Heliyon*. 2017;3(8):e00390.

62. Shiraishi K, Yokoyama M. Toxicity and immunogenicity concerns related to PEGylated-micelle carrier systems: a review. *Science and Technology of Advanced Materials*. 2019;20(1):324–36.

63. Pan Z, Ye H, Wu D. Recent advances on polymeric hydrogels as wound dressings. *APL Bioengineering*. 2021;5(1):011504.

64. Dai T, Tanaka M, Huang Y-YY, Hamblin MR. Chitosan preparations for wounds and burns: antimicrobial and wound-healing effects. *Expert Rev Anti Infect Ther*. 2011;9(7):857–79.

65. Dovedytis M, Liu Z, Bartlett S. Hyaluronic acid and its biomedical applications: A review. *Engineered Regeneration*. 2020;1:102–13.

66. Hesse E, Hefferan T, Tarara J, Haasper C, Meller R, Krettek C, et al. Collagen type I hydrogel allows migration, proliferation, and osteogenic differentiation of rat bone marrow stromal cells. *Journal of Biomedical Materials Research* Part A. 2010;9999A:NA–NA.

67. Kim H, Hong J, Kim Y, Han S-B. Stimulatory Effect of β-glucans on Immune Cells. *Immune Network*. 2011;11(4):191.

68. Lee BM, Park SJ, Noh I, Kim C-HH. The effects of the molecular weights of hyaluronic acid on the immune responses. *Biomater Res*. 2021;25(1):27.

69. Mathew-Steiner S, Roy S, Sen C. Collagen in Wound Healing. *Bioengineering*. 2021;8(5):63.

70. Farokhi M, Mottaghitalab F, Fatahi Y, Khademhosseini A, Kaplan D. Overview of Silk Fibroin Use in Wound Dressings. *Trends in Biotechnology*. 2018;36(9):907–22.

71. Lippens E, Swennen I, Gironès J, Declercq H, Vertenten G, Vlaminck L, et al. Cell survival and proliferation after encapsulation in a chemically modified Pluronic(R) F127 hydrogel. *J Biomater Appl*. 2013;27(7):828–39.

72. Russo E, Villa C. Poloxamer Hydrogels for Biomedical Applications. *Pharmaceutics*. 2019;11(12).

73. Devi RD, Sandhya P, Hari VB. Poloxamer: A novel functional molecule for drug delivery and gene therapy. *J Pharm Sci Res*. 2013;5(8):159–65.

74. Sriadibhatla S, Yang Z, Gebhart C, Alakhov VY, Kabanov A. Transcriptional activation of gene expression by pluronic block copolymers in stably and transiently transfected cells. *Mol Ther*. 2006;13(4):804–13.

75. Chung HJ, Lee Y, Park TG. Thermo-sensitive and biodegradable hydrogels based on stereocomplexed Pluronic multi-block copolymers for controlled protein delivery. *J Control Release*. 2008;127(1):22–30.

76. Park KM, Lee SY, Joung YK, Na JS, Lee MC, Park KD. Thermosensitive chitosan-Pluronic hydrogel as an injectable cell delivery carrier for cartilage regeneration. *Acta Biomater*. 2009;5(6):1956–65.

77. Park Y-JJ, Kwon R, Quan QZ, Oh DH, Kim JO, Hwang MR, et al. Development of novel ibuprofen-loaded solid dispersion with improved bioavailability using aqueous solution. *Arch Pharm Res*. 2009;32(5):767–72.

78. Yuan Y, Cui Y, Zhang L, Zhu H-PP, Guo Y-SS, Zhong B, et al. Thermosensitive and mucoadhesive in situ gel based on poloxamer as new carrier for rectal administration of nimesulide. *Int J Pharm*. 2012;430(1-2):114–9.

79. De Souza Ferreira SB, Moço TD, Borghi-Pangoni FB, Junqueira MV, Bruschi ML. Rheological, mucoadhesive and textural properties of thermoresponsive polymer blends for biomedical applications. *J Mech Behav Biomed Mater*. 2015;55:164–78.

80. Lee JH, Baek H-RR, Lee KM, Lee H-KK, Im SB, Kim YS, et al. The effect of poloxamer 407-based hydrogel on the osteoinductivity of demineralized bone matrix. Clin Orthop Surg. 2014;6(4):455–61.

81. Kikuchi A, Okano T. Nanostructured designs of biomedical materials: applications of cell sheet engineering to functional regenerative tissues and organs. *J Control Release*. 2005;101(1-3):69–84.

82. Dumortier G, Grossiord JL, Agnely F, Chaumeil JC. A review of poloxamer 407 pharmaceutical and pharmacological characteristics. *Pharm Res*. 2006;23(12):2709–28.

83. Soriano-Arandes A, Noguera-Julian A, López-Lacort M, Soler-Palacín P, Mur A, Méndez M, et al. Pregnancy as an opportunity to diagnose human-immunodeficiency virus immigrant women in Catalonia. *Enferm Infecc Microbiol Clin (Engl Ed)*. 2018;36(1):9–15.

84. Mayol L, Quaglia F, Borzacchiello A, Ambrosio L, La Rotonda MI. A novel poloxamers/hyaluronic acid in situ forming hydrogel for drug delivery: rheological, mucoadhesive and in vitro release properties. *Eur J Pharm Biopharm*. 2008;70(1):199–206.

85. Liu Y, Zhu YY, Wei G, Lu WY. Effect of carrageenan on poloxamer-based in situ gel for vaginal use: Improved in vitro and in vivo sustained-release properties. *Eur J Pharm Sci*. 2009;37(3-4):306–12.

86. Almeida H, Amaral MH, Lobão P, Lobo JMM. Influence of drug incorporation, temperature and storage time on the pH, textural and rheological properties of different poloxamer hydrogels. *Curr Drug Deliv*. 2013;10(6):753–64.

87. Qi H, Chen W, Huang C, Li L, Chen C, Li W, et al. Development of a poloxamer analogs/carbopol-based in situ gelling and mucoadhesive ophthalmic delivery system for puerarin. *Int J Pharm*. 2007;337(1-2):178–87.

88. M A Fathalla Z, Vangala A, Longman M, Khaled KA, Hussein AK, El-Garhy OH, et al. Poloxamer-based thermoresponsive ketorolac tromethamine in situ gel preparations: Design, characterisation, toxicity and transcorneal permeation studies. *Eur J Pharm Biopharm*. 2017;114:119–34.

89. Yu S, Zhang X, Tan G, Tian L, Liu D, Liu Y, et al. A novel pH-induced thermosensitive hydrogel composed of carboxymethyl chitosan and poloxamer cross-linked by glutaraldehyde for ophthalmic drug delivery. *Carbohydr Polym*. 2017;155:208–17.

90. Lou J, Hu W, Tian R, Zhang H, Jia Y, Zhang J, et al. Optimization and evaluation of a thermoresponsive ophthalmic in situ gel containing curcumin-loaded albumin nanoparticles. *Int J Nanomedicine*. 2014;9:2517–25.

91. Koffi AA, Agnely F, Ponchel G, Grossiord JL. Modulation of the rheological and mucoadhesive properties of thermosensitive poloxamer-based hydrogels intended for the rectal administration of quinine. *Eur J Pharm Sci.* 2006;27(4):328–35.

92. Ci T, Yuan L, Bao X, Hou Y, Wu H, Sun H, et al. Development and anti-Candida evaluation of the vaginal delivery system of amphotericin B nanosuspension-loaded thermogel. *J Drug Target*. 2018;26(9):829–39.

93. Mei L, Chen J, Yu S, Huang Y, Xie Y, Wang H, et al. Expansible thermal gelling foam aerosol for vaginal drug delivery. *Drug Deliv.* 2017;24(1):1325–37.

94. Hussain A, Ahsan F. The vagina as a route for systemic drug delivery. *J Control Release.* 2005;103(2):301–13.

95. Klouda L, Mikos AG. Thermoresponsive hydrogels in biomedical applications. *Eur J Pharm Biopharm*. 2008;68(1):34–45.

96. Ibrahim E-SA l-S, Ismail S, Fetih G, Shaaban O, Hassanein K, Abdellah NH. Development and characterization of thermosensitive pluronic-based metronidazole in situ gelling formulations for vaginal application. *Acta Pharm*. 2012;62(1):59–70.

97. Cafaggi S, Russo E, Caviglioli G, Parodi B, Stefani R, Sillo G, et al. Poloxamer 407 as a solubilising agent for tolfenamic acid and as a base for a gel formulation. *Eur J Pharm Sci*. 2008;35(1-2):19–29.

98. Liaw J, Lin Y. Evaluation of poly(ethylene oxide)-poly(propylene oxide)-poly(ethylene oxide) (PEO-PPO-PEO) gels as a release vehicle for percutaneous fentanyl. *J Control Release*. 2000;68(2):273–82.

99. Shin S-CC, Cho C-WW, Yang K-HH. Development of lidocaine gels for enhanced local anesthetic action. *Int J Pharm*. 2004;287(1-2):73–8.

100. Sivaraman A, Banga AK. Novel in situ forming hydrogel microneedles for transdermal drug delivery. *Drug Deliv Transl Res*. 2017;7(1):16–26.

101. Cui N, Dai C-YY, Mao X, Lv X, Gu Y, Lee E-SS, et al. Poloxamer-Based Scaffolds for Tissue Engineering Applications: A Review. *Gels*. 2022;8(6).

102. Pan JF, Liu NH, Sun H, Xu F. Preparation and characterization of electrospun PLCL/Poloxamer nanofibers and dextran/gelatin hydrogels for skin tissue engineering. *PLoS One*. 2014;9(11):e112885.

103. Yang X, Yang R, Chen M, Zhou Q, Zheng Y, Lu C, et al. KGF-2 and FGF-21 poloxamer 407 hydrogel coordinates inflammation and proliferation homeostasis to enhance wound repair of scalded skin in diabetic rats. *BMJ Open Diabetes Res Care*. 2020;8(1).

104. Lin S, Pei L, Zhang W, Shu G, Lin J, Li H, et al. Chitosan-poloxamer-based thermosensitive hydrogels containing zinc gluconate/recombinant human epidermal growth factor benefit for antibacterial and wound healing. *Mater Sci Eng C Mater Biol Appl*. 2021;130:112450.

105. Tonguc-Altin K, Sandalli N, Duman G, Selvi-Kuvvetli S, Topcuoglu N, Kulekci G. Development of novel formulations containing Lysozyme and Lactoferrin and evaluation of antibacterial effects on Mutans Streptococci and Lactobacilli. *Arch Oral Biol*. 2015;60(5):706–14.

106. Demirci S, Doğan A, Karakuş E, Halıcı Z, Topçu A, Demirci E, et al. Boron and Poloxamer (F68 and F127) Containing Hydrogel Formulation for Burn Wound Healing. *Biol Trace Elem Res*. 2015;168(1):169–80.

107. Suntornnond R, Tan EYSY, An J, Chua CK. A highly printable and biocompatible hydrogel composite for direct printing of soft and perfusable vasculature-like structures. *Sci Rep*. 2017;7(1):16902.

108. Suntornnond R, An J, Chua CK. Roles of support materials in 3D bioprinting - Present and future. *Int J Bioprint*. 2017;3(1):006.

109. Suntornnond R, Ng WL, Huang X, Yeow CHEH, Yeong WY. Improving printability of hydrogel-based bio-inks for thermal inkjet bioprinting applications via saponification and heat treatment processes. *J Mater Chem B*. 2022;10(31):5989–6000.

110. Li X, Li A, Feng F, Jiang Q, Sun H, Chai Y, et al. Effect of the hyaluronic acid-poloxamer hydrogel on skin-wound healing: in vitro and in vivo studies. *Animal Model Exp Med*. 2019;2(2):107–13.

111. Soriano-Ruiz JLL, Calpena-Campmany AC, Silva-Abreu M, Halbout-Bellowa L, Bozal-de Febrer N, Rodríguez-Lagunas MJJ, et al. Design and evaluation of a multifunctional thermosensitive poloxamer-chitosan-hyaluronic acid gel for the treatment of skin burns. *Int J Biol Macromol*. 2020;142:412–22.

112. Peng X, Ding C, Zhao Y, Hao M, Liu W, Yang M, et al. Poloxamer 407 and Hyaluronic Acid Thermosensitive Hydrogel-Encapsulated Ginsenoside Rg3 to Promote Skin Wound Healing. *Front Bioeng Biotechnol*. 2022;10:831007.

113. Jiang D, Liang J, Noble PW. Hyaluronan in tissue injury and repair. *Annu Rev Cell Dev Biol*. 2007;23:435–61.

114. Itano N, Kimata K. Mammalian hyaluronan synthases. *IUBMB Life*. 2002;54(4):195–9.

115. Yoshihara S, Kon A, Kudo D, Nakazawa H, Kakizaki I, Sasaki M, et al. A hyaluronan synthase suppressor, 4-methylumbelliferone, inhibits liver metastasis of melanoma cells. *FEBS Lett*. 2005;579(12):2722–6.

116. Masters KS, Shah DN, Walker G, Leinwand LA, Anseth KS. Designing scaffolds for valvular interstitial cells: cell adhesion and function on naturally derived materials. *J Biomed Mater Res A*. 2004;71(1):172–80.

117. Munakata H, Takagaki K, Majima M, Endo M. Interaction between collagens and glycosaminoglycans investigated using a surface plasmon resonance biosensor. *Glycobiology*. 1999;9(10):1023–7.

118. Tolg C, McCarthy JB, Yazdani A, Turley EA. Hyaluronan and RHAMM in wound repair and the "cancerization" of stromal tissues. *Biomed Res Int*. 2014;2014:103923.

119. Tolg C, Telmer P, Turley E. Specific sizes of hyaluronan oligosaccharides stimulate fibroblast migration and excisional wound repair. *PLoS ONE*. 2014;9(2):e88479.

120. Kreger ST, Voytik-Harbin SL. Hyaluronan concentration within a 3D collagen matrix modulates matrix viscoelasticity, but not fibroblast response. *Matrix Biol*. 2009;28(6):336–46.

121. Croce MA, Dyne K, Boraldi F, Quaglino D, Cetta G, Tiozzo R, et al. Hyaluronan affects protein and collagen synthesis by in vitro human skin fibroblasts. *Tissue Cell*. 2001;33(4):326–31.

122. David-Raoudi M, Tranchepain F, Deschrevel B, Vincent J-CC, Bogdanowicz P, Boumediene K, et al. Differential effects of hyaluronan and its fragments on fibroblasts: relation to wound healing. *Wound Repair Regen*. 2008;16(2):274–87.

123. Tolg C, Hamilton SR, Nakrieko K-AA, Kooshesh F, Walton P, McCarthy JB, et al. Rhamm-/- fibroblasts are defective in CD44-mediated ERK1,2 motogenic signaling, leading to defective skin wound repair. *J Cell Biol*. 2006;175(6):1017–28.

124. Kaya G, Rodriguez I, Jorcano JL, Vassalli P, Stamenkovic I. Selective suppression of CD44 in keratinocytes of mice bearing an antisense CD44 transgene driven by a tissue-specific promoter disrupts hyaluronate metabolism in the skin and impairs keratinocyte proliferation. *Genes Dev*. 1997;11(8):996–1007.

125. Smithmyer ME, Sawicki LA, Kloxin AM. Hydrogel scaffolds as in vitro models to study fibroblast activation in wound healing and disease. *Biomater Sci*. 2014;2(5):634–50.

126. Ghosh K, Ren X-DD, Shu XZ, Prestwich GD, Clark RA. Fibronectin functional domains coupled to hyaluronan stimulate adult human dermal fibroblast responses critical for wound healing. *Tissue Eng*. 2006;12(3):601–13.

127. Farran AJ, Teller SS, Jha AK, Jiao T, Hule RA, Clifton RJ, et al. Effects of matrix composition, microstructure, and viscoelasticity on the behaviors of vocal fold fibroblasts cultured in three-dimensional hydrogel networks. *Tissue Eng Part A*. 2010;16(4):1247–61.

128. Neuman MG, Nanau RM, Oruña-Sanchez L, Coto G. Hyaluronic acid and wound healing. *J Pharm Pharm Sci.* 2015;18(1):53–60.

129. Litwiniuk M, Krejner A, Speyrer MS, Gauto AR, Grzela T. Hyaluronic Acid in Inflammation and Tissue Regeneration. *Wounds*. 2016;28(3):78–88.

130. Huang G, Chen J. Preparation and applications of hyaluronic acid and its derivatives. *Int J Biol Macromol*. 2019;125:478–84.

131. Hirakura T, Yasugi K, Nemoto T, Sato M, Shimoboji T, Aso Y, et al. Hybrid hyaluronan hydrogel encapsulating nanogel as a protein nanocarrier: new system for sustained delivery of protein with a chaperone-like function. *J Control Release*. 2010;142(3):483–9.

132. Hahn SK, Kim JS, Shimobouji T. Injectable hyaluronic acid microhydrogels for controlled release formulation of erythropoietin. *J Biomed Mater Res A*. 2007;80(4):916–24.

133. Jung Y-SS, Park W, Park H, Lee D-KK, Na K. Thermo-sensitive injectable hydrogel based on the physical mixing of hyaluronic acid and Pluronic F-127 for sustained NSAID delivery. *Carbohydr Polym*. 2017;156:403–8.

134. Ilomuanya MO, Hameedat AT, Akang EN, Ekama SO, Silva BO, Akanmu AS. Development and evaluation of mucoadhesive bigel containing tenofovir and maraviroc for HIV prophylaxis. *Futur J Pharm Sci*. 2020;6(1):81.

135. Soriano JLL, Calpena AC, Rincón M, Pérez N, Halbaut L, Rodríguez-Lagunas MJJ, et al. Melatonin nanogel promotes skin healing response in burn wounds of rats. *Nanomedicine (Lond).* 2020;15(22):2133–47.

136. Ogundele MO. A novel anti-inflammatory activity of lysozyme: modulation of serum complement activation. *Mediators Inflamm*. 1998;7(5):363–5.

137. Lee W, Ku S-KK, Na DH, Bae J-SS. Anti-Inflammatory Effects of Lysozyme Against HMGB1 in Human Endothelial Cells and in Mice. *Inflammation*. 2015;38(5):1911–24.

138. Brock JH. Lactoferrin in human milk: its role in iron absorption and protection against enteric infection in the newborn infant. *Arch Dis Child*. 1980;55(6):417–21.

139. Kondo T, Ohshima T, Mori R, Guan DW, Ohshima K, Eisenmenger W. Immunohistochemical detection of chemokines in human skin wounds and its application to wound age determination. *Int J Legal Med*. 2002;116(2):87–91.

140. Engelmayer J, Blezinger P, Varadhachary A. Talactoferrin stimulates wound healing with modulation of inflammation. *J Surg Res*. 2008;149(2):278–86.

141. Tang L, Cui T, Wu JJ, Liu-Mares W, Huang N, Li J. A rice-derived recombinant human lactoferrin stimulates fibroblast proliferation, migration, and sustains cell survival. *Wound Repair Regen*. 2010;18(1):123–31.

142. Takayama Y, Mizumachi K. Effects of lactoferrin on collagen gel contractile activity and myosin light chain phosphorylation in human fibroblasts. *FEBS Lett*. 2001;508(1):111–6.

143. Heldin CH, Westermark B. Mechanism of action and in vivo role of platelet-derived growth factor. *Physiol Rev*. 1999;79(4):1283–316.

144. Tang L, Wu JJ, Ma Q, Cui T, Andreopoulos FM, Gil J, et al. Human lactoferrin stimulates skin keratinocyte function and wound re-epithelialization. *Br J Dermatol*. 2010;163(1):38–47.

145. Saito S, Takayama Y, Mizumachi K, Suzuki C. Lactoferrin promotes hyaluronan synthesis in human dermal fibroblasts. *Biotechnol Lett*. 2011;33(1):33–9.

146. Mast BA, Diegelmann RF, Krummel TM, Cohen IK. Hyaluronic acid modulates proliferation, collagen and protein synthesis of cultured fetal fibroblasts. *Matrix*. 1993;13(6):441–6.

147. Norrby K. Human apo-lactoferrin enhances angiogenesis mediated by vascular endothelial growth factor A in vivo. *J Vasc Res*. 2004;41(4):293–304.

148. Icriverzi M, Dinca V, Moisei M, Evans RW, Trif M, Roseanu A. Lactoferrin in Bone Tissue Regeneration. *Curr Med Chem*. 2020;27(6):838–53.

149. Amini AA, Kan H-MM, Cui Z, Maye P, Nair LS. Enzymatically cross-linked bovine lactoferrin as injectable hydrogel for cell delivery. *Tissue Eng Part A*. 2014;20(21-22):2830–9.

150. Amini AA, Nair LS. Recombinant human lactoferrin as a biomaterial for bone tissue engineering: mechanism of antiapoptotic and osteogenic activity. *Adv Healthc Mater*. 2014;3(6):897–905.

151. Bastos AR, da Silva LPP, Maia FR, Pina S, Rodrigues T, Sousa F, et al. Lactoferrin-Hydroxyapatite Containing Spongy-Like Hydrogels for Bone Tissue Engineering. *Materials (Basel)*. 2019;12(13).

152. Amirthalingam S, Lee SS, Rajendran AK, Kim I, Hwang NS, Rangasamy J. Addition of lactoferrin and substance P in a chitin/PLGA-CaSO4 hydrogel for regeneration of calvarial bone defects. *Mater Sci Eng C Mater Biol Appl*. 2021;126:112172.

153. Park YE, Chandramouli K, Watson M, Zhu M, Callon KE, Tuari D, et al. Sustained Delivery of Lactoferrin Using Poloxamer Gels for Local Bone Regeneration in a Rat Calvarial Defect Model. *Materials (Basel)*. 2021;15(1).

154. Suleman Ismail Abdalla S, Katas H, Chan JY, Ganasan P, Azmi F, Fauzi MB. Gelatin Hydrogels Loaded with Lactoferrin-Functionalized Bio-Nanosilver as a Potential Antibacterial and Anti-Biofilm Dressing for Infected Wounds: Synthesis, Characterization, and Deciphering of Cytotoxicity. *Mol Pharm*. 2021;18(5):1956–69.

155. Ammons MC, Ward LS, James GA. Anti-biofilm efficacy of a lactoferrin/xylitol wound hydrogel used in combination with silver wound dressings. *Int Wound J*. 2011;8(3):268–73.

156. Abeyrathne ED, Lee HY, Ahn DU. Egg white proteins and their potential use in food processing or as nutraceutical and pharmaceutical agents--a review. *Poult Sci*. 2013;92(12):3292–9.

157. Witholt B, Heerikhuizen HV, De Leij L. How does lysozyme penetrate through the bacterial outer membrane? *Biochim Biophys Acta*. 1976;443(3):534–44.

158. Bianchi C. Is Fleming's lysozyme an analgesic agent? An experimental reappraisal of clinical data. *Eur J Pharmacol*. 1981;71(2-3):211–21.

159. Gordon LI, Douglas SD, Kay NE, Yamada O, Osserman EF, Jacob HS. Modulation of neutrophil function by lysozyme. Potential negative feedback system of inflammation. *J Clin Invest*. 1979;64(1):226–32.

160. Gasior-Chrzan B. Effect of ovalbumin lysozyme on healing of standard skin wounds in guinea pigs. *Przegl Dermatol*. 1988;75(6):431–4.

161. Gasior-Chrzan B. Clinical trial of lysozyme treatment of crural ulcers in humans. *Przegl Dermatol*. 1988;75(6):435–8.

162. Li W, Jiang Y-XX, Chen Q-YY, Wang G-GG. Recombinant fusion protein by lysozyme and antibacterial peptide enhances ischemic wound healing via angiogenesis and reduction of inflammation in diabetic db/db mice. *PeerJ*. 2021;9:e11256.

163. Chen Q, Li W, Wang J, Qu X, Wang G. Lysozyme-Antimicrobial Peptide Fusion Protein Promotes the Diabetic Wound Size Reduction in Streptozotocin (STZ)-Induced Diabetic Rats. *Med Sci Monit*. 2018;24:8449–58.

164. Han HB, Li, Yu, Ma WZ, Cao ZC, An GF, et al. Egg White Lysozyme Promoted Collagen Secreting of Dermal Fibroblasts in Mice. *Asian Journal of Animal and Veterinary Advances*. 2011;6(7):667–77.

165. Yang Y, Zhang C, Cao Y, Qu Y, Li T, Yang T, et al. Bidirectional regulation of i-type lysozyme on cutaneous wound healing. *Biomedicine & Pharmacotherapy*. 2020;131:110700.

166. Charernsriwilaiwat N, Opanasopit P, Rojanarata T, Ngawhirunpat T. Lysozyme-loaded, electrospun chitosan-based nanofiber mats for wound healing. *Int J Pharm*. 2012;427(2):379–84.

167. Tonglairoum P, Ngawhirunpat T, Rojanarata T, Opanasopit P. Lysozyme-immobilized electrospun PAMA/PVA and PSSA-MA/PVA ion-exchange nanofiber for wound healing. *Pharm Dev Technol*. 2015;20(8):976–83.

168. Kim S, Fan J, Lee C-SS, Lee M. Dual Functional Lysozyme-Chitosan Conjugate for Tunable Degradation and Antibacterial Activity. *ACS Appl Bio Mater*. 2020;3(4):2334–43.

169. Xiao L, Ni W, Zhao X, Guo Y, Li X, Wang F, et al. A moisture balanced antibacterial dressing loaded with lysozyme possesses antibacterial activity and promotes wound healing. *Soft Matter*. 2021;17(11):3162–73.

170. Zhao X, Wang L, Gao J, Chen X, Wang K. Hyaluronic acid/lysozyme self-assembled coacervate to promote cutaneous wound healing. *Biomater Sci*. 2020;8(6):1702–10.

171. Tan H, Sun J, Jin D, Song J, Lei M, Antoshin A, et al. Coupling PEG-LZM polymer networks with polyphenols yields suturable biohydrogels for tissue patching. *Biomater Sci*. 2020;8(12):3334–47.

172. Lee JB, Yoon JJ, Lee DS, Park TG. Photo-crosslinkable, thermo-sensitive and biodegradable pluronic hydrogels for sustained release of protein. *J Biomater Sci Polym Ed*. 2004;15(12):1571–83.

173. Blanco D, Alonso MJ. Protein encapsulation and release from poly(lactide-co-glycolide) microspheres: effect of the protein and polymer properties and of the co-encapsulation of surfactants. *Eur J Pharm Biopharm*. 1998;45(3):285–94.

174. Paillard-Giteau A, Tran VT, Thomas O, Garric X, Coudane J, Marchal S, et al. Effect of various additives and polymers on lysozyme release from PLGA microspheres prepared by an s/o/w emulsion technique. *Eur J Pharm Biopharm*. 2010;75(2):128–36.

175. Hiwale P, Lampis S, Conti G, Caddeo C, Murgia S, Fadda AM, et al. In vitro release of lysozyme from gelatin microspheres: effect of cross-linking agents and thermoreversible gel as suspending medium. *Biomacromolecules*. 2011;12(9):3186–93.

176. Lee RC, Despa F, Guo L, Betala P, Kuo A, Thiyagarajan P. Surfactant copolymers prevent aggregation of heat denatured lysozyme. *Ann Biomed Eng*. 2006;34(7):1190–200.

177. Giuliano E, Paolino D, Fresta M, Cosco D. Mucosal Applications of Poloxamer 407-Based Hydrogels: An Overview. *Pharmaceutics*. 2018;10(3).

178. Niaz B, Saeed F, Ahmed A, Imran M, Maan A, Khan M, et al. Lactoferrin (LF): a natural antimicrobial protein. *International Journal of Food Properties*. 2019;22(1):1626–41.

179. Cory AH, Owen TC, Barltrop JA, Cory JG. Use of an aqueous soluble tetrazolium/formazan assay for cell growth assays in culture. *Cancer Commun*. 1991;3(7):207–12.

180. Chen H-CC. Boyden chamber assay. *Methods Mol Biol*. 2005;294:15–22.

181. Liang C-CC, Park AY, Guan J-LL. In vitro scratch assay: a convenient and inexpensive method for analysis of cell migration in vitro. *Nat Protoc*. 2007;2(2):329–33.

182. Vang Mouritzen M, Jenssen H. Optimized Scratch Assay for In Vitro Testing of Cell Migration with an Automated Optical Camera. *J Vis Exp*. 2018;(138).

183. Moniri M, Boroumand Moghaddam A, Azizi S, Abdul Rahim R, Zuhainis Saad W, Navaderi M, et al. Molecular study of wound healing after using biosynthesized BNC/Fe3O4 nanocomposites assisted with a bioinformatics approach. *Int J Nanomedicine*. 2018;13:2955–71.

184. Reiss MJ, Han Y-PP, Garcia E, Goldberg M, Yu H, Garner WL. Matrix metalloproteinase-9 delays wound healing in a murine wound model. *Surgery*. 2010;147(2):295–302.

185. Hariono M, Yuliani S, Istyastono E, Riswanto F, Adhipandito C. Matrix metalloproteinase 9 (MMP9) in wound healing of diabetic foot ulcer: Molecular target and structure-based drug design. *Wound Medicine*. 2018;22:1–13.

186. Zhang Q, Pan Y, Ji J, Xu Y, Zhang Q, Qin L. Roles and action mechanisms of WNT4 in cell differentiation and human diseases: a review. *Cell Death Discov*. 2021;7(1):287.

187. Zhang B, Wang M, Gong A, Zhang X, Wu X, Zhu Y, et al. HucMSC-Exosome Mediated-Wnt4 Signaling Is Required for Cutaneous Wound Healing. *Stem Cells*. 2015;33(7):2158–68.

188. Choi S, Yoon M, Choi K-Y. Approaches for Regenerative Healing of Cutaneous Wound with an Emphasis on Strategies Activating the Wnt/β-Catenin Pathway. *Advances in Wound Care*. 2022;11(2):70–86.

189. Zhang H, Nie X, Shi X, Zhao J, Chen Y, Yao Q, et al. Regulatory Mechanisms of the Wnt/β-Catenin Pathway in Diabetic Cutaneous Ulcers. *Frontiers in Pharmacology*. 2018;9.

190. Ding X, Tang Q, Xu Z, Xu Y, Zhang H, Zheng D, et al. Challenges and innovations in treating chronic and acute wound infections: from basic science to clinical practice. *Burns Trauma*. 2022;10:tkac014.

191. Yen C-CC, Shen C-JJ, Hsu W-HH, Chang Y-HH, Lin H-TT, Chen H-LL, et al. Lactoferrin: an iron-binding antimicrobial protein against Escherichia coli infection. *Biometals*. 2011;24(4):585–94.

192. Da Silva AS, Honjoya ER, Cardoso SC, De Souza CHH, Costa MDR de R, De Santana EH, et al. Antimicrobial action of lactoferrin on Staphylococcus aureus inoculated in Minas frescal cheese. *Arch Latinoam Nutr*. 2012;62(1):68–72.

193. Aguila A, Herrera A, Morrison D, Cosgrove B, Perojo A, Montesinos I, et al. Bacteriostatic activity of human lactoferrin against Staphylococcus aureus is a function of its iron-binding properties and is not influenced by antibiotic resistance. *FEMS Immunology & Medical Microbiology*. 2001;31(2):145–52.

194. Bera A, Herbert S, Jakob A, Vollmer W, Götz F. Why are pathogenic staphylococci so lysozyme resistant? The peptidoglycan O-acetyltransferase OatA is the major determinant for lysozyme resistance of Staphylococcus aureus. *Molecular Microbiology*. 2005;55(3):778–87.

195. Shimada T, Park B, Wolf A, Brikos C, Goodridge H, Becker C, et al. Staphylococcus aureus Evades Lysozyme-Based Peptidoglycan Digestion that Links Phagocytosis, Inflammasome Activation, and IL-1β Secretion. *Cell Host & Microbe*. 2010;7(1):38–49.

196. Graham DR, Dixon RE, Hughes JM, Thornsberry C. Disk diffusion antimicrobial susceptibility testing for clinical and epidemiologic purposes. *Am J Infect Control*. 1985;13(6):241–9.

197. Melo RS, Albuquerque Azevedo ÁMM, Gomes Pereira AMM, Rocha RR, Bastos Cavalcante RM, Carneiro Matos MN, et al. Chemical Composition and Antimicrobial Effectiveness of Ocimum gratissimum L. Essential Oil Against Multidrug-Resistant Isolates of Staphylococcus aureus and Escherichia coli. *Molecules*. 2019;24(21).

198. Ibrahim MM, Chen L, Bond JE, Medina MA, Ren L, Kokosis G, et al. Myofibroblasts contribute to but are not necessary for wound contraction. *Lab Invest*. 2015;95(12):1429–38.

199. Cho H, Jammalamadaka U, Tappa K, Egbulefu C, Prior J, Tang R, et al. 3D Printing of Poloxamer 407 Nanogel Discs and Their Applications in Adjuvant Ovarian Cancer Therapy. *Mol Pharm*. 2019;16(2):552–60.

APPENDIX A: ETHICAL APPROVAL FORM

YEDİTEPE ÜNİVERSİTESİ

T.C. YEDİTEPE ÜNİVERSİTESİ, DENEY HAYVANLARI ETİK KURULU

(YÜDHEK)

ETİK KURUL KARARI

Toplantı Tarihi	Karar No	İlgi	Proje Yürütücüsü
24.10.2017	625	16.10.2017	Dr. Öğr. Üyesi Gülengül Duman

'Laktoferin ve Lizozim İçeren Pluronic F127 Hidrojel Formülasyonlarının Yara İyileştirme Etkisinin Sıçanlar Üzerinde Araştırılması' adlı bilimsel çalışma etik kurulumuzda görüşülmüş olup, çalışmanın etik kurallara uygun olduğuna oy birliğiyle karar verilmiştir.

Etik Onay Geçerlilik Süresi: 3 Yıl	**Hayvan Türü ve cinsiyeti:** **Sıçan / Dişi**	**Hayvan Sayısı:** 36

GÖREVİ	ADI SOYADI	
Başkan	Prof. Dr. Bayram YILMAZ	
Başkan Yardımcısı	Prof. Dr. Erdem YEŞİLADA	**Katılmadı**
Raportör	Vet. Hekim Engin SÜMER	
Üye	Prof. Dr. M. Ece GENÇ	
Üye	Doç. Dr. Rukset ATTAR	
Üye	Doç. Dr. Soner DOĞAN	**Katılmadı**
Üye	Doç. Dr. Ediz DENİZ	
Üye	Prof. Dr. Gamze TORUN KÖSE	
Üye	Doç. Dr. Aylin YABA UÇAR	
Üye	Hakan GÖKSEL	
Üye	Ahmet ŞENKARDEŞLER	

APPENDIX B: NUMERICAL DATA OF GRAPHICAL IMAGES

Table B.1. to Table B.3. represent the data obtained from spectrophotometric measurements following MTS and MTT assays. Table B.4. shows the numbers of the fibroblasts that migrated towards the lower compartments in transwell migration assay. Table B.5. and Table B.6. demonstrate the data obtained from the scratch assay that was performed with 1% FBS, by means of area measurements and percent healing rates, respectively. They were followed by the same for 5% FBS treatment, which were shown in Tables B.7. and B.8. Table B.9. demonstrates the calculated ΔCT values for the QRT-PCR analysis, when it is supported by Table B.10., which indicates the relative mRNA expression values for Mmp9, Wnt4 and β-cat. Measured dimensions of *in vivo* wounds at different time points are mentioned in Table B.11. Finally, damage and healing scores obtained from histopathological observations for each animal are represented in Table B.12.

Table B.1. Spectrophotometric data obtained from MTS assay for tested concentrations of LF and LYZ

		Lactoferrin				Lysozyme			
	Control	400 µg/ml	200 µg/ml	100 µg/ml	50 µg/ml	400 µg/ml	200 µg/ml	100 µg/ml	50 µg/ml
Replicate 1	0.931341	0.978331	0.929112	0.961396	0.976887	0.819038	1.00261	1.00228	1.02243
Replicate 2	0.911163	1.09468	0.973599	1.01661	0.917302	0.907775	1.00123	0.975224	0.984014
Replicate 3	0.949749	1.09821	1.06327	0.957965	0.928151	0.94712	1.00241	0.988019	0.913643
% viability 1	100.0633897	105.112001	99.82390564	103.2925025	104.9568574	87.99754177	107.7205397	107.6850844	109.85
% viability 2	97.89546291	117.6125516	104.6035943	109.2247013	98.55503781	97.53145578	107.5722723	104.7781845	105.7226
% viability 3	102.0411474	117.9918152	114.2378574	102.9238755	99.72065569	101.7586873	107.6990516	106.1528808	98.16191
Mean	100	113.5721226	106.2217858	105.1470264	101.077517	95.76256163	107.6639545	106.2053833	104.5782
SD	1.693062057	5.98421277	5.994687034	2.887276223	2.784077104	5.755520349	0.065419967	1.187317467	4.839774

Table B.2. Spectrophotometric data obtained from MTT assay for combinationally-tested LF and LYZ concentrations

Protein concentration (µl/ml)	LF 800-LYZ 800	LF 800-LYZ 400	LF 800-LYZ 200	LF 400-LYZ 800	LF 400-LYZ 400	LF 400-LYZ 200	LF 200-LYZ 800	LF 200-LYZ 400	LF 200-LYZ 200
Replicate 1	0.477988	0.396146	0.409981	0.366471	0.411594	0.480582	0.360371	0.415418	0.381547
Replicate 2	0.343988	0.405736	0.379608	0.360961	0.369662	0.447405	0.344211	0.392416	0.385174

Replicate 3	0.392768	0.334534	0.379431	0.351731	0.423391	0.451044	0.372911	0.400679	0.387614
% viability	131.0997	108.6526	112.4472	100.5134	112.8895	131.8112	98.84037	113.9384	104.6484
% viability	94.34703	111.2829	104.1167	99.00219	101.3886	122.7116	94.4081	107.6296	105.6432
% viability	107.7261	91.75405	104.0681	96.47064	116.1251	123.7097	102.2798	109.8959	106.3124
Mean	111.0576	103.8965	106.8773	98.66209	110.1344	126.0775	98.50941	110.488	105.5347
SD	15.18803	8.652912	3.938538	1.667894	6.323696	4.07476	3.222102	2.609381	0.683654

Table B.3. Spectrophotometric data obtained from MTT assay for solely-tested LF and LYZ concentrations

Protein concentration (µl/ml)	LF 800	LF 400	LF 200	LYZ 800	LYZ 400	LYZ 200
Replicate 1	0.517553	0.475345	0.451395	0.324286	0.361826	0.432144
Replicate 2	0.477938	0.405765	0.359207	0.295744	0.338655	0.467811
Replicate 3	0.445213	0.393052	0.367493	0.414676	0.371074	0.442068
% viability	141.9512	130.3746	123.8059	88.9431	99.23953	118.5258
% viability	131.0858	111.2907	98.52111	81.11478	92.88433	128.3084
% viability	122.1102	107.8038	100.7937	113.7347	101.776	121.2477
Mean	131.7158	116.4897	107.7069	94.59754	97.96662	122.694
SD	8.112282	9.920789	11.42143	13.90431	3.739941	4.122555

Table B.4. Numbers of the migrated cells on transwell inserts

	Control 1	Control 2	Control 3	LF 1	LF 2	LF 3	LYZ 1	LYZ 2	LYZ 3	LF-LYZ 1	LF-LYZ 2	LF-LYZ 3
Area 1	91	118	79	46	63	65	135	133	123	97	104	100
Area 2	117	86	82	75	45	54	109	159	80	131	73	82
Area 3	135	122	133	114	116	122	144	161	146	135	140	121
Area 4	22	136	64	93	71	55	146	152	141	132	130	97
Area 5	111	78	75	66	74	97	56	71	129	110	120	139
Total	476	540	433	394	369	393	590	676	619	605	567	539
Average	95.2	108	86.6	78.8	73.8	78.6	118	135.2	123.8	121	113.4	107.8
Replicates average	96.6			77.06667			125.6667			114.0667		
SD	8.792421			2.311325			7.144851			5.409457		

Table B.5. Scratch wound areas measured by ImageJ Software at different time points for the trial with 1% FBS

Time point	Control	Area	LF	Area	LYZ	Area	LF-LYZ	Area

0 hours	1	3914768	1	4424416	1	4418640	1	4053056
	2	4251648	2	4584192	2	4168384	2	4199552
	3	4443120	3	4314112	3	4834800	3	4767072
	4	3895296	4	4455360	4	4748912	4	4779584
	5	4272800	5	4419296	5	4712400	5	4553584
	6	4614624	6	4309424	6	4021696	6	4077472
6 hours	1	3720960	1	4021696	1	3889248	1	3767328
	2	4046144	2	4051440	2	4063680	2	3621024
	3	4156160	3	3850560	3	4018080	3	3782160
	4	3813888	4	4187344	4	4058368	4	4237248
	5	4107264	5	4081248	5	4363968	5	4019664
	6	4119488	6	4046144	6	3640624	6	3544960
18 hours	1	2505920	1	2843392	1	2496960	1	3011040
	2	2820048	2	2897088	2	2815200	2	2922240
	3	3276032	3	2970944	3	2877312	3	3280320
	4	3499104	4	3332784	4	3451680	4	3606080
	5	3745440	5	2904672	5	2860416	5	3348400
	6	3382656	6	2860416	6	2958208	6	2840736
24 hours	1	2459552	1	2481472	1	1804416	1	2970432
	2	2706624	2	2276640	2	2276640	2	2649136

	3	3072240	3	2144800	3	2689280	3	2922240
	4	2840736	4	2508256	4	2276640	4	3141152
	5	3361600	5	2060448	5	2236992	5	2922240
	6	3153792	6	2091520	6	2624720	6	2483904
48 hours	1	12224	1	12272	1	12272	1	1870272
	2	12192	2	476736	2	12224	2	852320
	3	1162800	3	12288	3	245760	3	878976
	4	257376	4	232560	4	697680	4	524944
	5	1018576	5	24416	5	12256	5	316160
	6	12288	6	12272	6	709920	6	12272

Table B.6. Percent healing rates of the scratches treated with the media containing 1% FBS

Time point	Control	LF	LYZ	LF-LYZ
6 hours	4.950689	9.102218	11.98088	7.049692874
	4.833514	11.6215	2.511861	13.77594562
	6.458525	10.74502	16.89253	20.66073263
	2.089905	6.015586	14.5411	11.34692894
	3.874181	7.649363	7.393939	11.72526959
	10.72971	6.109401	9.475405	13.0598567

Average	4.441363	8.540514	10.46595	12.93640439
18 hours	35.98803	35.73407	43.4903	25.70939064
	33.67165	36.80265	32.46304	30.41543479
	26.26731	31.13429	40.48747	31.18794933
	10.17104	25.19608	27.3164	24.55242967
	12.34226	34.27297	39.30023	26.46671281
	26.69704	33.62417	26.44377	30.33095016
Average	24.18955	32.79404	34.91687	28.1104779
24 hours	37.17247	43.91413	59.16354	26.7113013
	36.33941	50.33716	45.38315	36.91860465
	30.85399	50.28409	44.3766	38.69947842
	27.07265	43.70251	52.05976	34.27980343
	21.32559	53.3761	52.52967	35.82549482
	31.65658	51.46637	34.73599	39.08225489
Average	30.73678	48.84673	48.04145	35.25282292

Table B.7. Scratch wound areas measured by ImageJ Software at different time points for the trial with 5% FBS

Area								
0 hours					24 hours			
Control	LF	LYZ	LF-LYZ		Control	LF	LYZ	LF-LYZ
4376906	4658360	4941958	4301003		2334797	1764771	593282	789077
4480028	5217306	4637980	4738444		2340010	1160155	368915	102356
4467084	5068179	5144744	4842809		1423426	931621	1143736	714243
4441339	4981282	4908227	4627419	Average	2032744	1285516	701977.7	535225.3

Table B.8. Percent healing rates of the scratches treated with the media containing 5% FBS

	Control	LF	LYZ	LF-LYZ
% healing	46.65645	62.11605	87.995	81.65365
	47.76796	77.76333	92.04578	97.83988
	68.13523	81.61823	77.76885	85.25147
Mean	54.18655	73.83254	85.93654	88.24834
SD	9.873641	8.432958	6.007533	6.939472

Table B.9. Delta cycle threshold (ΔCT) values from QRT-PCR for Mmp9, Wnt4 and β-cat

ΔCT		
Ctrl-MMP9	Ctrl-Wnt4	Ctrl-β-cat
0.87	8.995	12.73
LF-MMP9	LF-Wnt4	LF- β-cat
0.27	7.51	11.04
LYZ-MMP9	LYZ-Wnt4	LYZ- β-cat
0.97	7.5	10.425
LF-LYZ-MMP9	LF-LYZ-Wnt4	LF-LYZ- β-cat
0.695	6.82	10.24

Table B.10. Relative mRNA expression levels of Mmp9, Wnt4 and β-cat

		Mmp9			Wnt4			β-cat		
	Control	LF	LYZ	LF-LYZ	LF	LYZ	LF-LYZ	LF	LYZ	LF-LYZ
	100	184.0375	92.65881	100.6956	450.0234	181.50383	489.0561	581.589	636.429187	751.618199
	100	124.8331	93.95227	126.5757	174.1101	437.71748	416.9863	179.005	383.7056477	419.886673
Mean	100	154.4353	93.30554	113.6356	312.0668	309.61066	453.0212	380.297	510.0674174	585.752436
SD	0	29.60224	0.646734	12.94005	137.9566	128.10682	36.0349	201.292	126.3617696	165.865763

Table B.11. Wound areas measured by a caliper at different time points

	Day 0		Day 3		Day 5		Day 7		Day 8	
Hydrogel										
Animal	Left	Right	Left	Right	Left	Right	Left	Right	Left	Right
1	55.045	55.61	42.8085	30.4196	16.512	17.1556	6.5394	7.5035	3.429	3.5224
2	37.5575	48.8475	21.4016	26.5762	21.7782	28.0795	8.602	9.563	4.2228	6.6708
3	33.1525	30.71	21.3003	21.0028	14.3538	14.523	8.8592	7.6857	1.9118	4.0375
4	48.505	45.765	29.6964	22.0293	26.502	15.8627	16.467	4.5461	9.801	2.95
5	50.085	32.085	31.428	21.912	20.5344	14.4228	6.8283	6.0415	4.8195	3.7674
6	41.31	38.885	28.0734	25.0206	26.4552	20.601	15.2932	5.427	6.3888	3.8808
Average	44.27583	41.98375	29.11803	24.49342	21.0226	18.44077	10.43152	6.794467	5.095483	4.13815
Hydrogel-LF-LYZ										
	Left	Right	Left	Right	Left	Right	Left	Right	Left	Right
1	40.9425	35.7175	30.6812	24.1844	16.3856	20.237	16.02	4.1987	5.52	3.075
2	44.4175	45.045	30.5983	25.0096	27.412	22.22	11.0021	6.9751	7.4683	2.244
3	38.4625	32.595	41.2692	27.702	33.7692	18.411	9.6728	5.8384	4.9764	3.0825
4	32.25	40.755	26.452	27.494	24.2481	27.1327	13.0134	8.2228	6.6006	3.5462
5	35.86	61.77	24.6636	44.7051	16.0085	26.989	5.525	8.2256	2.809	3.42

6	43.8325	37.0125	38.7994	32.41	32.5707	19.4565	12.3216	11.556	7.8016	4.1474
Average	39.29417	42.14917	32.07728	30.25085	25.06568	22.4077	11.25915	7.502767	5.86265	3.252517
Hydrogel-LF										
	Left	Right	Left	Right	Left	Right	Left	Right	Left	Right
1	38.72	45.315	34.6884	26.334	20.0655	15.2881	8.712	12.712	3.2657	4.6299
2	40.7	33.605	34.6579	33.2775	19.4742	12.6882	7.5646	9.282	3.8106	3.0414
3	40.26	37.95	28.1784	24.0426	20.1366	23.52	9.5613	10.9224	3.7908	3.78
4	61.2	47.31	48.0145	33.7174	20.3848	15.9125	22.1088	8.9838	8.4807	3.8232
5	47.1225	35.7	37.1259	22.8552	21.125	13.166	11.3364	7.5744	4.5424	2.2479
6	39.1375	28.1475	30.1464	23.1231	22.1368	13.908	10.282	6.357	4.3992	2.5344
Average	44.52333	38.00458	35.46858	27.22497	20.55382	15.74713	11.59418	9.305267	4.7149	3.3428
Hydrogel-LYZ										
	Left	Right	Left	Right	Left	Right	Left	Right	Left	Right
1	37.536	40.5405	54.1101	30.32	29.026	25.6859	8.96	7.1238	8.8298	4.8336
2	31.6572	38.5029	34.3824	33.232	23.2245	13.366	6.1236	7.0761	3.969	7.4562
3	37.4468	38.3454	28.1655	26.3304	29.1456	19.0356	12.5118	8.4138	8.4474	6.0352
4	48.1164	28.8225	32.24	30.4484	20.4798	21.66	N/A	6.7236	N/A	5.5533
5	43.0268	37.3748	34.888	33.698	27.9285	34.128	6.7914	6.9112	3.0282	3.7389
6	73.2547	43.8084	39.38	24.934		22.23		7.4304		5.8596
Average	45.17298	37.89908	37.19433	29.82713	25.96088	22.68425	8.5967	7.279817	6.0686	5.579467

Madecassol®										
	Left	Right	Left	Right	Left	Right	Left	Right	Left	Right
1	41.7998	48.603	32.7096	30.5106	25.3125	21.8564	7.6356	17.2341	5.8308	4.9408
2	59.2516	64.8	42.9538	48.0318	43.173	12.3921	29.7305	5.7984	21.462	6.6222
3	38.2966	41.2985	48.8074	26.3289	36.2516	23.5926	14.2709	31.6589	13.8807	17.0156
4	29.4892	32.2092	23.374	39.837	26.2548	17.5985	17.9744	14.7048	9.4872	9.8048
5	41.0326	45.1113	38.8994	20.0716	38.2528	15.0297	8.9994	4.4436	4.8114	4.6665
6	43.5942	47.3871	42.8127	34.009	35.9046	34.1562	35.7406	10.4808	8.164	4.3212
Average	42.244	46.56818	38.25948	33.13148	34.19155	20.77092	19.05857	14.05343	10.60602	7.895183
Isotonic										
	Left	Right	Left	Right	Left	Right	Left	Right	Left	Right
1	42.7638	43.6852	39.4632	31.0708	15.4607	12.654	5.4015	7.9722	3.161	3.5316
2	38.0224	34.7072	39.0978	18.9024	40.824	22.3054	11.5775	5.61	5.6244	2.736
3	55.751	42.4125	47.724	28.4275	31.242	12.8714	15.0588	3.32	9.5232	2.9784
4	26.964	38.537	29.6078	25.7004	21.7035	17.7536	12.44	7.8228	5.3848	2.7807
5	47.8431	47.9408	35.659	37.8882	37.44	30.528	10.6166	8.2566	7.9401	4.9196
6	37.45	38.3554	37.9293	25.3101	19.158	14.964	10.8336	8.8168	5.3714	4.165
Average	41.46572	40.93968	38.24685	27.88323	27.63803	18.51273	10.988	6.9664	6.167483	3.51855

Table B.12. Damage and healing scores obtained from histopathological analysis

	Animal	Edema	Degeneration of epithelium	Congestion	Mononucleic cell infiltration	Damage total score	Fiber regeneration	Tissue regeneration	Healing total score
Hydrogel	1	1	0	1	1	3	3	2	5
	2	1	2	1	0	4	3	2	5
	3	1	2	2	1	6	3	2	5
	4	1	1	2	1	5	1	2	1
	5	1	1	1	1	4	2	2	1
	6	0	1	1	1	3	3	3	1
Mean						4.166666667			3
SD						1.169045194			2.19089023
	Animal	Edema	Degeneration of epithelium	Congestion	Mononucleic cell infiltration	Damage total score	Fiber regeneration	Tissue regeneration	Healing total score
Hydrogel LF	1	0	1	1	0	2	0	1	1
	2	0	1	1	0	2	0	0	0

LYZ	3	1	1	0	1	3	1	0	1
	4	0	0	0	1	1	1	0	1
	5	0	0	0	1	1	1	1	2
	6	1	1	1	1	4	0	1	1
Mean						2.166666667			1
SD						1.169045194			0.632455532
	Animal	Edema	Degeneration of epithelium	Congestion	Mononucleic cell infiltration	Damage total score	Fiber regeneration	Tissue regeneration	Healing total score
Hydrogel LF	1	1	1	0	2	4	1	0	1
	2	0	1	0	1	2	0	1	1
	3	0	0	1	1	2	1	0	1
	4	0	0	1	1	2	0	1	1
	5	0	0	0	0	0	1	0	1
	6	0	1	1	0	2	1	1	2
Mean						2			1.166666667
SD						1.264911064			0.40824829

	Animal	Edema	Degeneration of epithelium	Congestion	Mononucleic cell infiltration	Damage total score	Fiber regeneration	Tissue regeneration	Healing total score
Hydrogel LYZ	1	0	2	0	2	4	0	0	0
	2	1	1	1	1	4	1	1	2
	3	1	1	0	1	3	1	1	2
	4	0	0	0	1	1	1	1	2
Mean						3			1.5
SD						1.414213562			1
	Animal	Edema	Degeneration of epithelium	Congestion	Mononucleic cell infiltration	Damage total score	Fiber regeneration	Tissue regeneration	Healing total score
Madecassol®	1	0	0	0	1	1	0	0	0
	2	1	0	0	0	1	0	0	0
	3	0	0	0	0	0	1	0	1
	4	0	1	0	0	1	0	1	1
	5	0	0	0	1	1	0	0	0
	6	0	0	1	0	1	0	0	0
Mean						0.833333333			0.333333333
SD						0.40824829			0.516397779

	Animal	Edema	Degeneration of epithelium	Congestion	Mononucleic cell infiltration	Damage total score	Fiber regeneration	Tissue regeneration	Healing total score
Isotonic	1	1	1	2	2	6	2	3	5
	2	1	1	2	2	6	2	3	5
	3	1	2	1	1	5	1	2	3
	4	2	2	2	1	7	2	3	5
	5	2	2	1	2	7	1	2	3
	6	1	2	1	2	6	2	2	4
Mean						6.166666667			4.166666667
SD						0.752772653			0.98319208
	Animal	Edema	Degeneration of epithelium	Congestion	Mononucleic cell infiltration	Total damage score	Fiber regeneration	Tissue regeneration	Total healing score
Untreated	1	3	1	2	2	8	2	3	5
	2	3	1	2	1	7	2	2	4
	3	3	1	2	2	8	2	2	4
	4	2	1	1	1	5	3	3	6
	5	2	1	2	1	6	2	3	5

	6	2	3	1	2	8	2	2	4
Mean						7			4.666666667
SD						1.264911064			0.816496581